Multiple-SLE$_\kappa$ connectivity weights for rectangles, hexagons, and octagons

Steven M. Flores[*]
Department of Mathematics & Statistics,
University of Helsinki, P.O. Box 68, 00014, Finland,
and
Department of Mathematics, University of Michigan,
Ann Arbor, Michigan, 48109-2136, USA

Jacob J. H. Simmons[†]
Maine Maritime Academy, Pleasant Street, Castine, ME, 04420, USA

Peter Kleban[‡]
LASST and Department of Physics & Astronomy,
University of Maine, Orono, Maine, 04469-5708, USA
(Dated: May 29, 2015)

In four previous articles [6–9], two of the authors determined, completely and rigorously, a solution space $\mathcal{S}_N$ for a homogeneous system of $2N + 3$ linear partial differential equations (PDEs) in $2N$ variables that arises in conformal field theory (CFT) and multiple Schramm-Löwner evolution (SLE$_\kappa$). The system comprises $2N$ null-state equations and three conformal Ward identities that govern CFT correlation functions of $2N$ one-leg boundary operators or SLE$_\kappa$ partition functions. In [1, 10], M. Bauer et al. conjecture a formula, expressed in terms of "pure SLE$_\kappa$ partition functions," for the probability that the growing curves of a multiple-SLE$_\kappa$ process join in a particular connectivity. In the last article [9], we rigorously define certain elements of $\mathcal{S}_N$, which we call "connectivity weights," argue that they are in fact pure SLE$_\kappa$ partition functions, and show how to find explicit formulas for them in terms of Coulomb gas contour integrals.

The formal definition of the connectivity weights in [9] immediately leads to a method for finding explicit expressions for them. However, this method gives very complicated formulas where simpler versions may be available, and it is not applicable for certain values of $\kappa \in (0, 8)$ corresponding to well-known critical lattice models in statistical mechanics. In this article, we determine expressions for all connectivity weights in $\mathcal{S}_N$ for $N \in \{1, 2, 3, 4\}$ (those with $N \in \{3, 4\}$ are new) and for so-called "rainbow connectivity weights" in $\mathcal{S}_N$ for all $N \in \mathbb{Z}^+ + 1$. We verify these formulas by explicitly showing that they satisfy the formal definition of a connectivity weight. In appendix B, we investigate logarithmic singularities of some of these expressions, appearing for certain values of κ predicted by logarithmic CFT. In a future article [24], we use these results to predict crossing probabilities for critical lattice models inside polygons conditioned on a particular free/fixed side-alternating boundary condition, verifying our results via computer simulation. These crossing probabilities generalize Cardy's formula for critical percolation in a rectangle ($N = 2$, $\kappa = 6$) [19].

Keywords: conformal field theory, Schramm-Löwner evolution, connectivity weights, crossing probability, pure SLE$_\kappa$ partition function

I. INTRODUCTION

This article proposes explicit formulas for special functions that arise in multiple SLE$_\kappa$ [1–5] (and that also have a CFT interpretation [6–9]). Called "connectivity weights" [9], they are the main ingredients of a formula conjectured in [1, 9, 10] to give a *crossing probability*, or the probability that the growing curves of a multiple-SLE$_\kappa$ process join together pairwise in some specified connectivity. In this introduction, we briefly discuss crossing probabilities as natural observables of certain critical models in statistical physics, review the definition of a connectivity weight given in [9], recall some results from [6–8] that support this definition, and describe the organization of this article.

Crossing probabilities are natural observables of various random walks and critical models of statistical physics that possess a conformally invariant continuum limit. Indeed, multiple SLE$_\kappa$, a generalization of ordinary SLE$_\kappa$, is expected

[*]Electronic address: steven.flores@helsinki.fi
[†]Electronic address: jacob.simmons@mma.edu
[‡]Electronic address: kleban@maine.edu

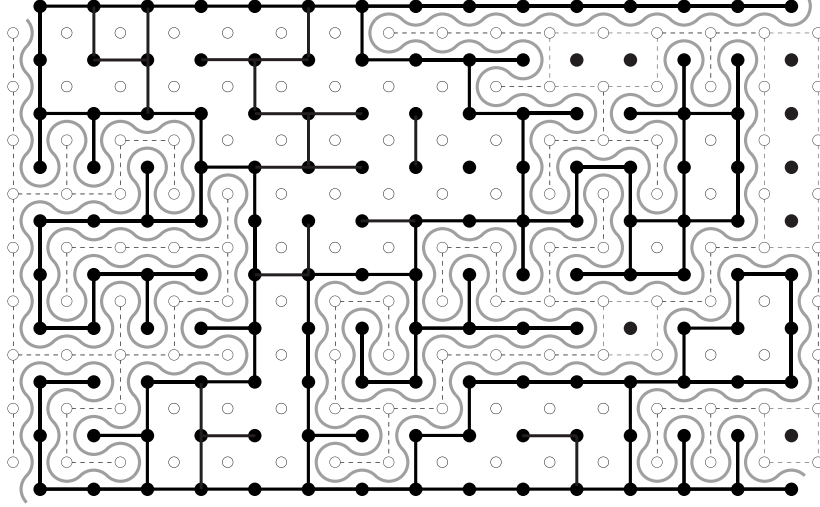arXiv:1505.07756v1 [math-ph] 28 May 2015

FIG. 1: A bond percolation configuration on a square lattice (black) in a rectangle, with a percolation cluster touching the top and bottom sides. Activated bonds are black, and activated dual bonds are dashed. Gray curves trace the cluster boundary.

to give the continuum limit of various mutually-avoiding random walks, including the loop-erased random walk ($\kappa = 2$) [11] and the self-avoiding random walk ($\kappa = 8/3$) [12], in a simply-connected domain. Crossing probabilities are also natural observables of various statistical mechanics models. Indeed, the archetypical example is the probability of a cluster-crossing event in critical percolation ($\kappa = 6$) [13]. Figure 1 illustrates this phenomenon for bond percolation on a discrete square lattice in a rectangle. In the continuum limit of this crossing event (where we send the lattice spacing to zero but simultaneously increase the system size so it always fills the rectangle), the boundaries of the percolation cluster touching both the rectangle's top and bottom sides are conjectured to approach random curves that fluctuate to the law of multiple SLE$_6$ (figure 1). (For site percolation on the triangular lattice, the marginal law for one of these curves is known to converge to SLE$_6$ [14], thanks in part to the "locality" property of cluster interfaces [15, 16].) As such, the percolation vertical crossing event is, in the continuum limit, identically the event that the four multiple-SLE$_6$ curves exploring the inside of the rectangle, each with an endpoint at its own corner, eventually join pairwise to form two random curves. One curve joins the two left corners of the rectangle, and the other curve joins the two right corners. The probability of this event is given by *Cardy's formula*,

$$\mathbb{P}\{\text{top-bottom crossing}\} = \frac{\Gamma(2/3)}{\Gamma(4/3)\Gamma(1/3)} \lambda^{1/3} \, {}_2F_1\left(\frac{1}{3}, \frac{2}{3}; \frac{4}{3} \,\middle|\, \lambda\right), \quad R = K(1-\lambda)/K(\lambda). \tag{1}$$

Here, $\lambda \in (0, 1)$ corresponds one-to-one with the aspect ratio $R \in (0, \infty)$ (that is, the ratio of the length of the bottom side to length of the left side) of the rectangle via the second equation in (1), with K the complete elliptic integral of the first kind [17, 18]. This formula (1) was first predicted by J. Cardy [19] using CFT methods. It was subsequently proven by S. Smirnov for critical site percolation on the triangular lattice [14]. The bond percolation crossing event, and its relation to multiple SLE$_\kappa$, generalizes to similar crossing events in the critical Potts model, the closely-related random cluster model [20–22], and level lines of various height models [23]. We study some of these generalizations for polygon crossing events in a forthcoming article [24].

Connectivity weights satisfy the system of differential equations that govern a correlation function comprising $2N$ one-leg boundary operators [6] in a conformal field theory (CFT) [25–27] with central charge $c \leq 1$. With $\boldsymbol{x} := (x_1, x_2, \ldots, x_{2N}) \in \Omega_0 := \{\boldsymbol{x} \in \mathbb{R}^{2N} \,|\, x_1 < x_2 < \ldots < x_{2N-1} < x_{2N}\}$ and $c = (6 - \kappa)(3\kappa - 8)/2\kappa$ [28], where $\kappa > 0$ is the multiple-SLE$_\kappa$ speed, this system is

$$\left[\frac{\kappa}{4}\partial_j^2 + \sum_{k \neq j}^{2N} \left(\frac{\partial_k}{x_k - x_j} - \frac{(6-\kappa)/2\kappa}{(x_k - x_j)^2}\right)\right] F(\boldsymbol{x}) = 0, \quad j \in \{1, 2, \ldots, 2N\}, \tag{2}$$

$$\sum_{k=1}^{2N} \partial_k F(\boldsymbol{x}) = 0, \quad \sum_{k=1}^{2N}\left[x_k\partial_k + \frac{(6-\kappa)}{2\kappa}\right]F(\boldsymbol{x}) = 0, \quad \sum_{k=1}^{2N}\left[x_k^2\partial_k + \frac{(6-\kappa)x_k}{\kappa}\right]F(\boldsymbol{x}) = 0. \tag{3}$$

Following CFT nomenclature, we call the first $2N$ equations (2) *null-state equations*, and we call the last three equations (3) *conformal Ward identities*. In [6–9], we study the vector space $\mathcal{S}_N$ (over the real numbers) comprising

all (classical) real-valued solutions $F : \Omega_0 \to \mathbb{R}$ of this system (2, 3) with the following property: there are positive constants C and p (possibly depending on F) such that

$$|F(\boldsymbol{x})| \leq C \prod_{i<j}^{2N} |x_j - x_i|^{\mu_{ij}(p)}, \quad \text{with} \quad \mu_{ij}(p) := \begin{cases} -p, & |x_j - x_i| < 1 \\ +p, & |x_j - x_i| \geq 1 \end{cases} \quad \text{for all } \boldsymbol{x} \in \Omega_0. \tag{4}$$

In [6–9], two authors of this article rigorously prove the following facts concerning the solution space $\mathcal{S}_N$ for all $\kappa \in (0, 8)$:

1. $\dim \mathcal{S}_N = C_N$, with C_N the Nth Catalan number:

$$C_N = \frac{(2N)!}{N!(N+1)!}. \tag{5}$$

2. $\mathcal{S}_N$ is spanned by real-valued *Coulomb gas solutions* [8]. These are linear combinations of (or limits as $\varkappa \to \kappa$ of linear combinations of) any functions that have the explicit formula [29, 30]

$$F(\kappa \,|\, \boldsymbol{x}) = \left(\prod_{\substack{j<k \\ j,k \neq c}}^{2N} (x_k - x_j)^{2/\kappa} \right) \left(\prod_{\substack{k=1 \\ k \neq c}}^{2N} |x_c - x_k|^{1-6/\kappa} \right) \mathcal{J}\left(\kappa \,\Big|\, \Gamma_1, \Gamma_2, \ldots, \Gamma_{N-1} \,\Big|\, \boldsymbol{x} \right), \tag{6}$$

where $c \in \{1, 2, \ldots, 2N\}$ (we call x_c *the point bearing the conjugate charge*), $\mathcal{J}$ is the *Coulomb gas integral* or *Dotsenko-Fateev integral* and is given by

$$\mathcal{J}\left(\kappa \,\Big|\, \Gamma_1, \Gamma_2, \ldots, \Gamma_{N-1} \,\Big|\, \boldsymbol{x} \right) = \oint_{\Gamma_{N-1}} \mathrm{d}u_{N-1} \oint_{\Gamma_{N-2}} \mathrm{d}u_{N-2} \cdots$$

$$\cdots \oint_{\Gamma_2} \mathrm{d}u_2 \oint_{\Gamma_1} \mathrm{d}u_1 \left(\prod_{\substack{l=1 \\ l \neq c}}^{2N} \prod_{m=1}^{N-1} (x_l - u_m)^{-4/\kappa} \right) \left(\prod_{m=1}^{N-1} (x_c - u_m)^{12/\kappa - 2} \right) \left(\prod_{p<q}^{N-1} (u_p - u_q)^{8/\kappa} \right), \tag{7}$$

and $\Gamma_1, \Gamma_2, \ldots, \Gamma_{N-1}$ are nonintersecting closed contours in the complex plane.

3. The dual space $\mathcal{S}_N^*$ has a basis $\mathscr{B}_N^* := \{[\mathscr{L}_1], [\mathscr{L}_2], \ldots, [\mathscr{L}_{C_N}]\}$ comprising equivalence classes of linear functionals $\mathscr{L}_\varsigma : \mathcal{S}_N \to \mathbb{R}$ called *allowable sequences of limits* [6]. We explain what these are below.

One may construct the Coulomb gas solutions (6, 7) via the CFT Coulomb gas formalism, introduced by V.S. Dotsenko and V.A. Fateev [29, 30]. In [31], J. Dubédat proves that these putative solutions indeed solve the system (2–3).

In [6–9], we use certain elements of the dual space $\mathcal{S}_N^*$ to prove, rigorously, items 1–3 above. To construct these linear functionals $\mathscr{L} : \mathcal{S}_N \to \mathbb{R}$, we prove in [6] that for all $F \in \mathcal{S}_N$ and all $i \in \{1, 2, \ldots, 2N-1\}$, the limits

$$\bar{\ell}_1 F(x_1, x_2, \ldots, x_i, x_{i+2}, \ldots, x_{2N}) := \lim_{x_{i+1} \to x_i} (x_{i+1} - x_i)^{6/\kappa - 1} F(x_1, x_2, \ldots, x_{2N}), \tag{8}$$

$$\underline{\ell}_1 F(x_2, x_3, \ldots, x_{2N-1}) := \lim_{R \to \infty} (2R)^{6/\kappa - 1} F(-R, x_2, x_3 \ldots, x_{2N-1}, R) \tag{9}$$

exist, (8) is independent of x_i, and, after trivially sending $x_i \to x_{i-1}$ in (8), both are in $\mathcal{S}_{N-1}$. Then, we let $\mathscr{L}$ be a composition of N such limits. These functionals gather into equivalence classes $[\mathscr{L}]$ whose elements differ only by the order in which we take their limits. For convenience, we represent every equivalence class $[\mathscr{L}]$ by a unique *polygon diagram*, in which N nonintersecting arcs inside a $2N$-sided polygon $\mathcal{P}$ join pairwise the vertices of $\mathcal{P}$ (enumerated
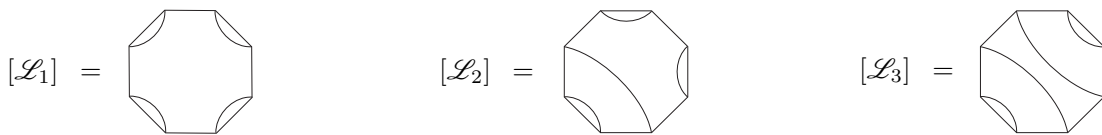

FIG. 2: Polygon diagrams for three different equivalence classes of allowable sequences of $N = 4$ limits. We find the other $C_4 - 3 = 11$ diagrams by rotating each of these three.
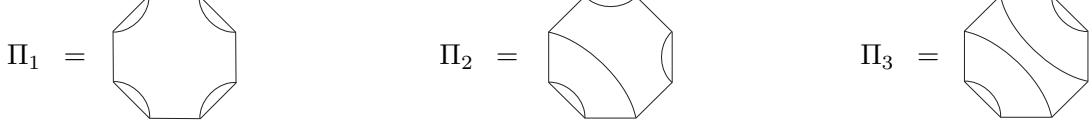
FIG. 3: Polygon diagrams for three different connectivity weights in $\mathscr{B}_4 \subset \mathcal{S}_4$. We find the other $C_4 - 3 = 11$ diagrams by rotating each of these three. Compare with the polygon diagrams in figure 2.

in counterclockwise order). The endpoints of the jth arc are the i_{2j-1}th and i_{2j}th vertices, where $x_{i_{2j-1}} < x_{i_{2j}}$ are the two points brought together by the jth limit of $\mathscr{L}$. There are C_N such diagrams, and they correspond one-to-one with the available equivalence classes (figure 2). We enumerate the equivalence classes $[\mathscr{L}_1], [\mathscr{L}_2], \ldots, [\mathscr{L}_{C_N}]$.

We conclude our analysis in [6] with a rigorous proof that the linear mapping $v : \mathcal{S}_N \to \mathbb{R}^{C_N}$ with $v(F)_\varsigma := [\mathscr{L}_\varsigma]F$ is well-defined and injective, so $\dim \mathcal{S}_N \leq C_N$. Then in [8], we use this map again to show that a certain subset of $\mathcal{S}_N$ comprising C_N distinct Coulomb gas solutions is linearly independent, thus establishing items 1 and 2 above. These results imply that v is an isomorphism, and item 3 above almost immediately follows from this fact.

Item 3 naturally leads us to consider the basis $\mathscr{B}_N$ for $\mathcal{S}_N$ dual to $\mathscr{B}_N^* \subset \mathcal{S}_N^*$. We call the elements of $\mathscr{B}_N$ *connectivity weights*, and we denote them as $\Pi_1, \Pi_2, \ldots, \Pi_{C_N}$, where Π_ϑ is defined through the duality relation

$$[\mathscr{L}_\varsigma]\Pi_\vartheta = \delta_{\varsigma,\vartheta} \text{ for all } \varsigma, \vartheta \in \{1, 2, \ldots, C_N\}, \tag{10}$$

$$\mathscr{B}_N^* = \{[\mathscr{L}_1], [\mathscr{L}_2], \ldots, [\mathscr{L}_{C_N}]\}, \quad \mathscr{B}_N = \{\Pi_1, \Pi_2, \ldots, \Pi_{C_N}\}. \tag{11}$$

We also define the *polygon diagram* of Π_ς to be that of its corresponding equivalence class $[\mathscr{L}_\varsigma]$ (figure 3).

The basis $\mathscr{B}_N$ (11) is natural. Indeed, because of the duality relation (10), any element $F \in \mathcal{S}_N$ has the decomposition over $\mathscr{B}_N$

$$F = a_1\Pi_1 + a_2\Pi_2 + \cdots + a_{C_N}\Pi_{C_N}, \quad a_\varsigma = [\mathscr{L}_\varsigma]F. \tag{12}$$

As we mentioned, the connectivity weights $\Pi_1, \Pi_2, \ldots, \Pi_{C_N}$ naturally arise in a certain stochastic process called *multiple Schramm Löwner evolution (SLE$_\kappa$)* [1–5]. In this process, $2N$ distinct self/mutually-avoiding fractal curves grow from the points $x_1 < x_2 < \ldots < x_{2N}$ in the real axis and explore the upper half-plane. This process stops once the tips of these $2N$ curves join pairwise to form N fractal curves called *boundary arcs*. The non-intersecting boundary arcs join the points $x_1 < x_2 < \ldots < x_{2N}$ together pairwise in any one of C_N distinct connectivities (figure 4), and we enumerate these connectivities in such a way that every element of $[\mathscr{L}_\varsigma]$ brings together the endpoints of each arc in the ςth connectivity. The boundary arcs are conjectured, and in some cases proven, to be conformally invariant scaling limits of cluster perimeters in various critical lattice models or of certain random walks [11, 12, 14, 21, 23, 32]. Thus, multiple SLE$_\kappa$ is useful for studying these systems.

The multiple-SLE$_\kappa$ process is completely determined up to an arbitrary nonzero solution of the system (2–3), called an *SLE$_\kappa$ partition function* [1, 9]. Without loss of generality, we suppose that an SLE$_\kappa$ partition function is always positive-valued. Refs. [9, 10] conjecture and give supporting arguments that

$$P_\varsigma = \frac{a_\varsigma \Pi_\varsigma}{F} = \frac{a_\varsigma \Pi_\varsigma}{a_1\Pi_1 + a_2\Pi_2 + \cdots + a_{C_N}\Pi_{C_N}}, \quad a_\varsigma := [\mathscr{L}_\varsigma]F \geq 0 \tag{13}$$

gives the probability of the growing curves in the multiple-SLE$_\kappa$ process, with partition function $F \in \mathcal{S}_N$, almost surely joining pairwise in the ςth connectivity (figure 4).
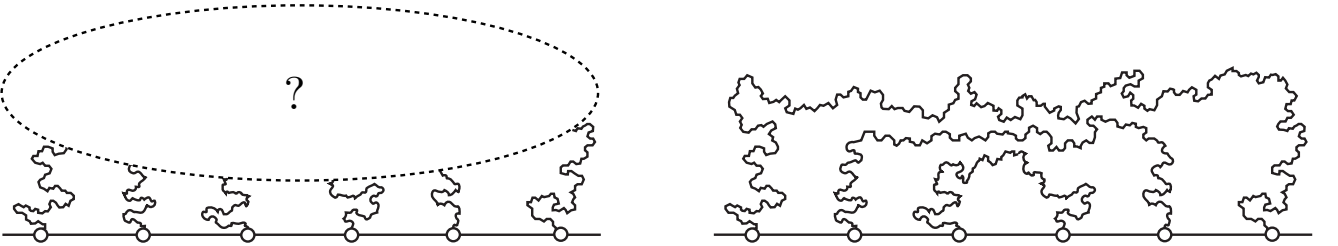

FIG. 4: Refs. [9, 10] conjecture a formula for the probability that the growing curves of a multiple-SLE$_\kappa$ process (left) eventually join pairwise in the ςth connectivity (right).

The proposed crossing-probability formula (13) predicts some fundamental properties of the connectivity weights that are not apparent from their formal definition (10). For each $\varsigma \in \{1, 2, \ldots, C_N\}$, if we choose F so $a_\varsigma > 0$ and assume, as is natural, that P_ς is positive-valued, then (13) immediately implies that Π_ς is positive-valued and is therefore itself an SLE_κ partition function. In fact, (13) gives $P_\varsigma = \delta_{\varsigma, \vartheta}$ for the multiple-SLE_κ process with partition function $F = \Pi_\vartheta$, meaning that the growing curves of this process join pairwise in the ϑth connectivity almost surely. Thanks to this special property, connectivity weights are also called *pure SLE_κ partition functions*, or more succinctly, *pure partition functions*, in the literature [1, 10, 33].

Explicit formulas for the connectivity weights $\Pi_1, \Pi_2, \ldots, \Pi_{C_N}$ are of interest because they are natural to use as a basis for $\mathcal{S}_N$ and are important to multiple SLE_κ. One way to determine such formulas is through finding another basis $\mathcal{B}_N = \{\mathcal{F}_1, \mathcal{F}_2, \ldots, \mathcal{F}_{C_N}\}$ comprising the explicit solutions (6, 7), computing the coefficients in the decomposition (12) of each basis element over $\mathscr{B}_N$, and inverting the collection of C_N resulting equations to find $\Pi_1, \Pi_2, \ldots, \Pi_{C_N}$. In fact, we use this approach in [9]. However, determining a convenient basis for $\mathcal{S}_N$ and calculating the coefficients in (12) may be difficult. Moreover, the connectivity weight formulas that result may be unnecessarily complicated. In addition, the so-called basis may fail to span $\mathcal{S}_N$ for certain $\kappa \in (0, 8)$, causing this approach to fail for those values.

Recently and independently of this work, K. Kytölä and E. Peltola developed a completely different approach for finding explicit solutions of the system (2, 3) that uses quantum group methods [34]. Called the *spin-chain Coulomb gas correspondence*, their formalism gives another means for determining connectivity weight formulas (which they call "pure partition functions") for all $N \in \mathbb{Z}^+$ and irrational $\kappa > 0$ [33]. Moreover, it has the advantage of explicitly determining the asymptotic properties of these formulas as two or more points x_j approach each other simultaneously. This information is expected to be useful for determining some anticipated, important properties of these functions, such as positivity [9, 34].

But perhaps the most straightforward (if not the most elegant) approach for finding formulas of connectivity weights is to simply guess and verify them directly through the duality relation (10). This approach is practical for small $N \in \mathbb{Z}^+ + 1$ but very unwieldy for large N. Fortunately, in most practical applications such as those involving lattice models or random walks inside $2N$-sided polygons, N is small. In section II, we apply this approach to find explicit formulas for all connectivity weights in $\mathcal{S}_N$ with $N \in \{1, 2, 3, 4\}$ and for special connectivity weights called "rainbow connectivity weights" in $\mathcal{S}_N$ for all $N \in \mathbb{Z}^+ + 1$. The cases $N \in \{1, 2, 3, 4\}$ respectively pertain to multiple SLE_κ in (or really, conformally mapped from the upper half-plane onto) the two-sided polygon, the rectangle, the hexagon, and the octagon. For $N \in \{1, 2\}$, these connectivity weight formulas are already known [1, 31], but for $N \in \{3, 4\}$, these formulas are new. In section III, we summarize our results. In appendix A, two authors of this article explicitly show that all singularities in $\kappa \in (0, 8)$ of factors in the connectivity weight formulas are removable singularities, and the connectivity weights are therefore analytic functions of $\kappa \in (0, 8)$ (and, actually, of $\kappa \in (0, 8) \times i\mathbb{R}$ too). Finally, in appendix B, we study logarithmic singularities of some of the connectivity weight formulas as one or more points x_j approach a common point x_i. These logarithmic singularities may arise only if κ is an *exceptional speed* [8, 9] and N is sufficiently large. Such κ correspond with CFT minimal models [9]. In appendix A of [9], we investigate the existence of logarithmic singularities in certain elements of $\mathcal{S}_N$ for $8/\kappa \in 2\mathbb{Z}^+ + 1$, and in appendix B of this article, we uncover a similar logarithmic behavior of the hexagon connectivity weight (28) for $12/\kappa \in \mathbb{Z}^+ + 1$ coprime with three. For both cases, we briefly discuss how logarithmic CFT predicts the appearance of these logarithmic singularities.

In [24], we conformally map the multiple-SLE_κ process with $N = 3$ onto a hexagon, and we use (13) and the results of section II C to find explicit formulas for crossing probabilities as functions of the hexagon's shape. To verify this formula for $\kappa = \{16/3, 24/5, 4\}$ we measure via computer simulation $Q \in \{2, 3, 4\}$ random cluster model crossing probabilities in a hexagon with a free/fixed side-alternating boundary condition [6]. (Multiple-SLE_κ at these values of κ corresponds with these respective models. See [6] for more details.) The $Q = 1$ random cluster model corresponds with critical percolation ($\kappa = 6$), and in [35], we provide similar verification for this case.

Actually, the case $\kappa = 6$ has a unique, interesting feature. In percolation, the free/fixed side-alternating boundary condition [6] of the $2N$-sided polygon does not influence the probabilities of the configurations of the interior sites or bonds. As such, the partition function for the system conditioned on this boundary-condition event approaches the free partition function, summing over all bond configurations, as we approach the continuum limit. According to [1, 24], it is natural to interpret F as the ratio of these two partition functions in this limit, which is then one. Upon inserting $F = 1$ into (13) with $\kappa = 6$, we find that $P_\varsigma = \Pi_\varsigma$. That is, if $\kappa = 6$, then the ςth connectivity weight gives the probability that percolation clusters join the fixed sides of the polygon in the ςth connectivity.

II. ANALYSIS

In this section, we present formulas for all connectivity weights in $\mathcal{S}_N$ with $N \in \{1, 2, 3, 4\}$ and for all so-called "rainbow connectivity weights" in $\mathcal{S}_N$ with $N \in \mathbb{Z}^+ + 1$. The $N \in \{3, 4\}$ and "rainbow" results are, to our knowledge, new. Our derivations proceed in two steps. First, we assume that each sought formula has the form (6) and prudently

choose integration contours for the Coulomb gas integral (7) of that formula. Second, we verify that our ansatz is correct. Because our candidate formula gives an element of $\mathcal{S}_N$, we must only verify that it satisfies the duality condition (10) of a connectivity weight.

Certain constraints limit the various possible integration contours available for use in (7). To begin, each contour must close in order for (6) to solve the system (2, 3). Furthermore, by Cauchy's theorem, each contour must circle around some of the branch points $x_1, x_2, \ldots, x_{2N}$, thereby passing onto different Riemann sheets of the integrand, in order for the integration to give something nontrivial. And finally, each contour must have a winding number of zero around these branch points in order to end on the same Riemann sheet on which it started. The simplest contour that satisfies these criteria is the *Pochhammer contour*, shown in the left illustration of figures 5 and 6. In [8, 9], we only consider Pochhammer contours that entwine together two branch points, but in this article, we consider Pochhammer contours that entwine together more than two branch points or that surround other integration contours or both.

Both theorem 5 and section IV B of [9] motivate our integration-contour selections for the Coulomb gas integral (7). In particular, theorem 5 says that for any $\Pi_\varsigma \in \mathscr{B}_N$ and $i \in \{1, 2, \ldots, 2N - 1\}$,

I. (x_i, x_{i+1}) is a *two-leg interval* of Π_ς (meaning that the limit $\bar{\ell}_1 \Pi_\varsigma$ (8) vanishes) if no arc joins the ith vertex with the $(i+1)$th vertex in the polygon diagram for Π_ς.

II. (x_i, x_{i+1}) is not a two-leg interval of Π_ς if an arc joins the ith vertex with the $(i+1)$th vertex in the polygon diagram for Π_ς.

On the other hand, the discussion in section IV B of [9] specifies two scenarios for the interaction of the integration contours with the interval (x_i, x_{i+1}) in which this interval is a two-leg interval of Π_ς.

(a) If no integration contour in a formula for Π_ς of the form (6, 7) either crosses (x_i, x_{i+1}) or touches its endpoints and if $c \notin \{i, i+1\}$, then (x_i, x_{i+1}) is a two-leg interval of Π_ς.

(b) If a Pochhammer contour in a formula for Π_ς of the form (6, 7) entwines together both endpoints of (x_i, x_{i+1}) (as in figure 5 with $j = i + 1$) and if $c \in \{i, i+1\}$, then (x_i, x_{i+1}) is a two-leg interval of Π_ς.

Selecting integration contours for connectivity weights based on items a and b above is equivalent to constructing conformal blocks in CFT via Coulomb gas methods [9, 26, 27, 29, 30].

In order for us to obtain numerical values of crossing probabilities (so we may, for example, compare these predicted values to computer simulation measurements), we must numerically evaluate the connectivity weights that appear in (13). Formulas for connectivity weights typically involve integration around a Pochhammer contour, and although this integration is not entirely straightforward, we may perform it by decomposing the contour into a collection of loops and line segments. This decomposition is simplest if a Pochhammer contour is *elementary*, meaning that it entwines together only two "endpoints" x_i and x_j. We denote such a contour by $\mathscr{P}(x_i, x_j)$. As figure 5 shows, for
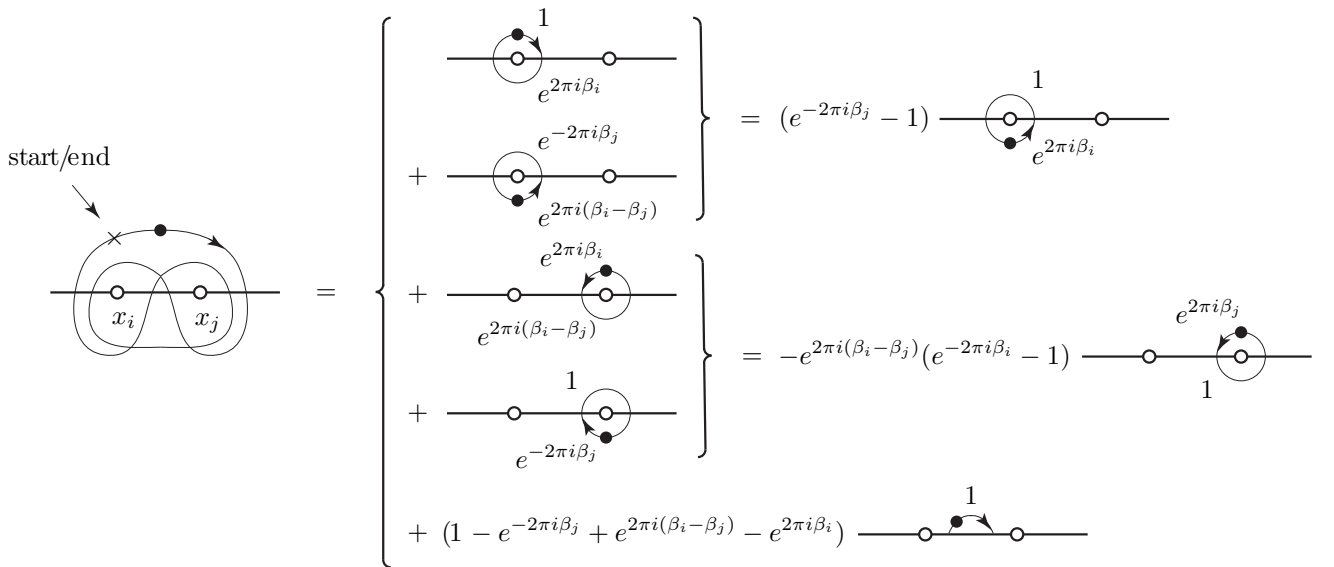

FIG. 5: The elementary Pochhammer contour $\mathscr{P}(x_i, x_j)$ (left) with "endpoints" x_i and x_j, and its decomposition (14) (right). The phase factor of the integrand at the start point and end point (at the tip of the arrow) of each contour is shown.

FIG. 6: If $e^{2\pi i \beta_i}$ and $e^{2\pi i \beta_j}$ are the monodromy factors associated with the endpoints x_i and x_j respectively, and $\mathrm{Re}\,\beta_i, \mathrm{Re}\,\beta_j > -1$, then we may replace the elementary Pochhammer contour $\mathscr{P}(x_i, x_j)$ with the simple contour on the right via (15).

any function $f(u)$ that is analytic in the interior of a region containing $\mathscr{P}(x_i, x_j)$, any $\beta_i, \beta_j \in \mathbb{C}$, and any positive $\epsilon \ll |x_j - x_i|$, we have (as we account for the phase factors, we take $-\pi < \arg(z) \leq \pi$ for all complex z)

$$\oint_{\mathscr{P}(x_i, x_j)} (u - x_i)^{\beta_i} (x_j - u)^{\beta_j} f(u)\, \mathrm{d}u = (e^{-2\pi i \beta_j} - 1) \oint_{x_i} (u - x_i)^{\beta_i} (x_j - u)^{\beta_j} f(u)\, \mathrm{d}u$$

$$- e^{2\pi i (\beta_i - \beta_j)} (e^{-2\pi i \beta_i} - 1) \oint_{x_j} (u - x_i)^{\beta_i} (x_j - u)^{\beta_j} f(u)\, \mathrm{d}u \qquad (14)$$

$$+ 4 e^{\pi i (\beta_i - \beta_j)} \sin \pi \beta_i \sin \pi \beta_j \int_{x_i + \epsilon}^{x_j - \epsilon} (u - x_i)^{\beta_i} (x_j - u)^{\beta_j} f(u)\, \mathrm{d}u,$$

where the subscript x_i (resp. x_j) on the first (resp. second) integral on the right side of (14) indicates that u traces counterclockwise a circle centered on x_i (resp. x_j) with radius ϵ, starting just above $x_i + \epsilon$ (resp. below $x_j - \epsilon$) where the integrand's phase is zero. If $\mathrm{Re}\,\beta_i, \mathrm{Re}\,\beta_j > -1$, then sending $\epsilon \to 0$ in (14) gives the useful identity

$$\oint_{\mathscr{P}(x_i, x_j)} (u - x_i)^{\beta_i} (x_j - u)^{\beta_j} f(u)\, \mathrm{d}u =$$

$$4 e^{\pi i (\beta_i - \beta_j)} \sin \pi \beta_i \sin \pi \beta_j \int_{x_i}^{x_j} (u - x_i)^{\beta_i} (x_j - u)^{\beta_j} f(u)\, \mathrm{d}u, \quad \mathrm{Re}\,\beta_i, \mathrm{Re}\,\beta_j > -1 \quad (15)$$

(figure 6). In other words, if $\mathrm{Re}\,\beta_i, \mathrm{Re}\,\beta_j > -1$, then we may discard the integrations in (14) around the loops. Because the right side of (15) is easier to evaluate numerically than the left side, we use the former whenever it converges. We note that $\beta_i, \beta_j \in \mathbb{Z}^+ \cup \{0\}$ are zeros of (14, 15).

If a Pochhammer contour is not elementary but surrounds several branch points and/or integration contours, then we may decompose it into a collection of loops, each of which surrounds a branch point of the integrand, and line segments that join these loops, although the decomposition is more complicated than (14). Furthermore, if the integrations along these segments converge, then we may shrink the radius of the loops to zero so the line segments terminate at the branch points. (This is convenient for numerical evaluation because the resulting decomposition only contains integrations along line segments.) As we account for the phase factors that arise in these decompositions, we take $-\pi < \arg(z) \leq \pi$ for all complex z. This sets the conventions of figure 7 for use throughout this article.

Ignoring the subtle issue of convergence, we express all formulas for connectivity weights Π_ς as sums of improper integrations along line segments that terminate at branch points, discarding the contributions that arise from integrating
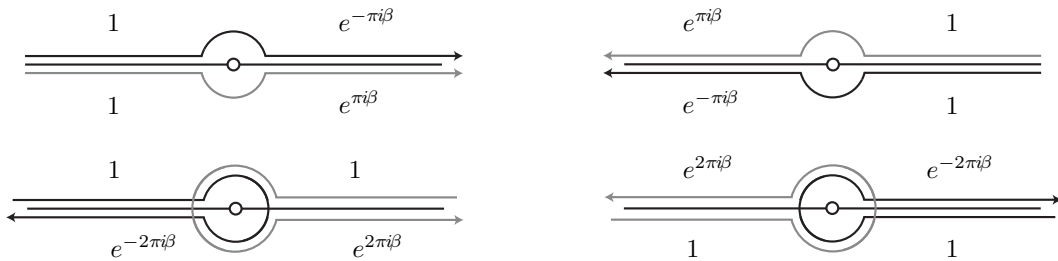

FIG. 7: Monodromy factors accrued by the function $(x - u)^\beta$ as u passes over or under (upper illustration) or encircles around (lower illustration) the branch point x (open circle on the real axis).
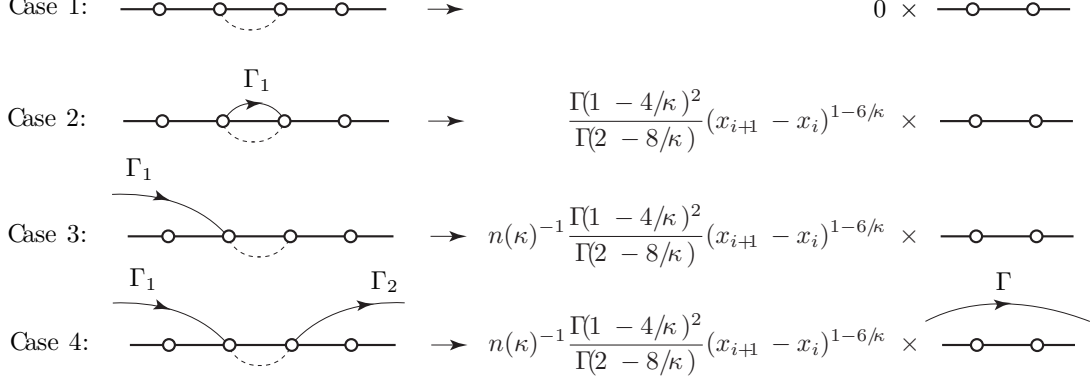
FIG. 8: Cases 1–4 (left) and their asymptotic behavior as $x_{i+1} \to x_i$ (right). The dashed curve connects x_i with x_{i+1} (neither present on the right), and solid curves are integration contours. The endpoints of Γ are the endpoints of Γ_1 and Γ_2, not shown.

around loops. If an improper integral does diverge, then we use identity (15) to make the replacement

$$\int_{x_i}^{x_j} (u - x_i)^{\beta_i} (x_j - u)^{\beta_j} f(u)\,\mathrm{d}u \quad \longmapsto \quad \frac{1}{4e^{\pi i(\beta_i - \beta_j)} \sin \pi\beta_i \sin \pi\beta_j} \oint_{\mathscr{P}(x_i, x_j)} (u - x_i)^{\beta_i} (x_j - u)^{\beta_j} f(u)\,\mathrm{d}u. \quad (16)$$

Although this replacement reintroduces a Pochhammer contour, this new Pochhammer contour is elementary, so we may use (14) to numerically integrate around it. To summarize, the decomposition has the form

$$\Pi_\varsigma \propto \oint_{\Gamma_1} \oint_{\Gamma_2} \cdots \oint_{\Gamma_{N-1}} \left[\ldots \text{integrand of (7)} \ldots \right] \mathrm{d}u_{N-1} \cdots \mathrm{d}u_2\,\mathrm{d}u_1, \quad \Gamma_m = \text{Pochhammer contour}, \quad (17)$$

$$= \sum \left[\ldots \text{integration along line segments } [x_i, x_j] \ldots \right] \quad (18)$$

$$= \sum \left[\ldots \text{integration around elementary } \mathscr{P}(x_i, x_j) \ldots \right], \quad (19)$$

and we give the formula for each Π_ς in the form (18), with the form (19) implicitly used, when needed, by making the replacement (15) for all contours. Every definite integral that appears in the sum (18) has $\beta_i, \beta_j \in \{-4/\kappa, 8/\kappa, 12/\kappa - 2\}$, with $\beta_i = -4/\kappa$ or $\beta_j = -4/\kappa$, so all (resp. none) of them diverge if $\kappa \in (0, 4]$ (resp. $\kappa \in (4, 8)$). Because the right sides of (17–19) are equal for $\kappa \in (4, 8)$ and (17) is analytic in $\kappa \in (0, 8) \times i\mathbb{R}$, it follows that (19) is also analytic in this region, in particular at the poles $\beta_i, \beta_j \in \mathbb{Z}^-$ of the right side of (16), so (19) gives the analytic continuation of (18) to the region $\kappa \in (0, 8) \times i\mathbb{R}$. This includes the line segment $\kappa \in (0, 8)$ of exclusive interest here.

In order to correctly normalize the connectivity weight $\Pi_\varsigma \in \mathscr{B}_N$ such that (10) is satisfied, it suffices to require that the limit (8) with $F = \Pi_\varsigma$ such that (x_i, x_{i+1}) is not a two-leg interval of Π_ς (item I) gives another connectivity weight $\Xi_{\varsigma'} \in \mathscr{B}_{N-1}$ for some $\varsigma' \in \{1, 2, \ldots, C_{N-1}\}$. Indeed, we then have

$$[\mathscr{L}_\varsigma]\Pi_\varsigma = [\mathscr{M}_{\varsigma'}]\left(\overbrace{\lim_{x_{i+1} \to x_i} (x_{i+1} - x_i)^{6/\kappa - 1} \Pi_\varsigma(\boldsymbol{x})}^{(8)} \right) = [\mathscr{M}_{\varsigma'}]\Xi_{\varsigma'} = 1, \quad (20)$$

where $[\mathscr{M}_{\varsigma'}] \in \mathscr{B}_{N-1}^*$ is the equivalence class produced by dropping the first limit $\bar{\ell}_1$ from all elements of $[\mathscr{L}_\varsigma]$ that send $x_{i+1} \to x_i$ first. Computing this limit involves determining the asymptotic behavior of the Coulomb gas integral (7) as $x_{i+1} \to x_i$ for $i \notin \{c, c-1\}$, which is generally complicated to do. To simplify this calculation for $\kappa \in (4, 8)$, we use (15) to decompose all Pochhammer contours that surround x_i or x_{i+1} into line segments that terminate at these points in one of the following four cases:

1. Neither x_i nor x_{i+1} are endpoints of an integration contour.

2. Both x_i and x_{i+1} are endpoints of one common contour, say Γ_1.

3. x_i (resp. x_{i+1}) is an endpoint of one contour, say Γ_1, and x_{i+1} (resp. x_i) is not an endpoint of any contour.

4. x_i is an endpoint of one contour, say Γ_1, and x_{i+1} is an endpoint of a different contour, say Γ_2.

Figure 8 illustrates cases 1–4 and shows the asymptotic behavior of the Coulomb gas integral (7) in each case, as was found in the proof of lemma 6 in [8]. (Cases 3 and 4 include situations in which one of the integration contours arcs over (x_i, x_{i+1}), not shown in figure 8.) In cases 3 and 4, we encounter the reciprocal of

$$n(\kappa) := -2\cos(4\pi/\kappa), \qquad (21)$$

called the *O(n)-model fugacity function* because loops in the loop-gas representation of the O(n) model are conjectured to fluctuate to the law of $\text{SLE}_\kappa/\text{CLE}_\kappa$ [20, 21, 36–40], with speed $\kappa \in (8/3, 8)$ related to the loop fugacity n through (21). Case 4 yields the result of case 3, but with the original two contours Γ_1 and Γ_2 replaced by one terminating at the other endpoints of Γ_1 and Γ_2.

Finally, to find formulas for all of the connectivity weights in $\mathscr{B}_N$ is somewhat redundant. Indeed, if rotating the polygon diagram for one connectivity weight Π_ς gives the diagram of another Π_ϑ, then a similar transformation of the formula for Π_ς gives the formula for Π_ϑ. Therefore, we give only one formula for each collection of connectivity weights whose polygon diagrams are identical up to rotation.

A. The SLE_κ connectivity weight ($N = 1$)

According to item 1 of the introduction I, the dimension of the solution space $\mathcal{S}_1$ for the system (2, 3) is $C_1 = 1$ (5), so there is only one connectivity weight that spans all of $\mathcal{S}_1$. In [6], we find that every element of $\mathcal{S}_1$ is a multiple of the function

$$\Pi_1(\kappa \,|\, x_1, x_2) = (x_2 - x_1)^{1-6/\kappa}. \qquad (22)$$

The limit (8) with $i = 1$ gives $\bar{\ell}_1 \Pi_1 = 1$, so according to the duality condition (10), the (aptly-named) function Π_1 (22) gives the formula for the lone connectivity weight we seek. This weight serves as the partition function for ordinary SLE_κ in the upper half-plane and from x_1 to x_2 [1, 4].

B. Rectangle connectivity weights ($N = 2$)

According to item 1 of the introduction I, the dimension of the solution space $\mathcal{S}_2$ for the system (2, 3) is $C_2 = 2$ (5), so there are two connectivity weights Π_1 and Π_2 that span $\mathcal{S}_2$. Because their diagrams are identical up to a rotation, we find a formula for only Π_1. An appropriate transformation then gives the formula for Π_2.

Now we find a formula for Π_1 in the form of (6) with $N = 2$. After choosing $c = 3$, we determine the integration contour of (7) for use in this formula. Figure 9 shows the polygon diagram for Π_1, and from this diagram and item I above, it is apparent that (x_3, x_4) is a two-leg interval of Π_1. Hence, following item b above, we entwine x_3 and x_4 with a Pochhammer contour $\Gamma_1 = \mathscr{P}(x_3, x_4)$. This choice of integration contour determines the formula for Π_1 up to normalization.

Assuming that $\kappa \in (4, 8)$, we replace the Pochhammer contour by an integration along $[x_3, x_4]$ via (15) (figure 6). Thus, the Coulomb gas integral (7) with $N = 2$ becomes (here, we implicitly order the differences in the factors of the integrand in (7) such that (23) is positive-valued)

$$I_3(\kappa \,|\, x_1, x_2, x_3, x_4) := \mathcal{J}\Big(\kappa \,\Big|\, [x_3, x_4] \,\Big|\, x_1, x_2, x_3, x_4\Big), \quad c = 3, \quad N = 2. \qquad (23)$$

After inserting the Coulomb gas integral (23) into (6), we find the proper normalization for the resulting formula by requiring that the limit (9) equals the $N = 1$ connectivity weight (22) with $(x_1, x_2) \mapsto (x_2, x_3)$. Upon using the results
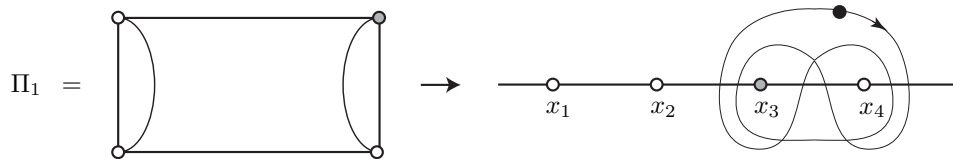

FIG. 9: The one topologically distinct rectangle connectivity, and the integration contour for its weight with $c = 3$. Moving counterclockwise around the rectangle corresponds to moving right along the real axis, with the bottom-left vertex sent to x_1.
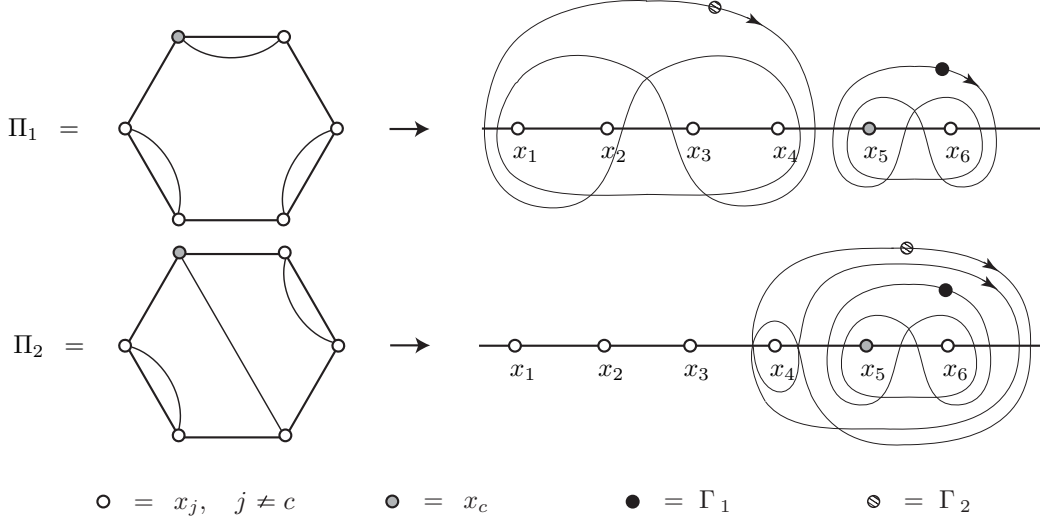
FIG. 10: The two topologically distinct hexagon connectivities, and the integration contours for their weights with $c = 5$. Moving counterclockwise around the hexagon corresponds to moving right along the real axis, with the bottom-left vertex sent to x_1.

of sections A 3 and A 5 of [8] to determine the asymptotic behavior of (23) as $x_4 = -x_1 \to \infty$ (figure 8), we find

$$\Pi_1(\kappa \,|\, x_1, x_2, x_3, x_4) = n(\kappa) \frac{\Gamma(2 - 8/\kappa)}{\Gamma(1 - 4/\kappa)^2} \left(\prod_{\substack{i<j \\ i,j \neq 3}}^{4} (x_j - x_i)^{2/\kappa} \right) \left(\prod_{k \neq 3}^{4} |x_3 - x_k|^{1 - 6/\kappa} \right) I_3(\kappa \,|\, x_1, x_2, x_3, x_4). \quad (24)$$

If $\kappa \in (0, 4]$, then the improper integral (23) diverges, and we regularize it via the replacement (16) with $x_i = x_3$, $x_j = x_4$, $\beta_i = 12/\kappa - 2$, and $\beta_j = -4/\kappa$.

Employing the contour-integral definition of the Gauss hypergeometric function [17, 18], we may write (24) in the alternative form

$$\Pi_1(\kappa \,|\, x_1, x_2, x_3, x_4) = \frac{\Gamma(12/\kappa - 1)\Gamma(4/\kappa)}{\Gamma(8/\kappa)\Gamma(8/\kappa - 1)} (x_3 - x_1)^{1 - 6/\kappa} (x_4 - x_2)^{1 - 6/\kappa}$$

$$\times \lambda^{2/\kappa}(1 - \lambda)^{1 - 6/\kappa} \, {}_2F_1\left(\frac{4}{\kappa}, 1 - \frac{4}{\kappa}; \frac{8}{\kappa} \,\middle|\, \lambda \right), \quad \lambda := \frac{(x_2 - x_1)(x_4 - x_3)}{(x_3 - x_1)(x_4 - x_2)}. \quad (25)$$

If $\kappa = 6$, corresponding to critical percolation [14], then (25) becomes Cardy's formula (1) [19] for the probability of a vertical percolation-cluster crossing in a rectangle with aspect ratio (bottom-side length to left-side length) $R = K(\lambda)/K(1 - \lambda)$, where K is the complete elliptic integral of the first kind [17, 18]. The polygon diagram for Π_1 illustrates the corresponding boundary arc connectivity (figure 9). Also, with the formula for Π_1 written in the form (25), we may use knowledge of the behavior of the hypergeometric function as $\lambda \to 0$ and $\lambda \to 1$ [17, 18] to verify the duality condition (10). This completes the proof that (24, 25) are indeed formulas for Π_1.

C. Hexagon connectivity weights ($N = 3$)

According to item 1 of the introduction I, the dimension of the solution space $\mathcal{S}_3$ for the system (2, 3) is $C_3 = 5$ (5), so there are five connectivity weights $\Pi_1, \Pi_2, \ldots, \Pi_5$ that span $\mathcal{S}_3$. These connectivity weights sort into two disjoint sets, with the diagrams in each set identical up to a rotation. Hence, we find formulas for only two connectivity weights Π_1 and Π_2 shown in figure 10, one per set. An appropriate transformation then gives the formulas for the other weights.

First, we find a formula for Π_1 in the form of (6) with $N = 3$. After choosing $c = 5$, we determine the two integration contours of (7) for use in this formula. Figure 10 shows the polygon diagram for Π_1, and from this diagram and item I above, it is apparent that (x_1, x_2), (x_3, x_4), and (x_5, x_6) are two-leg intervals of Π_1. Hence, following item b above, we entwine x_5 and x_6 with a Pochhammer contour $\Gamma_1 = \mathscr{P}(x_5, x_6)$. Moreover, item a above
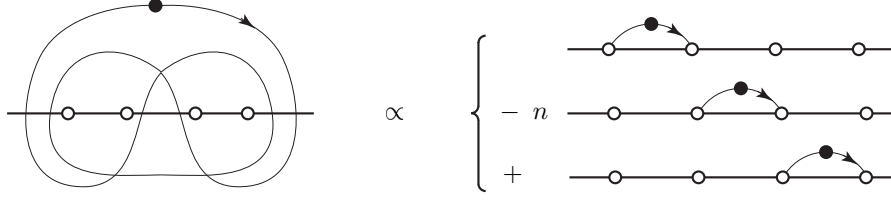
FIG. 11: Integration around the Pochhammer contour on the left is proportional to the combination of three integrations along line segments on the right. We use this decomposition to find the first hexagon (28) and octagon (46) connectivity weights.

requires that no integration contour crosses the other two-leg intervals. In order to satisfy item a, we entwine $[x_1, x_2]$ and $[x_3, x_4]$ with a Pochhammer contour Γ_2. These choices of integration contours determine the formula for Π_1 up to normalization.

Assuming that $\kappa \in (4, 8)$, we decompose the Coulomb gas integral (7) of Π_1, with Γ_1 and Γ_2 as specified, into a linear combination of the simpler definite integrals of type (here, we implicitly order the differences in the factors of the integrand in (7) such that (26) is positive-valued, and we note that by Fubini's theorem that $I_{ij} = I_{ji}$)

$$i \neq j: \quad I_{ij}(\kappa \,|\, x_1, x_2, \ldots, x_6) := \mathcal{J}\Big(\kappa \,\Big|\, [x_i, x_{i+1}], [x_j, x_{j+1}] \,\Big|\, x_1, x_2, \ldots, x_6\Big), \quad c = 5, \quad N = 3, \quad i, j < 2N. \quad (26)$$

To obtain this decomposition, we replace Γ_1 by an integration along $[x_5, x_6]$ (figure 6) and decompose the integration along Γ_2 into integrations along $[x_1, x_2]$, $[x_2, x_3]$, and $[x_3, x_4]$ (figure 11), finding

$$\mathcal{J}(\kappa \,|\, \Gamma_1, \Gamma_2) \propto [e^{4\pi i/\kappa} I_{15} + e^{8\pi i/\kappa} I_{25} + e^{12\pi i/\kappa} I_{35} - e^{20\pi i/\kappa} I_{15} - e^{24\pi i/\kappa} I_{25} - e^{20\pi i\kappa} I_{35}$$
$$+ e^{12\pi i/\kappa} I_{15} + e^{8\pi i/\kappa} I_{25} + e^{4\pi i\kappa} I_{35} - e^{-4\pi i/\kappa} I_{15} - e^{-8\pi i/\kappa} I_{25} - e^{-4\pi i/\kappa} I_{35}](\kappa)$$
$$= (e^{4\pi i/\kappa} - e^{20\pi i/\kappa} + e^{12\pi i/\kappa} - e^{-4\pi i/\kappa})[I_{15} + I_{35} - nI_{25}](\kappa). \quad (27)$$

After inserting this decomposition (27) into (6), we find the proper normalization for the resulting formula by requiring that the limit (8) with $i = 2$ equals the rectangle connectivity weight (24) with $(x_2, x_3, x_4) \mapsto (x_4, x_5, x_6)$. Upon using the results of sections A 2 and A 3 in [8] (figure 8) with the decomposition (27) (figure 11) to determine the asymptotic behavior of $\mathcal{J}(\Gamma_1, \Gamma_2)$ as $x_3 \to x_2$, we find

$$\Pi_1(\kappa \,|\, x_1, x_2, \ldots, x_6) = \frac{n(\kappa)^2}{n(\kappa)^2 - 2} \frac{\Gamma(2 - 8/\kappa)^2}{\Gamma(1 - 4/\kappa)^4} \left(\prod_{\substack{i<j \\ i,j\neq 5}}^{6} (x_j - x_i)^{2/\kappa} \right) \left(\prod_{k\neq 5}^{6} |x_5 - x_k|^{1-6/\kappa} \right)$$
$$\times [nI_{25} - I_{15} - I_{35}](\kappa \,|\, x_1, x_2, \ldots, x_6). \quad (28)$$

If $\kappa \in (0, 4]$, then the improper integrals in (28) diverge, and we regularize them via the replacement (16).

Presently, the formula (28) for Π_1 is a well-motivated guess. To prove that it is indeed correct, we must verify the duality condition (10) for $\vartheta = 1$ and all $\varsigma \in \{1, 2, 3, 4, 5\}$. We begin with $\varsigma = 1$. By the preceding paragraph, $\bar{\ell}_1 \Pi_1$ (8) with $i = 2$ gives the rectangle connectivity weight (24), and thanks to (20), this is sufficient to confirm the duality condition (10) for $\varsigma = 1$. For all other ς, we note that the polygon diagram for $[\mathscr{L}_\varsigma]$ has an arc whose two endpoints correspond with the endpoints of either (x_1, x_2), (x_3, x_4), or (x_5, x_6). As such, to compute $[\mathscr{L}_\varsigma]\Pi_1$, we may take the limit (8) respectively with $i = 1$, $i = 3$, or $i = 5$ first. But because all of these intervals are two-leg intervals of Π_1, these limits, and therefore $[\mathscr{L}_\varsigma]$, annihilate Π_1, confirming the duality condition (10) for $\varsigma \in \{2, 3, 4, 5\}$.

Next, we find a formula for Π_2 in the form of (6) with $N = 3$. After choosing $c = 5$, we determine the two integration contours of (7) for use in this formula. Figure 10 shows the polygon diagram for Π_2, and from this diagram and item I above, it is apparent that (x_1, x_2), (x_2, x_3), (x_4, x_5), and (x_5, x_6) are two-leg intervals of Π_2. Hence, following item b above, we entwine x_5 and x_6 with a Pochhammer contour $\Gamma_1 = \mathscr{P}(x_5, x_6)$. Moreover, item a above requires that no integration contour crosses (x_1, x_2) or (x_2, x_3). In order to satisfy item a, we entwine x_4 and Γ_1 with a Pochhammer contour Γ_2. These choices of integration contours determine the formula for Π_2 up to normalization.

Assuming that $\kappa \in (4, 8)$, we decompose the Coulomb gas integral (7) of Π_2, with Γ_1 and Γ_2 as specified, into a linear combination of the simpler definite integrals of type (26). Specifically, we replace Γ_1 by an integration along $[x_5, x_6]$ (figure 6), freeze u_1 somewhere within (x_5, x_6), and decompose the integration along Γ_2 into (figure 7)
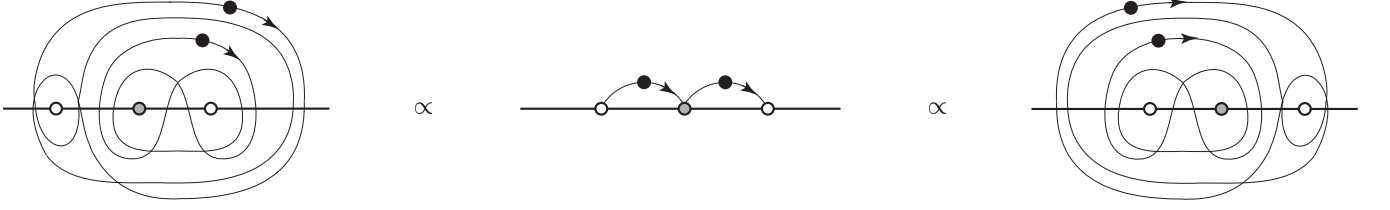
FIG. 12: Integration around the above nested pair of Pochhammer contours (left, right) is proportional to performing the first integration along the right interval and the second integration along the left interval (middle). The gray circle is x_c in (7).

$$e^{4\pi i/\kappa} J_{x_4}^{x_5} + e^{-8\pi i/\kappa} J_{x_5}^{u_1} + e^{-16\pi i/\kappa} J_{u_1}^{x_6} - e^{-28\pi i/\kappa} J_{x_4}^{x_5} - e^{-16\pi i/\kappa} J_{x_5}^{u_1} - e^{-8\pi i/\kappa} J_{u_1}^{x_6}$$
$$+ e^{-36\pi i/\kappa} J_{x_4}^{x_5} + e^{-24\pi i/\kappa} J_{x_5}^{u_1} + e^{-16\pi i/\kappa} J_{u_1}^{x_6} - e^{-4\pi i/\kappa} J_{x_4}^{x_5} - e^{-16\pi i/\kappa} J_{x_5}^{u_1} - e^{-24\pi i/\kappa} J_{u_1}^{x_6}, \quad (29)$$

where J_a^b is the magnitude of the integrand of I_{ij} (26) with $x_5 < u_1 < x_6$ and with u_2 integrated from a to b. We factor (29) into

$$2i \sin\left(\frac{4\pi}{\kappa}\right)(1 - e^{-32\pi i/\kappa})J_{x_4}^{x_5} + (e^{-8\pi i/\kappa} - 2e^{-16/\pi i/\kappa} + e^{-24\pi i/\kappa})(J_{x_5}^{u_1} - J_{u_1}^{x_6}). \quad (30)$$

Now, the integrations of $J_{x_5}^{u_1}$ and $J_{u_1}^{x_6}$ with respect to u_1 along $[x_5, x_6]$ are equal because their integrands exchange under the switch $(u_1, u_2) \mapsto (u_2, u_1)$. Integrating u_1 along $[x_5, x_6]$ in (30) therefore gives (figure 12)

$$\mathcal{J}(\Gamma_1, \Gamma_2) \propto I_{45}. \quad (31)$$

After inserting the decomposition (31) into (6), we find the proper normalization for the resulting formula by requiring that the limit (8) with $i = 3$ equals the rectangle connectivity weight (24) with $(x_3, x_4) \mapsto (x_5, x_6)$. Upon using the results of section A 3 in [8] (figure 8) with the decomposition (31) (figure 12) to determine the asymptotic behavior of $\mathcal{J}(\Gamma_1, \Gamma_2)$ as $x_4 \to x_3$, we find

$$\Pi_2(\kappa \,|\, x_1, x_2, \ldots, x_6) = n(\kappa)^2 \frac{\Gamma(2 - 8/\kappa)^2}{\Gamma(1 - 4/\kappa)^4} \left(\prod_{\substack{i<j \\ i,j\neq 5}}^6 (x_j - x_i)^{2/\kappa}\right)\left(\prod_{k\neq 5}^6 |x_5 - x_k|^{1-6/\kappa}\right) I_{45}(\kappa \,|\, x_1, x_2, \ldots, x_6). \quad (32)$$

If $\kappa \in (0, 4]$, then the improper integral in (32) diverges, and we regularize it via the replacement (16).

Presently, the formula (32) for Π_2 is a well-motivated guess. To prove that it is indeed correct, we must verify the duality condition (10) for $\vartheta = 2$ and all $\varsigma \in \{1, 2, 3, 4, 5\}$. We first note that (x_4, x_5) is indeed a two-leg interval of Π_2 thanks to the symmetry property of the decomposition (31) shown in figure 12. Then the verification proceeds similarly to that for Π_1 (28) above. Section II E generalizes this particular connectivity weight formula to arbitrary $N \in \mathbb{Z}^+ + 1$.

The formulas (28, 32) found for Π_1 and Π_2 respectively are singular at any $\kappa \in (0, 8) \times i\mathbb{R}$ such that $8/\kappa \in \mathbb{Z}^+ + 1$ or $12/\kappa \in \mathbb{Z}^+ + 1$. Also, the formula (28) for Π_1 is singular at any κ such that $n(\kappa)^2 = 2$ (21), and both formulas appear to vanish if $n(\kappa) = 0$ (that is, if $8/\kappa \in 2\mathbb{Z}^+ + 1$). Because section III of [9] shows that Π_1 and Π_2 are continuous functions of κ, these singularities must be removable. Furthermore, because they are elements of a basis, there is no $\kappa \in (0, 8)$, including those with $n(\kappa) = 0$, such that $\Pi_1(\kappa)$ or $\Pi_2(\kappa)$ vanish for all $\boldsymbol{x} \in \Omega_0$. Although we already know these facts, it is interesting to verify them directly from the formulas themselves, which we do in Appendix A.

D. Connectivity weights in octagons ($N = 4$)

According to item 1 of the introduction I, the dimension of the solution space $\mathcal{S}_4$ for the system (2, 3) is $C_4 = 14$ (5), so there are fourteen connectivity weights $\Pi_1, \Pi_2, \ldots, \Pi_{14}$ that span $\mathcal{S}_4$. These connectivity weights sort into three disjoint sets, with the diagrams in each set identical up to a rotation. Hence, we find formulas for only three connectivity weights Π_1, Π_2, and Π_3 shown in figure 13, one per set. An appropriate transformation then gives the formulas for the other weights.
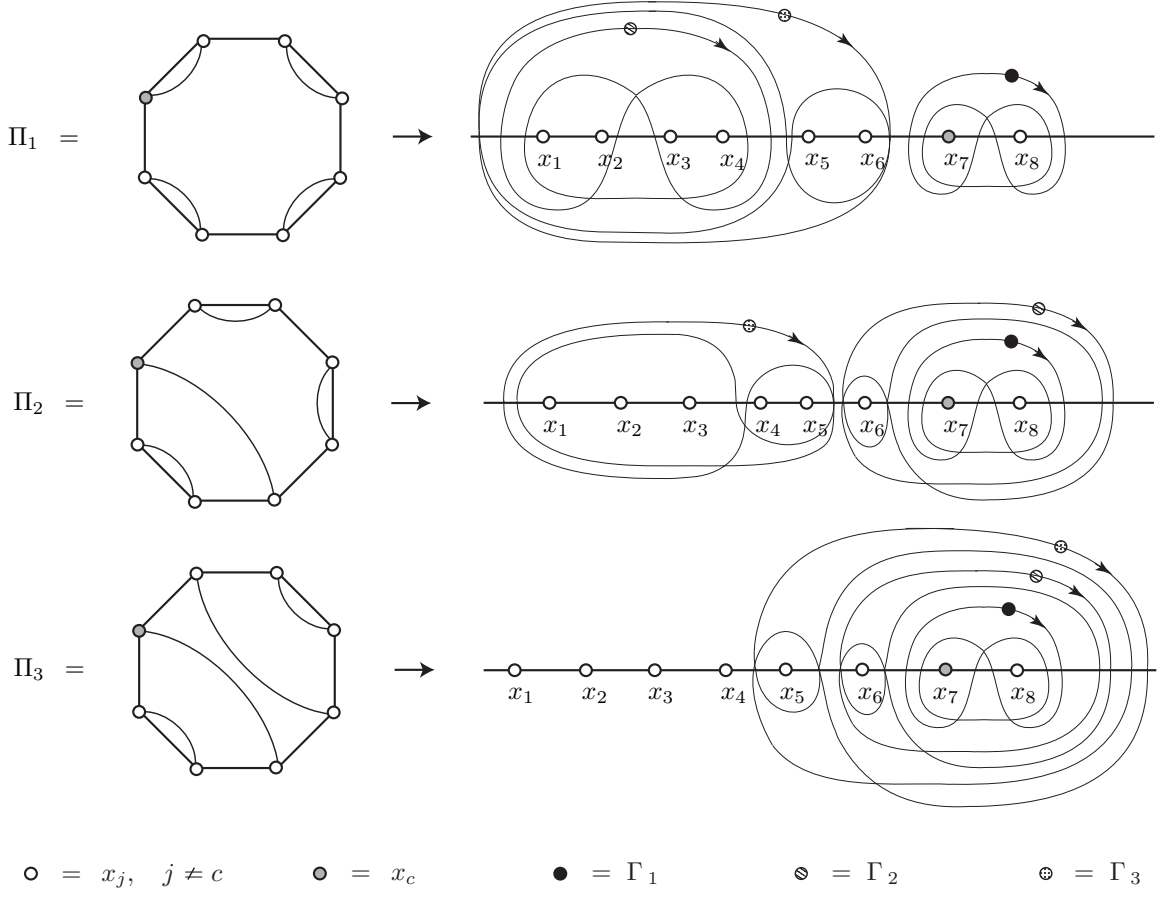
FIG. 13: The three topologically distinct octagon connectivities, and integration contours for their weights with $c = 7$. Moving counterclockwise around the hexagon corresponds to moving right along the real axis, with the bottom-left vertex sent to x_1. In (45), we note that Π_1 (46) does not exactly correspond with the collection of integration contours for "Π_0" (42) to its right.

Here, we first find a formula for Π_2 in the form of (6) with $N = 4$. After choosing $c = 7$, we determine the three integration contours of (7) for use in this formula. Figure 13 shows the polygon diagram for Π_2, and from this diagram and item I above, it is apparent that (x_1, x_2), (x_2, x_3), (x_4, x_5), (x_6, x_7), and (x_7, x_8) are two-leg intervals of Π_2. Hence, following item b above, we entwine x_7 and x_8 with a Pochhammer contour $\Gamma_1 = \mathscr{P}(x_7, x_8)$. Furthermore, the formula for the second hexagon connectivity weight (32) suggests that we entwine Γ_1 and x_6 with another Pochhammer contour Γ_2 in order for (x_6, x_7) to be a two-leg interval of Π_2 as well. Finally, item a above suggests that no integration contour crosses the other two-leg intervals. In order to satisfy item a, we entwine $[x_1, x_3]$ and $[x_4, x_5]$ with a Pochhammer contour Γ_3. These choices of integration contours determine the formula for Π_2 up to normalization.

Assuming that $\kappa \in (4, 8)$, we decompose the Coulomb gas integral (7) of Π_2, with Γ_1, Γ_2, and Γ_3 as specified, into a linear combination of the simpler definite integrals

$$
\begin{aligned}
i \neq j \neq k: \quad & I_{ijk}(\kappa \,|\, x_1, x_2, \ldots, x_8) := \mathcal{J}\Big(\kappa \,\Big|\, [x_i, x_{i+1}], [x_j, x_{j+1}], [x_k, x_{k+1}] \,\Big|\, x_1, x_2, \ldots, x_8\Big), \quad && c = 7, \quad N = 4, \\
i = j \neq k: \quad & I_{iik}(\kappa \,|\, x_1, x_2, \ldots, x_8) := \mathcal{J}\Big(\kappa \,\Big|\, [x_i, u_2], [x_i, x_{i+1}], [x_k, x_{k+1}] \,\Big|\, x_1, x_2, \ldots, x_8\Big). && i, j, k < 2N.
\end{aligned}
\tag{33}
$$

In the definition for I_{iik} on the bottom line of (33), the right endpoint of the first contour $[x_i, u_2]$ is the second integration variable u_2, integrated after the first (u_1). We implicitly order the differences in the factors of the integrand in (7) such that (33) is positive-valued. Figure 12 shows that integration over the nested pair $\Gamma_2 \times \Gamma_1$ decomposes into integration along $[x_6, x_7] \times [x_7, x_8]$ (section II C). Using this fact and then decomposing the integration along Γ_3

into integrations along line segments similar to what figure 11 shows, we find

$$
\mathcal{J}(\kappa \,|\, \Gamma_1, \Gamma_2, \Gamma_3) \propto
\left\{
\begin{array}{l}
+\, e^{4\pi i/\kappa} I_{167} + e^{8\pi i/\kappa} I_{267} + e^{12\pi i/\kappa} I_{367} + e^{16\pi i/\kappa} I_{467} \\[4pt]
-\, e^{20\pi i/\kappa} I_{167} - e^{24\pi i/\kappa} I_{267} - e^{28\pi i/\kappa} I_{367} - e^{24\pi i/\kappa} I_{467} \\[4pt]
+\, e^{12\pi i/\kappa} I_{167} + e^{8\pi i/\kappa} I_{267} + e^{4\pi i/\kappa} I_{367} + I_{467} \\[4pt]
-\, e^{-4\pi i/\kappa} I_{167} - e^{-8\pi i/\kappa} I_{267} - e^{-12\pi i/\kappa} I_{367} - e^{-8\pi i/\kappa} I_{467}
\end{array}
\right\} (\kappa)
$$
$$
= e^{8\pi i/\kappa} (n(\kappa)^2 - 4)[n(I_{167} - n I_{267}) + (n^2 - 1)(n I_{367} - I_{467})](\kappa). \tag{34}
$$

After inserting (34) into (6), we find the proper normalization for the resulting formula by requiring that the limit (8) with $i = 3$ equals the second hexagon connectivity weight (32) with $(x_3, x_4, x_5, x_6) \mapsto (x_5, x_6, x_7, x_8)$. Upon using the results of sections A 2 and A 3 in [8] (figure 8) with the decomposition (34) to determine the asymptotic behavior of $\mathcal{J}(\Gamma_1, \Gamma_2, \Gamma_3)$ as $x_4 \to x_3$, we find

$$
\Pi_2(\kappa \,|\, x_1, x_2, \ldots, x_8) = \frac{n(\kappa)^3}{n(\kappa)^4 - 3n(\kappa)^2 + 1} \frac{\Gamma(2 - 8/\kappa)^3}{\Gamma(1 - 4/\kappa)^6} \left(\prod_{\substack{i < j \\ i, j \neq 7}}^{8} (x_j - x_i)^{2/\kappa} \right) \left(\prod_{k \neq 7}^{8} |x_7 - x_k|^{1 - 6/\kappa} \right)
$$
$$
\times [n(I_{167} - n I_{267}) + (n^2 - 1)(n I_{367} - I_{467})](\kappa \,|\, x_1, x_2, \ldots, x_8). \tag{35}
$$

If $\kappa \in (0, 4]$, then the improper integrals in (35) diverge, and we regularize them via the replacement (16).

Presently, the formula (35) for Π_2 is a well-motivated guess. To prove that it is indeed correct, we must verify the duality condition (10) for $\vartheta = 2$ and all $\varsigma \in \{1, 2, \ldots, 14\}$. We begin with $\varsigma = 2$. By the preceding paragraph, $\bar{\ell}_1 \Pi_2$ (8) with $i = 3$ gives the hexagon connectivity weight (32), and thanks to (20), this is sufficient to confirm the duality condition (10) for $\varsigma = 2$. For all other ς, we note that the polygon diagram for $[\mathscr{L}_\varsigma]$ has an arc whose two endpoints correspond with the endpoints of either (x_1, x_2), (x_2, x_3), (x_4, x_5), (x_6, x_7), or (x_7, x_8). As such, to compute $[\mathscr{L}_\varsigma]\Pi_2$, we may take the limit (8) respectively with $i = 1$, $i = 2$, $i = 4$, $i = 6$, or $i = 7$ first. However, all of (x_1, x_2), (x_2, x_3), (x_4, x_5), and (x_7, x_8) are two-leg intervals of Π_2. Indeed, this follows from item a and figure 13 above. Furthermore, (x_6, x_7) is a two-leg interval of Π_2, and this is manifest from item b above and the right illustration of figure 12. Thus, these limits, and therefore $[\mathscr{L}_\varsigma]$, annihilate Π_2, confirming the duality condition (10) for $\varsigma \in \{1, 3, 4, \ldots, 14\}$.

Next, we find a formula for Π_3 in the form of (6) with $N = 4$. After choosing $c = 7$, we determine the three integration contours of (7) for use in this formula. Figure 13 shows the polygon diagram for Π_3, and from this diagram and item I above, it is apparent that (x_1, x_2), (x_2, x_3), (x_3, x_4), (x_5, x_6), (x_6, x_7), and (x_7, x_8) are two-leg intervals of Π_3. Hence, following item b above, we entwine x_7 and x_8 with a Pochhammer contour $\Gamma_1 = \mathscr{P}(x_7, x_8)$. Furthermore, the formula for the second hexagon connectivity weight (32) and figure 12 suggest that we entwine Γ_1 and x_6 with another Pochhammer contour Γ_2 in order for (x_6, x_7) to be a two-leg interval of Π_3 as well. Finally, item a above suggests that no integration contour crosses the other two-leg intervals. In order to satisfy item a, we entwine x_5 and Γ_2 with a Pochhammer contour Γ_3. These choices of integration contours determine the formula for Π_3 up to normalization.

Assuming that $\kappa \in (4, 8)$, we decompose the Coulomb gas integral (7) of Π_3, with Γ_1, Γ_2, and Γ_3 as specified, into a linear combination of the simpler definite integrals of type (33). Figure 12 shows that the integration over the nested pair $\Gamma_2 \times \Gamma_1$ decomposes into integration along $[x_6, x_7] \times [x_7, x_8]$. After inserting that decomposition into the Coulomb gas integral $\mathcal{J}(\Gamma_1, \Gamma_2, \Gamma_3)$, we freeze u_1 and u_2 at locations within (x_7, x_8) and (x_6, x_7) respectively, and we
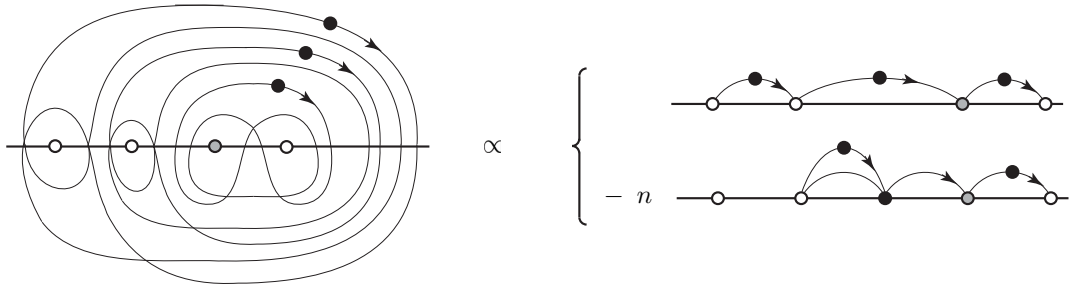

FIG. 14: Integration around the three nested Pochhammer contours on the left is proportional to the difference of the two integrations on the right. The gray circle is x_c in (7).

decompose the integration along Γ_3 into

$$
\begin{aligned}
&+ e^{4\pi i/\kappa} J_{x_5}^{x_6} + e^{8\pi i/\kappa} J_{x_6}^{u_2} + J_{u_2}^{x_7} + e^{-12\pi i/\kappa} J_{x_7}^{u_1} + e^{-20\pi i/\kappa} J_{u_1}^{x_8} \\
&- e^{-36\pi i/\kappa} J_{x_5}^{x_6} - e^{-40\pi i/\kappa} J_{x_6}^{u_2} - e^{-32\pi i/\kappa} J_{u_2}^{x_7} - e^{-20\pi i/\kappa} J_{x_7}^{u_1} - e^{-12\pi i/\kappa} J_{u_1}^{x_8} \\
&+ e^{-44\pi i/\kappa} J_{x_5}^{x_6} + e^{-48\pi i/\kappa} J_{x_6}^{u_2} + e^{-40\pi i/\kappa} J_{u_2}^{x_7} + e^{-28\pi i/\kappa} J_{x_7}^{u_1} + e^{-20\pi i/\kappa} J_{u_1}^{x_8} \\
&- e^{-4\pi i/\kappa} J_{x_5}^{x_6} - J_{x_6}^{u_2} - e^{-8\pi i/\kappa} J_{u_2}^{x_7} - e^{-20\pi i/\kappa} J_{x_7}^{u_1} - e^{-28\pi i/\kappa} J_{u_1}^{x_8}
\end{aligned}
\tag{36}
$$

where J_a^b is the magnitude of the integrand of I_{i67} (33) with $x_7 < u_1 < x_8$ and $x_6 < u_2 < x_7$ and with u_3 integrated from a to b. We may factor (36) into

$$
2i \sin\left(\frac{4\pi}{\kappa}\right) [(1 - e^{-40\pi i/\kappa})J_{x_5}^{x_6} + (1 - e^{-40\pi i/\kappa})(e^{4\pi i/\kappa} + e^{-4\pi i/\kappa})J_{x_6}^{u_2}
$$
$$
+ (e^{-4\pi i/\kappa} - e^{-36\pi i/\kappa})(J_{u_2}^{x_7} - J_{x_6}^{u_2}) + (e^{-16\pi i/\kappa} - e^{-24\pi i/\kappa})(J_{x_7}^{u_1} - J_{u_1}^{x_8})]. \tag{37}
$$

Now, the integrations of $J_{x_7}^{u_1}$ and $J_{u_1}^{x_8}$ (resp. $J_{u_2}^{x_7}$ and $J_{x_6}^{u_2}$) with respect to u_1 along $[x_7, x_8]$ (resp. u_2 along $[x_6, x_7]$) are equal because their integrands exchange under the switch $(u_1, u_3) \mapsto (u_3, u_1)$ (resp. $(u_2, u_3) \mapsto (u_3, u_2)$). Integrating u_1 and u_2 along $[x_7, x_8]$ and $[x_6, x_7]$ respectively in (37) therefore gives (figure 14)

$$
\mathcal{J}(\Gamma_1, \Gamma_2, \Gamma_3) \propto I_{567} - n I_{667}. \tag{38}
$$

After inserting the decomposition (38) into (6), we find the proper normalization for the resulting formula by requiring that the limit (8) with $i = 4$ equals the second hexagon connectivity weight (32) with $(x_4, x_5, x_6) \mapsto (x_6, x_7, x_8)$. Upon using the results of section A 3 in [8] (figure 8) with the decomposition (38) (figure 14) to determine the asymptotic behavior of $\mathcal{J}(\Gamma_1, \Gamma_2, \Gamma_3)$ as $x_5 \to x_4$, we find

$$
\Pi_3(\kappa \,|\, x_1, x_2, \ldots, x_8) = n(\kappa)^3 \frac{\Gamma(2 - 8/\kappa)^3}{\Gamma(1 - 4/\kappa)^6} \left(\prod_{\substack{i<j \\ i,j \neq 7}}^{8} (x_j - x_i)^{2/\kappa} \right)
$$
$$
\times \left(\prod_{k \neq 7}^{8} |x_7 - x_k|^{1 - 6/\kappa} \right) [I_{567} - n I_{667}](\kappa \,|\, x_1, x_2, \ldots, x_8). \tag{39}
$$

If $\kappa \in (0, 4]$, then the improper integrals in (39) diverge, and we regularize them via the replacement (16).

Presently, the formula (39) for Π_3 is a well-motivated guess. To prove that it is indeed correct, we must verify the duality condition (10) for $\vartheta = 3$ and all $\varsigma \in \{1, 2, \ldots, 14\}$. This proceeds along the same lines as that for Π_2 (35) above. Section II E generalizes this particular connectivity weight formula to arbitrary $N \in \mathbb{Z}^+ + 1$.

Finally, we seek a formula for Π_1 in the form of (6) with $N = 4$. After choosing $c = 7$, we determine the three integration contours of (7) for use in this formula. Figure 13 shows the polygon diagram for Π_1, and from this diagram and item I above, it is apparent that (x_1, x_2), (x_3, x_4), (x_5, x_6), and (x_7, x_8) are two-leg intervals of Π_1. Hence, following item b above, we entwine x_7 and x_8 with a Pochhammer contour $\Gamma_1 = \mathscr{P}(x_7, x_8)$. Moreover, item a above requires that no integration contour crosses the other two-leg intervals. In order to satisfy item a, the formula for the first hexagon connectivity weight (28) (figure 10) suggests that we entwine (x_1, x_2) and (x_3, x_4) with a Pochhammer contour Γ_2 and that we entwine (x_5, x_6) and Γ_2 with another contour Γ_3. These choices of integration contours determine the prospective formula for Π_1 up to normalization.
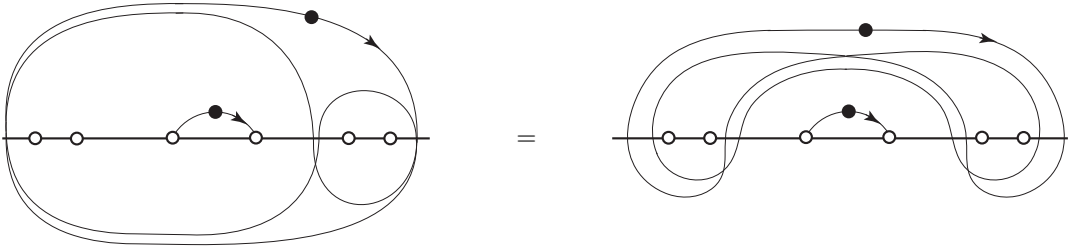

FIG. 15: The first octagon connectivity weight has a Pochhammer contour Γ_2 nested in another Γ_3 (figure 13). We decompose Γ_2 into three segments (figure 11), one shown on the left, and we deform Γ_3 (figure 16) so it does not surround those segments.
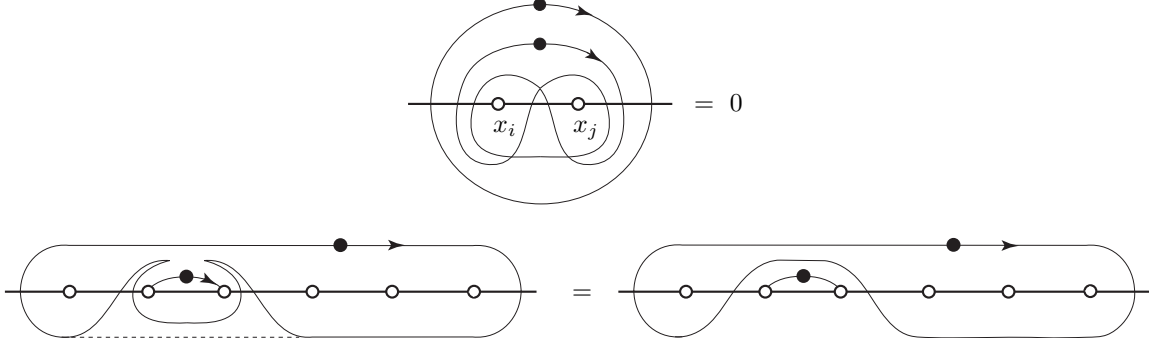
FIG. 16: Integrating (7) around an elementary Pochhammer contour $\mathscr{P}(x_i, x_j)$ (or line segment $[x_i, x_j]$) with $i, j \neq c$ and then around a loop that tightly wraps around $\mathscr{P}(x_i, x_j)$ gives zero. Thus, we may deform an integration contour through $\mathscr{P}(x_i, x_j)$.

Assuming that $\kappa \in (4, 8)$, we decompose the Coulomb gas integral (7) of Π_1, with Γ_1, Γ_2, and Γ_3 as specified, into a linear combination of the simpler definite integrals of type (33). Specifically, we replace Γ_1 with an integration along $[x_5, x_6]$ (figure 6) and decompose the integration along Γ_2 into integrations along $[x_1, x_2]$, $[x_2, x_3]$, and $[x_3, x_4]$, just as we did for first the hexagon connectivity weight (28) (figure 11). We call the corresponding terms in the decomposition the "first term," the "second term," and the "third term" respectively. The left illustration of figure 15 shows the contours $[x_3, x_4]$ and Γ_3 for the third term. Now, to decompose Γ_3 into simple contours, we recall identity (B1) from appendix B of [8]. This identity says that if Γ is a line segment or an elementary Pochhammer contour with endpoints at $x_i < x_j$, if $i, j \neq c$, and if Γ_0 is a simple loop surrounding Γ, then (top illustration of figure 16)

$$\int_\Gamma \oint_{\Gamma_0} [\ldots \text{ the integrand of } \mathcal{J} \text{ (7) } \ldots] \, \mathrm{d}u_2 \, \mathrm{d}u_1 = 0. \tag{40}$$

Using identity (40), we deform Γ_3 such that it no longer surrounds the contour originally inside it (bottom illustration of figure 16). After this deformation, Γ_3 entwines $[x_3, x_4]$ (resp. $\{x_1, x_4\}$, resp. $[x_1, x_2]$) and $[x_5, x_6]$ together in the first (resp. second, resp. third) term. For example, the right illustration of figure 15 shows the contours $[x_3, x_4]$ and Γ_3 for the third term after this deformation. Next, we decompose Γ_3 in the same way that we decomposed Γ_2 for

FIG. 17: The decomposition (41) of $\mathcal{J}(\Gamma_1, \Gamma_2, \Gamma_3)$ into nine terms (boxed), and the calculation of the limits (43, 44) using figure 8 (with Gamma functions dropped). Course-dashed (resp. fine-dashed) arcs join the points brought together by $\mathscr{L}_3$ (resp. $\mathscr{L}_1$).

each of the three terms (figure 11). In so doing, we find nine terms in total, illustrated in the boxed part of figure 17. Some of these terms have an integration contour that arcs over another integration contour, and by decomposing that outer contour as figure 18 shows, we ultimately find

$$\mathcal{J}(\Gamma_1, \Gamma_2, \Gamma_3) \propto I_{357} - nI_{347} + n^2 I_{337} - 2nI_{237} + 2I_{137} - nI_{257} + n^2 I_{247} + n^2 I_{227} - nI_{127} + I_{157} - nI_{147}. \tag{41}$$

After inserting the decomposition (41) into (6), we find the proper normalization for the resulting formula by requiring that the limit (8) with $i = 2$ equals the first hexagon connectivity weight (28) with $(x_2, x_3, x_4, x_5, x_6) \mapsto (x_4, x_5, x_6, x_7, x_8)$. Upon using the results of sections A 2–A 4 in [8] (figure 8) with the boxed decomposition of figure 17 to determine the asymptotic behavior of $\mathcal{J}(\Gamma_1, \Gamma_2, \Gamma_3)$ as $x_3 \to x_2$, we find the function

$$\Pi_0(\kappa \,|\, x_1, x_2, \ldots, x_8) = \frac{n(\kappa)^3}{[n(\kappa)^2 - 2]^2} \frac{\Gamma(2 - 8/\kappa)^3}{\Gamma(1 - 4/\kappa)^6} \left(\prod_{\substack{i < j \\ i, j \neq 7}}^{8} (x_j - x_i)^{2/\kappa} \right) \left(\prod_{k \neq 7}^{8} |x_7 - x_k|^{1 - 6/\kappa} \right)$$

$$\times [I_{357} - nI_{347} + n^2 I_{337} - 2nI_{237} + 2I_{137} - nI_{257}$$
$$+ n^2 I_{247} + n^2 I_{227} - nI_{127} + I_{157} - nI_{147}](\kappa \,|\, x_1, x_2, \ldots, x_8). \tag{42}$$

While it is a well-motivated guess, the function Π_0 (42) is unfortunately not the connectivity weight Π_1 we seek. Indeed, the identification of Π_1 with the collection of integration contours in the top illustration of figure 13 is incomplete. More terms must be added to generate a formula for Π_1. Perhaps this is not surprising, for to satisfy the various two-leg interval conditions for Π_1, we could have just as well entwined $[x_3, x_4]$ and $[x_5, x_6]$ together with a Pochhammer contour Γ_2 and entwined $[x_1, x_2]$ and Γ_2 together with another Pochhammer contour Γ_3. As one might suspect, this seemingly equally valid choice of integration contours yields a different function. Furthermore, neither it nor Π_0 gives a formula for Π_1.

Fortunately, however, Π_0 needs only a small correction to give a formula for Π_1. To find this correction, we act on both sides of (42) with $[\mathscr{L}_\varsigma]$ for each $\varsigma \in \{1, 2, \ldots, 14\}$, beginning with $\varsigma = 1$. Above, we note that $\bar{\ell}_1 \Pi_1$ (8) with $i = 2$ gives the hexagon connectivity weight (28), and thanks to (20), this is sufficient to confirm that $[\mathscr{L}_1] \Pi_0 = 1$. For all other $\varsigma \in \{2, 3, 4, \ldots, 14\}$, we note that the polygon diagrams for all but two of the $[\mathscr{L}_\varsigma]$ with $\varsigma \geq 2$ has an arc whose two endpoints correspond with the endpoints of either (x_1, x_2), (x_3, x_4), (x_5, x_6), or (x_7, x_8). Because all of these intervals are two-leg intervals of Π_0, these $[\mathscr{L}_\varsigma]$ annihilate Π_0, confirming the duality condition (10) for these particular ς. The only two $[\mathscr{L}_\varsigma]$ with $\varsigma \geq 2$ whose polygon diagram has no such arc are $[\mathscr{L}_3]$, whose polygon diagram matches that of Π_3 in figure 13, and the equivalence class, call it $[\mathscr{L}_4]$, whose polygon diagram we obtain by rotating that for $[\mathscr{L}_3]$ by $\pi/2$ radians.

It is easy to show that $[\mathscr{L}_4]$ annihilates Π_0. Indeed, we may choose an element $\mathscr{L}_4 \in [\mathscr{L}_4]$ whose first limit is (8) with $i = 2$ and whose next limit is (8) with $i = 1$ and $i + 1 \mapsto 4$. Above (42), we note that the first limit sends Π_0 to the first hexagon connectivity weight (28) with $(x_2, x_3, x_4, x_5, x_6) \mapsto (x_4, x_5, x_6, x_7, x_8)$. Because (x_1, x_4) is a two-leg interval of this new weight, the next limit, and therefore $[\mathscr{L}_4]$, annihilates Π_0 altogether.

Next, we show that $[\mathscr{L}_3]$ does not annihilate Π_0, which is the main feature of Π_0 that distinguishes it from Π_1. The boxed part of figure 17 shows the decomposition (41) of the Coulomb gas integral $\mathcal{J}(\Gamma_1, \Gamma_2, \Gamma_3)$ (7), and the part of this figure beneath the boxed area shows the calculation of $\mathscr{L}_3\{n^{-3}(n^2 - 2)^2 \Pi_0\}$ and $\mathscr{L}_1\{n^{-3}(n^2 - 2)^2 \Pi_0\}$, where $\mathscr{L}_3$ and $\mathscr{L}_1$ are allowable sequences of limits whose respective equivalence classes $[\mathscr{L}_3]$ and $[\mathscr{L}_1]$ are the only two that do not annihilate Π_0. Their actions are respectively given by

$$\mathscr{L}_3\{n^{-3}(n^2 - 2)^2 \Pi_0\}(\kappa) = \lim_{x_7 \to x_2} \lim_{R \to \infty} \lim_{x_6 \to x_3} \lim_{x_5 \to x_4} [(x_7 - x_2)(2R)(x_6 - x_3)(x_5 - x_4)]^{6/\kappa - 1}$$
$$\times \; n(\kappa)^{-3}[n(\kappa)^2 - 2]^2 \, \Pi_0(\kappa \,|\, x_1 = -R, x_2, x_3, x_4, x_5, x_6, x_7, x_8 = R), \tag{43}$$
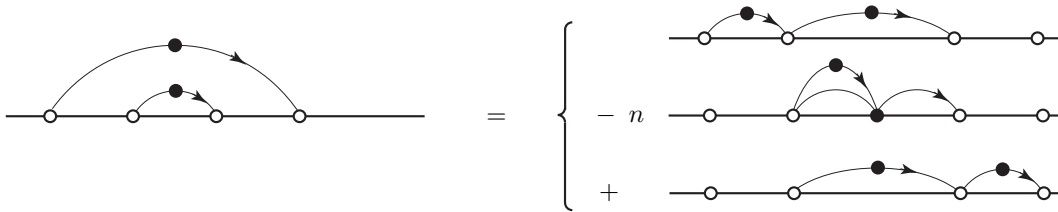

FIG. 18: Integration along the pair of nested contours shown on the left equals the sum of integrations shown on the right. We use this identity to decompose the two terms in the boxed part of figure 17 that have nested contours, ultimately finding (41).

$$\mathscr{L}_1\{n^{-3}(n^2-2)^2\Pi_0\}(\kappa) = \lim_{x_7\to x_6}\lim_{R\to\infty}\lim_{x_3\to x_2}\lim_{x_5\to x_4}[(x_7-x_6)(2R)(x_3-x_2)(x_5-x_4)]^{6/\kappa-1}$$
$$\times\ n(\kappa)^{-3}[n(\kappa)^2-2]^2\,\Pi_0(\kappa\,|\,x_1=-R,x_2,x_3,x_4,x_5,x_6,x_7,x_8=R). \tag{44}$$

With the help of figure 17 and figure 8, we may find the limits (43, 44). Now with the image of Π_0 under all fourteen equivalence classes $[\mathscr{L}_\varsigma]\in\mathscr{B}_4^*$ known, (12) gives the decomposition of Π_0 over $\mathscr{B}_4$. The result is

$$\mathscr{L}_\varsigma\{n^{-3}(n^2-2)^2\Pi_0\} = \left\{\begin{array}{ll} n^{-3}(n^2-2)^2, & \varsigma=1 \\ n^{-2}(n^2-2), & \varsigma=3 \\ 0, & \varsigma\in\{2,4,5,\ldots,14\} \end{array}\right\} \implies \Pi_0=\Pi_1+\left(\frac{n}{n^2-2}\right)\Pi_3. \tag{45}$$

Finally, upon isolating Π_1 from (45) and substituting the formulas (42) and (39) for Π_0 and Π_3 respectively into the result, we find

$$\Pi_1(\kappa\,|\,x_1,x_2,\ldots,x_8) = \frac{n(\kappa)^3}{[n(\kappa)^2-2]^2}\frac{\Gamma(2-8/\kappa)^3}{\Gamma(1-4/\kappa)^6}\left(\prod_{\substack{i<j\\i,j\neq7}}^{8}(x_j-x_i)^{2/\kappa}\right)\left(\prod_{k\neq7}^{8}|x_7-x_k|^{1-6/\kappa}\right)$$
$$\times[I_{357}-nI_{347}+n^2I_{337}-2nI_{237}+2I_{137}-nI_{257}+n^2I_{247}+n^2I_{227}$$
$$-nI_{127}+I_{157}-nI_{147}-(n^2-2)(nI_{567}-n^2I_{667})](\kappa\,|\,x_1,x_2,\ldots,x_8). \tag{46}$$

If $\kappa\in(0,4]$, then the improper integrals in (46) diverge, and we regularize them via the replacement (16).

The formulas (35, 39, 46) found for Π_2, Π_3, and Π_1 respectively are singular at any $\kappa\in(0,8)\times i\mathbb{R}$ such that $8/\kappa\in\mathbb{Z}^++1$ or $12/\kappa\in\mathbb{Z}^++1$. Also, the formula (35) for Π_2 is singular at any κ such that $n(\kappa)^4-3n(\kappa)^2+1=0$, the formula (46) for Π_1 is singular at any κ such that $n(\kappa)^2=2$ (21), and all three formulas appear to vanish if $n(\kappa)=0$ (that is, if $8/\kappa\in2\mathbb{Z}^++1$). Because section III of [9] shows that Π_1, Π_2, and Π_3 are continuous functions of κ, these singularities must be removable. Furthermore, because they are elements of a basis, there is no $\kappa\in(0,8)$, including those with $n(\kappa)=0$, such that $\Pi_1(\kappa)$ or $\Pi_2(\kappa)$ or $\Pi_3(\kappa)$ vanish for all $\boldsymbol{x}\in\Omega_0$. Although we already know these facts, it is interesting to verify them directly from the formulas themselves, which we do in appendix A.

E. Rainbow connectivity weights for arbitrary N

For $N>4$, correctly guessing a collection of integration contours for (6) that gives a formula for some connectivity weight is generally difficult. However, among the C_N connectivity weights that span $\mathcal{S}_N$, there is a set of N weights that we may always determine explicitly. (This explicit formula, however, is not always in the form of (18, 19), that is, in terms of integrations along line segments or elementary Pochhammer contours.) The polygon diagram for one of these, denoted Π_{N-1}, has an arc with its endpoints at the jth vertex and the $(2N-j+1)$th vertex of the polygon for all $j\in\{1,2,\ldots,N\}$, and the polygon diagrams for the other $N-1$ weights follow from rotating the diagram for Π_{N-1}. After continuously mapping the polygon diagram for Π_{N-1} onto the upper half-plane, we see that the image of the jth arc joins x_j with x_{2N-j+1} and that the collection of N arcs sequentially nest each other in the upper half-plane to form a rainbow (figure 19). For this reason, we call this polygon diagram (and the others generated by rotating it) a *rainbow diagram* [41], and we call its associated connectivity weight a *rainbow connectivity weight* [8].
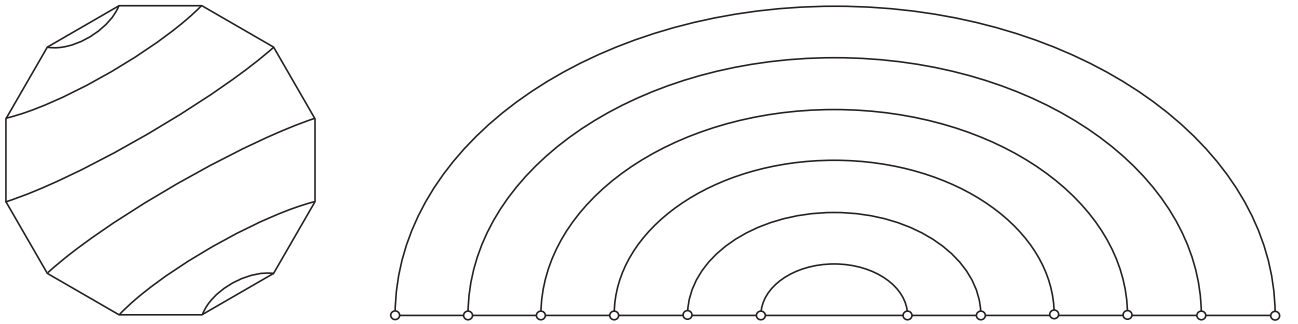

FIG. 19: The $N=6$ rainbow diagram (left) for the connectivity weight $\Pi_5\in\mathscr{B}_6$, and its image under a conformal map onto the upper half-plane (right). Each but the middle interval and the outer interval containing infinity is a two-leg interval of Π_5.

As usual, we find an explicit formula only for Π_{N-1}. An appropriate transformation then gives the formulas for the other $N-1$ rainbow connectivity weights.

Now we find a formula for Π_{N-1} in the form (6). After choosing $c = 2N$, we determine the integration contours of (7) for use in this formula. From the rainbow diagram for Π_{N-1}, it is apparent that all intervals among (x_1, x_2), $(x_2, x_3), \ldots, (x_{2N-2}, x_{2N-1})$ and (x_{2N-1}, x_{2N}), except (x_N, x_{N+1}), are two-leg intervals of Π_{N-1}. Hence, following item b above, we entwine x_{2N-1} and x_{2N} with a Pochhammer contour $\Gamma_1 = \mathscr{P}(x_{2N-1}, x_{2N})$. Furthermore, the formula for the second hexagon connectivity weight (32) suggests that we entwine Γ_1 and x_{2N-2} with another Pochhammer contour Γ_2 in order for (x_{2N-2}, x_{2N-1}) to be a two-leg interval of Π_{N-1}, and we denote this contour by $\mathscr{P}(x_{2N-2}, \Gamma_1)$. Moreover, the formula for the third octagon connectivity weight (39) suggests that we entwine Γ_2 and x_{2N-3} with another Pochhammer contour Γ_3 in order for (x_{2N-3}, x_{2N-2}) to be a two-leg interval of Π_{N-1}, and we denote this contour by $\mathscr{P}(x_{2N-3}, \Gamma_2)$. Repeating these selections, the mth contour Γ_m is then the Pochhammer contour $\mathscr{P}(x_{2N-m}, \Gamma_{m-1})$ entwining x_{2N-m} with Γ_{m-1} for all $m \in \{2, 3, \ldots, N-1\}$. No integration contour crosses the other intervals $(x_1, x_2), (x_2, x_3), \ldots, (x_{N-1}, x_N)$, and according to item a above, these are thus two-leg intervals of Π_{N-1}, as they must be. These choices of integration contours determine the formula for Π_{N-1} up to normalization. With $\mathcal{J}(\Gamma_1, \Gamma_2, \ldots, \Gamma_{N-1})$ defined in (7) with $c = 2N$ and the integration contours defined above, we have

$$
\Pi_{N-1}(\kappa \,|\, x_1, x_2, \ldots, x_{2N}) = A_N \left(\prod_{i<j}^{2N-1} (x_j - x_i)^{2/\kappa} \right)
$$
$$
\times \left(\prod_{k=1}^{2N-1} (x_{2N} - x_k)^{1-6/\kappa} \right) \mathcal{J}\left(\kappa \,\Big|\, \Gamma_1, \Gamma_2, \ldots, \Gamma_{N-1} \,\Big|\, x_1, x_2, \ldots, x_{2N} \right), \quad c = 2N, \quad (47)
$$

where A_N is a presently unspecified constant that we later choose in order to satisfy the duality condition (10) below. (Equation (55) gives the formula for A_N.)

Presently, the formula (6) for Π_{N-1} that follows from this selection of integration contours is a well-motivated guess. To prove that it is indeed correct, we must verify the duality condition (10) for $\vartheta = N-1$ and all $\varsigma \in \{1, 2, \ldots, C_N\}$. For $\varsigma \neq N-1$, this verification is easy. Indeed, every polygon diagram, except for the rainbow diagram with its jth arc joining the jth and $(2N-j+1)$th polygon vertex (i.e., the polygon diagrams of $[\mathscr{L}_{N-1}]$ and Π_{N-1}), has at least one arc with both of its endpoints among the first N vertices of the polygon. We pick one of these arcs. There are two possibilities. Either the arc has its endpoints at the ith and $(i+1)$th vertices for some $i \in \{1, 2, \ldots, N-1\}$, or an arc nested within it does. Thus, $[\mathscr{L}_\varsigma]$ with $\varsigma \neq N-1$ includes a limit (8) that sends $x_{i+1} \to x_i$ for some i in this range. However, because the polygon diagram of Π_{N-1} does not have such an arc in its diagram, it follows from item I above, and from item a with the previous paragraph, that (x_i, x_{i+1}) is a two-leg interval of Π_{N-1}. Hence, the limit $[\mathscr{L}_\varsigma]$ annihilates Π_{N-1} for all $\varsigma \neq N-1$. This confirms the duality condition (10) for $\varsigma \neq N-1$.

To finish the analysis, we must find a suitable normalization for Π_{N-1} such that the duality condition (10) is true for $\vartheta = \varsigma = N-1$ too. That is, we must find the normalization coefficient A_N of (47) such that

$$
[\mathscr{L}_{N-1}]\Pi_{N-1} := A_N \lim_{x_{2N} \to x_1} \lim_{x_{2N-1} \to x_2} \cdots \lim_{x_{N+2} \to x_{N-1}} \lim_{x_{N+1} \to x_N} [(x_{2N} - x_1)(x_{2N-1} - x_2) \cdots (x_{N+2} - x_{N-1}) \times
$$
$$
(x_{N+1} - x_N)]^{6/\kappa - 1} \left(\prod_{i<j}^{2N-1} (x_j - x_i)^{2/\kappa} \right) \left(\prod_{k=1}^{2N-1} (x_{2N} - x_k)^{1-6/\kappa} \right) \mathcal{J}\left(\kappa \,\Big|\, \Gamma_1, \Gamma_2, \ldots, \Gamma_{N-1} \,\Big|\, x_1, x_2, \ldots, x_{2N} \right) = 1, \quad (48)
$$

where $\mathcal{J}(\Gamma_1, \Gamma_2, \ldots, \Gamma_{N-1})$ is given by (7) with $c = 2N$ and where the integration contours are as described above (47). To compute the first limit of (48), we find the asymptotic behavior of $\mathcal{J}(\Gamma_1, \Gamma_2, \ldots, \Gamma_{N-1} \,|\, x_1, x_2, \ldots, x_{2N})$ as $x_{N+1} \to x_N$ by replacing Γ_{N-1} with a large, simple loop that surrounds all of $[x_1, x_{2N}]$ and $\Gamma_1, \Gamma_2, \ldots, \Gamma_{N-2}$. Because the residue at infinity of the integrand of (7), when viewed as a function of u_{N-1}, is zero, the integration around this large loop vanishes by the Cauchy integral theorem. Assuming that $\kappa \in (4, 8)$, we contract the large loop tightly around $[x_1, x_{2N}]$ and the other contours, pinch its upper and lower halves together at x_{N+1}, and divide it into a left loop Γ_l and a right loop Γ_r surrounding $\Gamma_1, \Gamma_2, \ldots, \Gamma_{N-1}$ (figure 20). We examine the integration around each loop.
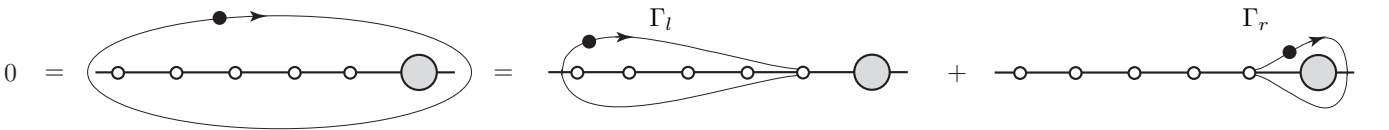

FIG. 20: Integrating u_{N-1} of (7) around a loop surrounding $[x_1, x_{2N}]$ and the Pochhammer contours $\Gamma_1, \Gamma_2, \ldots, \Gamma_{N-2}$, represented by the large gray circle, gives zero. We separate the loop into a left half and right half at x_{N+1}. ($N = 4$ shown.)
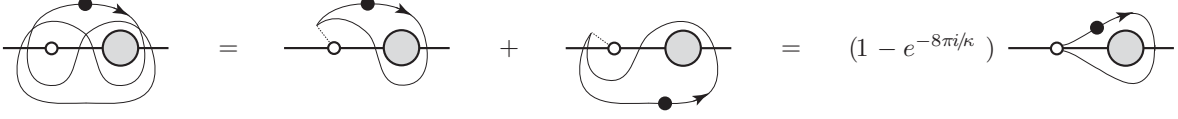
FIG. 21: We separate the Pochhammer contour Γ_{N-1} that entwines x_{N+1} (left point) with the Pochhammer contours Γ_1, $\Gamma_2, \ldots, \Gamma_{N-2}$ (gray circle) into two copies of the loop Γ_r (figure 20). The monodromy factor associated with x_{N+1} is $\exp[-8\pi i/\kappa]$.

1. The integration around Γ_r is proportional to what we find from integrating around the original Pochhammer contour $\Gamma_{N-1} = \mathscr{P}(x_{N+1}, \Gamma_{N-2})$. Indeed, we may decompose Γ_{N-1} into these two simple loops (figure 21):

   (a) The first loop starts at x_{N+1}, winds clockwise once around Γ_{N-2}, and finally ends at x_{N+1}. This end point is the start point of the second loop.

   (b) The second loop starts at x_{N+1}, winds counterclockwise once around this point, then winds counterclockwise once around Γ_{N-2}, then winds clockwise once around x_{N+1}, and finally ends at x_{N+1}.

   Because it has opposite orientation and passes around x_{N+1} before attaching to the first loop, the integration around the second loop gives $-\exp[2\pi i(-4/\kappa)]$ times the integration around the first loop. We therefore have

$$\mathcal{J}\Big(\kappa \,\Big|\, \Gamma_1, \Gamma_2, \ldots, \Gamma_{N-2}, \Gamma_r\Big) = (1 - e^{-8\pi i/\kappa})^{-1} \mathcal{J}\Big(\kappa \,\Big|\, \Gamma_1, \Gamma_2, \ldots, \Gamma_{N-2}, \Gamma_{N-1}\Big). \tag{49}$$

2. The integration around Γ_l decomposes into a sum of integrations both immediately above and below $[x_1, x_2]$, $[x_2, x_3], \ldots, [x_{N-1}, x_N]$, and $[x_N, x_{N+1}]$. Accounting for their relative phase difference, we have

$$\mathcal{J}\Big(\kappa \,\Big|\, \Gamma_1, \Gamma_2, \ldots, \Gamma_{N-2}, \Gamma_l\Big) = \sum_{j=1}^{N}(1 - e^{2\pi ij(-4/\kappa)})\mathcal{J}\Big(\kappa \,\Big|\, \Gamma_1, \Gamma_2, \ldots, \Gamma_{N-2}, [x_j, x_{j+1}]\Big). \tag{50}$$

The integration around Γ_l combines with the integration around Γ_r to give the integration around the large loop, which vanishes (figure 20). Therefore, upon identifying (49) with the opposite of (50), we find that if $\kappa \in (4, 8)$, then

$$\mathcal{J}\Big(\kappa \,\Big|\, \Gamma_1, \Gamma_2, \ldots, \Gamma_{N-2}, \Gamma_{N-1}\Big) = (e^{-8\pi i/\kappa} - 1)$$

$$\times \sum_{j=1}^{N} 2i \sin\left(\frac{4\pi j}{\kappa}\right) e^{-4\pi ij/\kappa} \mathcal{J}\Big(\kappa \,\Big|\, \Gamma_1, \Gamma_2, \ldots, \Gamma_{N-2}, [x_j, x_{j+1}]\Big). \tag{51}$$

Because the left side of (51) is an analytic function of all $\kappa \in (0, 8) \times i\mathbb{R}$ and the equality (51) holds for all $\kappa \in (4, 8)$, the replacement (16) with $\beta_i \mapsto \beta_j = -4/\kappa$ and $\beta_j \mapsto \beta_{j+1} = -4/\kappa$ gives the analytic continuation of (51) to this strip, which includes $\kappa \in (0, 4]$.

Now we determine the asymptotic behavior of (51) as $x_{N+1} \to x_N$. For this purpose, we write the jth Coulomb gas integral on the right side of (51) as (assuming $\kappa \in (4, 8)$, otherwise we replace $[x_j, x_{j+1}]$ with $\mathscr{P}(x_j, x_{j+1})$)

$$\mathcal{J}\Big(\kappa \,\Big|\, \Gamma_1, \Gamma_2, \ldots, \Gamma_{N-2}, [x_j, x_{j+1}] \,\Big|\, x_1, x_2, \ldots, x_{2N}\Big) = \oint_{\Gamma_1} du_1 \oint_{\Gamma_2} du_2 \cdots$$

$$\cdots \oint_{\Gamma_{N-2}} du_{N-2} \left(\prod_{l=1}^{2N-1}\prod_{m=1}^{N-2}(x_l - u_m)^{-4/\kappa}\right)\left(\prod_{m=1}^{N-2}(x_{2N} - u_m)^{12/\kappa - 2}\right)\left(\prod_{p<q}^{N-2}(u_p - u_q)^{8/\kappa}\right)$$

$$\times e^{4\pi ij/\kappa} \int_{x_j}^{x_{j+1}} du_{N-1} \mathcal{N}\left[\left(\prod_{l=1}^{2N-1}(x_l - u_{N-1})^{-4/\kappa}\right)(x_{2N} - u_{N-1})^{12/\kappa - 2}\left(\prod_{p=1}^{N-2}(u_p - u_{N-1})^{8/\kappa}\right)\right], \tag{52}$$

where the symbol $\mathcal{N}[\ldots]$ orders the enclosed terms so each difference is positive. Now the integrand in (52) approaches its limit as $x_{N+1} \to x_N$ uniformly over $\Gamma_1, \Gamma_2, \ldots, \Gamma_{N-2}$, and over $[x_j, x_{j+1}]$ too, unless $j \in \{N-1, N\}$. In the former case, we find the limit of (52) by setting $x_{N+1} = x_N$. If $j = N-1$ (resp. $j = N$), then (A15, A23) of section A 3 (resp. (A7, A9) of section A 2) in [8], here with $i = N$ and $\beta_i = \beta_{i+1} = -4/\kappa$, give the asymptotic behavior of the integration with respect to u_{N-1}. After inserting this into (52) and setting $x_{N+1} = x_N$ in all other factors, we find

$$\mathscr{I}\left(\kappa \,\middle|\, \Gamma_1, \Gamma_2, \ldots, \Gamma_{N-2}, \begin{matrix}[x_{N-1}, x_N]\\ [x_N, x_{N+1}]\end{matrix} \,\middle|\, x_1, x_2, \ldots, x_{2N}\right) \underset{x_{N+1}\to x_N}{\sim} \left\{\begin{matrix} e^{4\pi i(N-1)/\kappa}\, n(\kappa)^{-1}\\ e^{4\pi i N/\kappa}\end{matrix}\right\} e^{8(N-2)\pi i/\kappa}$$

$$\times \left(x_{N+1} - x_N\right)^{1-8/\kappa}\left(x_{2N} - x_N\right)^{12/\kappa - 2}\left(\prod_{k=1}^{N-1}(x_N - x_k)^{-4/\kappa}\right)\left(\prod_{k=N+2}^{2N-1}(x_k - x_N)^{-4/\kappa}\right)\frac{\Gamma(1-4/\kappa)^2}{\Gamma(2-8/\kappa)}$$

$$\times \oint_{\Gamma_1} du_1 \oint_{\Gamma_2} du_2 \cdots \oint_{\Gamma_{N-2}} du_{N-2} \left(\prod_{\substack{l\neq N,\\ N+1}}^{2N-1}\prod_{m=1}^{N-2}(x_l - u_m)^{-4/\kappa}\right)\left(\prod_{m=1}^{N-2}(x_{2N}-u_m)^{12/\kappa-2}\right)\left(\prod_{p<q}^{N-2}(u_p-u_q)^{8/\kappa}\right). \tag{53}$$

(In particular, each of the $N-2$ identical phase factors $\exp[8\pi i/\kappa]$ that appears on the right side of (53) arises as the limit of the product $(x_N - u_p)^{-4/\kappa}(x_{N+1} - u_p)^{-4/\kappa}(u_p - u_{N-1})^{8/\kappa}$ as $x_{N+1} \to x_N$, with $u_{N-1} \in [x_N, x_{N+1}]$, for some $p \in \{1, 2, \ldots, N-2\}$.) Equation (53) gives the asymptotic behavior of the $j = N-1$ and $j = N$ terms on the right side of (51) as $x_{N+1} \to x_N$. For $\kappa \in (0, 8)$, the factor $(x_{N+1} - x_N)^{1-8/\kappa}$ dominates the other terms in (51), which have finite limits. After dropping these latter terms from (51), replacing the $j = N$ and $j = N+1$ terms of (51) with the right side of (53), inserting the right side of (51) into (47), and simplifying the result, we find

$$\Pi_{N-1}(\kappa\,|\,x_1, x_2, \ldots, x_{2N}) \underset{x_{N+1}\to x_N}{\sim} (x_{N+1} - x_N)^{1-6/\kappa}4e^{4\pi i(2N-5)/\kappa}n(\kappa)^{-1}$$

$$\times \frac{A_N}{A_{N-1}}\sin\left(-\frac{4\pi}{\kappa}\right)\sin\left(\frac{4\pi(N+1)}{\kappa}\right)\frac{\Gamma(1-4/\kappa)^2}{\Gamma(2-8/\kappa)}\Xi_{N-2}(\kappa\,|\,x_1, x_2, \ldots, x_{N-1}, x_{N+2}, \ldots, x_{2N}), \tag{54}$$

where Ξ_{N-2} is the rainbow connectivity weight in $\mathscr{B}_{N-1}$ whose polygon diagram follows from removing the arc joining the Nth and $(N+1)$th vertices of the polygon diagram for Π_{N-1}.

Returning to the task of finding the normalization A_N in (48), we use (54) to find the first limit on the right side of (48). Then we repeat this process another $N-2$ times to compute all limits in (48). Upon doing this and applying the condition $[\mathscr{L}_{N-1}]\Pi_{N-1} = 1$, we find the following normalization constant for use in (47):

$$A_N = \prod_{m=1}^{N-1}\frac{n(\kappa)e^{-4\pi i(2m-3)/\kappa}\,\Gamma(2-8/\kappa)}{4\sin(-4\pi/\kappa)\sin(4\pi(m+2)/\kappa)\,\Gamma(1-4/\kappa)^2}. \tag{55}$$

This normalization constant (55) leads to $[\mathscr{L}_{N-1}]\Pi_{N-1} = 1$ only if $c = 2N$, so x_{2N} is the point bearing the conjugate charge. If $c = 2N-1$ instead, as it does in sections II B–II D, then the $m = 1$ factor in (55) must be altered. To find A_N in this situation, we perform all steps spanning (49–54) $N-2$ times, finding that the ratio A_N/A_2 equals the product of all factors in (55), excluding the factor with $m = 1$. Now, repeating this process one last time to determine A_2 would send the point x_{2N-1} bearing the conjugate charge to x_2, producing a complicated result. Instead, we determine A_2 by directly comparing (47) with $N = 2$ to the normalized rectangle connectivity weight formula (24) with $(x_3, x_4) \mapsto (x_{2N-1}, x_{2N})$, previously found in section II B. We find that A_2 equals the $m = 1$ factor in (55) with the phase factor replaced by $\exp[-12\pi i/\kappa]$, so A_N equals the product (55) but with the phase factor in the $m = 1$ factor replaced by $\exp[-12\pi i/\kappa]$. Upon inserting this replacement into (55, 47) with $N = 2$, $N = 3$, and $N = 4$ and decomposing the integration contours as we did in sections II B–II D, we recover the connectivity weight formulas Π_1 (24) for the rectangle, Π_2 (32) for the hexagon, and Π_3 (39) for the octagon respectively.

For convenience, we replace the factor $(x_l - u_m)^{-4/\kappa}$ of the integrand in (47) with $(u_m - x_l)^{-4/\kappa}$ for all $m \in \{1, 2, \ldots, N-1\}$ and $l \in \{1, 2, \ldots, 2N-m\}$. In so doing, the branch cuts anchored to points either to the left of or in the left (resp. points in the right) cycle of each Pochhammer contour follow the real axis leftward (resp. rightward) to negative (resp. positive) infinity, as we have in (14, 15). For each m, this adjustment multiplies the mth factor of (55) by $\exp[4\pi i(2N-m)/\kappa]$, or one phase factor of $\exp[4\pi i/\kappa]$ for each replacement. Thus, we find the following alternative formula for Π_{N-1} (47),

$$\Pi_{N-1}(\kappa\,|\,x_1, x_2, \ldots, x_{2N}) = \left(\prod_{m=1}^{N-1}\frac{n(\kappa)e^{4\pi i(m+3)/\kappa}\Gamma(2-8/\kappa)}{4\sin(-4\pi/\kappa)\sin(4\pi(m+2)/\kappa)\Gamma(1-4/\kappa)^2}\right)\left(\prod_{j<k}^{2N-1}(x_k - x_j)^{2/\kappa}\right)$$

$$\times \left(\prod_{k=1}^{2N-1}(x_{2N}-x_k)^{1-6/\kappa}\right)\oint_{\Gamma_{N-1}}du_{N-1}\cdots\oint_{\Gamma_2}du_2\oint_{\Gamma_1}du_1\left(\prod_{m=1}^{N-1}\prod_{l=1}^{2N-m}(u_m - x_l)^{-4/\kappa}\right)$$

$$\times \left(\prod_{m=1}^{N-1}\prod_{l=2N-m+1}^{2N-1}(x_l - u_m)^{-4/\kappa}\right)\left(\prod_{m=1}^{N-1}(x_{2N}-u_m)^{12/\kappa-2}\right)\left(\prod_{p<q}^{N-1}(u_p - u_q)^{8/\kappa}\right), \tag{56}$$

after using the following identity to simplify the adjusted formula for A_N:

$$\left(\prod_{m=1}^{N-1} e^{-4\pi i(2m-3)/\kappa} \right) \left(\prod_{m=1}^{N-1} e^{4\pi i(2N-m)/\kappa} \right) = \prod_{m=1}^{N-1} e^{4\pi i(m+3)/\kappa}. \tag{57}$$

Part of the prefactor in (56) is a natural generalization of part of the prefactor on the right side of (16). This comes about for the following reason. The left cycle of Γ_m surrounds the branch point x_{2N-m}, so after $u_m \in \Gamma_m$ traces this cycle counterclockwise once, the integrand acquires a phase factor of $\exp[2\pi i \beta_i]$ with $\beta_i = -4/\kappa$. And if $m > 1$ (resp. $m = 1$), then the right cycle of Γ_m surrounds the branch points x_j with $j \in \{2N-m+1, 2N-m+2, \ldots, 2N\}$ and u_n with $n \in \{1, 2, \ldots, m-1\}$ (resp. the one branch point x_{2N}). Hence, after $u_m \in \Gamma_m$ traces this cycle counterclockwise once, the integrand acquires a phase factor of $\exp[2\pi i \beta_j]$, with

$$\beta_j = \overbrace{(-4/\kappa)(m-1)}^{\{x_j\}_{j=2N-m+1}^{2N-1}} + \overbrace{(8/\kappa)(m-1)}^{\{u_n\}_{n=1}^{m-1}} + \overbrace{12/\kappa - 2}^{x_{2N}} = (4/\kappa)(m+2) - 2. \tag{58}$$

After inserting these expressions for β_i and β_j (58) into the prefactor on the right side of (16), we recover part of the prefactor in (56):

$$4e^{\pi i(\beta_i - \beta_j)} \sin \pi \beta_i \sin \pi \beta_j = 4e^{-4\pi i(m+3)/\kappa} \sin(-4\pi/\kappa) \sin(4\pi(m+2)/\kappa). \tag{59}$$

A natural interpretation of this result is to say that the right side of (59) generalizes the prefactor on the right side of (15, 16) to situations in which the right cycle of a Pochhammer contour surrounds several branch points.

III.   SUMMARY

This article presents formulas for "connectivity weights" or "pure SLE$_\kappa$ partition functions" Π_ς [9], special functions that arise in multiple SLE$_\kappa$ (Schramm-Löwner Evolution) [1–5] and that also have a conformal field theory interpretation [9]. The connectivity weights are the main ingredients of the conjectured formula (13) for the *crossing probability* P_ς [9, 10], that is, the probability that the $2N$ growing curves of a multiple-SLE$_\kappa$ process anchored at $x_1, x_2, \ldots, x_{2N}$ almost surely join together pairwise in the ςth connectivity. (Figure 4 shows an example. The index $\varsigma \in \{1, 2, \ldots, C_N\}$, with C_N the Nth Catalan number, enumerates all of the possible connectivities, as explained in the introduction I.)

In this article, using rigorous results from [6–9], we find explicit formulas for all of the connectivity weights from the solution space $\mathcal{S}_N$ of the system of PDEs (2, 3) with $N \in \{1, 2, 3, 4\}$ (those with $N \in \{3, 4\}$ are new), and for so-called "rainbow connectivity weights" for all $N \in \mathbb{Z}^+ + 1$. These formulas are expected to give cluster-crossing probabilities for critical statistical mechanics lattice models inside rectangles ($N = 2$), hexagons ($N = 3$), and octagons ($N = 4$) with a free/fixed side-alternating boundary condition, a topic that we investigate in [24]. In the case of critical percolation ($\kappa = 6$), Π_ς itself gives the probability that percolation clusters join the fixed sides of a polygon with $2N$ sides in the ςth connectivity (again, with a free/fixed side-alternating boundary condition on the polygon's perimeter). These probabilities generalize Cardy's formula (1) [19] for the probability that a percolation cluster joins the opposite sides of a rectangle ($N = 2$).

In section II, we find formulas for the connectivity weights by choosing a suitable collection of integration contours to use in the Coulomb gas solutions (6, 7) for the system of equations (2, 3) and then verifying that the resulting formulas satisfy the duality condition (10). This verification is a sufficient last step because the duality condition (10) uniquely defines each connectivity weight. We give a formula for only one connectivity weight per collection of weights that are identical up to rotation of their polygon diagrams (figure 3). A suitable transformation then gives formulas for the other weights in the collection. For $N = 1$, the formula for the unique connectivity weight is (22); for $N = 2$, the formula is (24); for $N = 3$, these formulas are (28, 32); and for $N = 4$, these formulas are (35, 39, 46). In addition, we find an explicit formula (56) for the "rainbow connectivity weight" (section II E), generating a multiple-SLE$_\kappa$ process in which the boundary arcs join the $2N$ marked points on the real axis to form a "rainbow" [4, 41] in the upper half-plane (figure 19). (Ref. [34] obtains an alternative explicit formula for the rainbow connectivity weight using the "spin-chain Coulomb gas correspondence," previously developed in [33].) In appendix A, we explicitly show that all singularities in $\kappa \in (0, 8) \times i\mathbb{R}$ of factors in these formulas are removable, so each connectivity weight is an analytic function of κ in this region. Finally, in appendix B, we study logarithmic singularities of some of the connectivity weight formulas as one or more points x_j approach a common point x_i. Predicted to occur by logarithmic CFT, these logarithmic singularities may arise only for certain κ corresponding to CFT minimal models [9] and for $N \in \mathbb{Z}^+$ sufficiently large. Some of the analysis in appendix B is a natural extension of the analysis in appendix A of [9].

IV. ACKNOWLEDGEMENTS

Appendix A: Investigation of connectivity weights near singular $\kappa \in (0, 8) \times i\mathbb{R}$

The prefactors that appear in the various connectivity weight formulas (24, 28, 32, 35, 39, 46) have poles exclusively at certain $\kappa \in (0, 8)$, yet in spite of this, the connectivity weights are analytic functions of $\kappa \in (0, 8) \times i\mathbb{R}$. Indeed, if we replace $F \in \mathcal{S}_N$ in (12) with each element of the Temperley-Lieb set $\mathcal{B}_N = \{\mathcal{F}_1, \mathcal{F}_2, \ldots, \mathcal{F}_{C_N}\}$ (which is a basis for $\mathcal{S}_N$ if and only if $\kappa \in (0, 8)$ is not an exceptional speed with $q \leq N + 1$, see definitions 4 and 5 and lemma 6 of [8]), then we obtain a $C_N \times C_N$ system of equations in the connectivity weights $\Pi_1, \Pi_2 \ldots, \Pi_{C_N}$ that is invertible if and only if $\kappa \in (0, 8)$ is not an exceptional speed with $q \leq N + 1$. In fact, each element of $\mathcal{B}_N$ and all coefficients of the system are analytic at any $\kappa \in (0, 8) \times i\mathbb{R}$. As such, it follows upon solving the system and applying analytic continuation that the connectivity weights are analytic at any κ in this region where the system is invertible. If $\kappa \in (0, 8)$ is among the mentioned exceptional speeds, then the system is not invertible. However, by using the basis from the proof of theorem 8 in [8], we encounter a different invertible $C_N \times C_N$ system of equations in all of the connectivity weights [9]. Then the same analysis shows that the connectivity weights are analytic at these speeds too.

Thanks to these observations, it is not necessary to directly verify that the connectivity weight formulas derived in this article have finite, non-vanishing limits as $\varkappa \to \kappa$, where κ is a pole of the formula prefactor. Indeed, because we know that this limit of any particular connectivity weight exists, we infer that the corresponding connectivity weight formula with the prefactor dropped must have a zero at $\varkappa = \kappa$. Furthermore, the order of the zero must equal the order of the pole, or else the connectivity weight would vanish at $\varkappa = \kappa$, thereby violating the duality relation (10) for $\varsigma = \vartheta$. (To complete the argument supporting this last point, we must first establish that the limits of the connectivity weight formulas as $\varkappa \to \kappa$ still satisfy the duality relation (10). Indeed, this follows from the fact that the limit $\varkappa \to \kappa$ commutes with all limits in every equivalence class $[\mathscr{L}_\varsigma]$ of the dual space $\mathscr{B}_N^*$. See the paragraph beneath (49) in [8].)

Thus, for any $N \in \mathbb{Z}^+$, all connectivity weights $\Pi_1, \Pi_2, \ldots, \Pi_{C_N}$ of $\mathscr{B}_N$ (11) are analytic functions of $\kappa \in (0, 8) \times i\mathbb{R}$. The remainder of this appendix demonstrates in detail how this comes about from the formulas for the cases $N \in \{2, 3, 4\}$ presented in this article. Logically, this is not necessary, and the reader may omit it. However, it is of interest as an illustration of relevant contour integral technology and because, as we show below, the singular behavior at the mentioned exceptional speeds sometimes occurs for reasons related to the linear dependence of $\mathcal{B}_N$ at this speed [8].

Throughout this section, we let $\varkappa \in (0, 8) \times i\mathbb{R}$ denote an arbitrary SLE_κ speed (we consider complex $\varkappa$ only for the occasional purpose of analytic continuation), and we let κ denote a particular SLE_κ speed that is a singularity of a prefactor appearing in a connectivity weight formula.

1. Singularities of the rectangle connectivity weight

Equation (24) gives a formula for the first rectangle connectivity weight. After using (16) to extend the integration in this formula to all speeds $\varkappa \in (0, 8) \times i\mathbb{R}$, we write it as

$$\frac{n(\varkappa)\, \Gamma(2 - 8/\varkappa)}{4e^{-16\pi i/\varkappa} \sin(-4\pi/\varkappa) \sin(12\pi/\varkappa)\, \Gamma(1 - 4/\varkappa)^2} \ \cdots \ \oint_{\mathscr{P}(x_3, x_4)} (x_4 - u)^{-4/\varkappa}(u - x_3)^{12/\varkappa - 2} \cdots \mathrm{d}u, \qquad \text{(A1)}$$

where the ellipses stand for omitted factors analytic for $\varkappa \in (0, 8)$ and over $u \in A$, where A is an open region containing $\mathscr{P}(x_3, x_4)$. Equation (21) defines the factor $n(\varkappa)$. Among speeds $\varkappa \in (0, 8)$, the prefactor in (A1) is singular at all κ such that $8/\kappa \in \mathbb{Z}^+ + 1$ or $12/\kappa \in \mathbb{Z}^+ + 1$. We divide these singularities into three cases.

1. $8/\kappa \in \mathbb{Z}^+ + 1$ and $4/\kappa \notin \mathbb{Z}^+$: In this case, only the factor $\Gamma(2 - 8/\varkappa)$ of (A1) has a pole at $\varkappa = \kappa$. However, $\varkappa = \kappa$ is a removable singularity of the product $n(\varkappa)\Gamma(2 - 8/\varkappa)$ and hence of (A1).

2. $12/\kappa \in \mathbb{Z}^+ + 1$ and $4/\kappa \notin \mathbb{Z}^+$: In this case, only the reciprocal of $\sin(12\pi/\varkappa)$ has a pole at $\varkappa = \kappa$. However, it follows from (14) that κ is a zero of the contour integral too. As such, κ is a removable singularity of

$$\frac{1}{\sin(12\pi/\varkappa)} \oint_{\mathscr{P}(x_3, x_4)} (x_4 - u)^{12/\varkappa - 2}(u - x_3)^{-4/\varkappa} \cdots \mathrm{d}u \qquad \text{(A2)}$$

and hence of (A1).

3. $4/\varkappa \in \mathbb{Z}^+$: In this case, almost every factor in (A1) vanishes or has a pole at $\varkappa = \kappa$. Upon writing (A1) as

$$\frac{n(\varkappa)}{4e^{-16\pi i/\varkappa}} \underbrace{\frac{\Gamma(2-8/\varkappa)}{\sin(-4\pi/\varkappa)\Gamma(1-4/\varkappa)^2}}_{1.} \cdots \underbrace{\frac{1}{\sin(12\pi/\varkappa)} \oint_{\mathscr{P}(x_3,x_4)}}_{2.} \cdots \tag{A3}$$

and using (14), we see that κ is a removable singularity of the first and second factors in (A3) and hence of (A1).

From these facts, we conclude that the first rectangle connectivity weight (24) is an analytic function of $\varkappa \in (0,8) \times i\mathbb{R}$.

2. Singularities of the hexagon connectivity weights

Equation (28) gives a formula for the first hexagon connectivity weight. After using (16) to extend the integration in this formula to all speeds $\varkappa \in (0,8) \times i\mathbb{R}$, we write the terms in this formula as

$$\frac{n(\varkappa)^2 \Gamma(2-8/\varkappa)^2}{4^2 e^{-16\pi i/\varkappa} \sin^3(-4\pi/\varkappa)\sin(12\pi/\varkappa)\Gamma(1-4/\varkappa)^4[n(\varkappa)^2-2]} \cdots \oint_{\mathscr{P}(x_i,x_{i+1})} (x_{i+1}-u_2)^{-4/\varkappa} \cdots$$

$$\cdots (u_2-x_i)^{-4/\varkappa} \cdots \oint_{\mathscr{P}(x_5,x_6)} (x_6-u_1)^{-4/\varkappa}(u_1-x_5)^{12/\varkappa-2} \cdots \mathrm{d}u_1 \, \mathrm{d}u_2, \quad i \in \{1,2,3\}, \quad \text{(A4)}$$

where the ellipses stand for omitted factors analytic over $\varkappa \in (0,8) \times i\mathbb{R}$, over $u_1 \in A$, and over $u_2 \in B$, where A and B are open regions containing $\mathscr{P}(x_5,x_6)$ and $\mathscr{P}(x_i,x_{i+1})$ respectively. Among speeds $\varkappa \in (0,8) \times i\mathbb{R}$, the prefactor in (A4) is singular at all κ such that $8/\kappa \in \mathbb{Z}^+ + 1$, $12/\kappa \in \mathbb{Z}^+ + 1$, or $n(\kappa)^2 = 2$. We divide these singularities into four cases.

1. $8/\kappa \in \mathbb{Z}^+ + 1$ and $4/\kappa \notin \mathbb{Z}^+$: The treatment of this case is identical to that of item 1 in section A 1.

2. $12/\kappa \in \mathbb{Z}^+ + 1$ and $4/\kappa \notin \mathbb{Z}^+$: The treatment of this case is identical to that of item 2 in section A 1.

3. $4/\kappa \in \mathbb{Z}^+$: In this case, almost every factor in (A4) vanishes or has a pole at $\varkappa = \kappa$. Upon writing (A4) as

$$\frac{n(\varkappa)^2}{4^2 e^{-16\pi i/\varkappa}[n(\varkappa)^2-2]} \overbrace{\frac{\Gamma(2-8/\varkappa)^2}{\sin^2(-4\pi/\varkappa)\Gamma(1-4/\varkappa)^4}}^{1.} \cdots$$

$$\cdots \underbrace{\frac{1}{\sin(-4\pi/\varkappa)} \oint_{\mathscr{P}(x_i,x_{i+1})}}_{2.} \cdots \underbrace{\frac{1}{\sin(12\pi/\varkappa)} \oint_{\mathscr{P}(x_5,x_6)}}_{3.} \cdots \tag{A5}$$

and using (14), we see that κ is a removable singularity of the first, second, and third factors in (A5) and hence of (A4).

4. $n(\kappa)^2 = 2$: In this case, $\kappa \in (0,8) \times i\mathbb{R}$ is any of the exceptional speeds $\kappa_{4,q'} = 16/q'$ [8], where $q' > 1$ is an integer coprime with four. Here, $n(\varkappa)^2 - 2 = O(\varkappa - \kappa)$ as $\varkappa \to \kappa$ (21). Also, (28, A4) with the factor $[n(\varkappa)^2-2]^{-1}$ dropped is an analytic function of $\varkappa \in (0,8) \times i\mathbb{R}$. Thus, if it vanishes at $\varkappa = \kappa$, then it is $O((\varkappa-\kappa)^m)$ as $\varkappa \to \kappa$ for some $m \in \mathbb{Z}^+$, so κ is a removable singularity of (28, A4). Indeed, this function does vanish at $\varkappa = \kappa$, as

$$[nI_{25} - I_{15} - I_{35}](\kappa) = 0 \quad \text{if } n(\kappa)^2 = 2. \tag{A6}$$

To derive (A6), we integrate u_2 of (A4) around a simple loop that surrounds $[x_1,x_6]$ and $\Gamma_1 = [x_5,x_6]$, pinch the upper and lower halves of the loop together between x_4 and x_5, and divide the loop into a left half that tightly surrounds $[x_1,x_4]$ and a right half that surrounds Γ_1. Now, as we cross the interval (x_4,x_5), the integrand of (7) with $N = 3$ and $c = 5$ does not acquire a phase factor. Indeed, it accumulates one phase factor of

$$e^{2\pi i(-4/\kappa)} = e^{2\pi i(-4q'/16)} = e^{2\pi i(-q'/4)} \tag{A7}$$
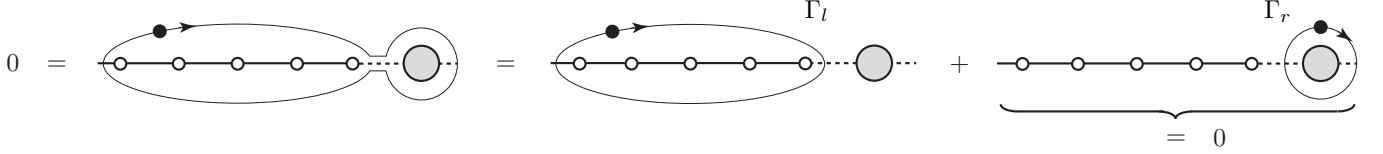
FIG. 22: If $\kappa = 4(N+1)/q'$ for some $q' \in \mathbb{Z}^+$ coprime with $N+1$, then the integrand of (7) does not have a branch cut immediately to the right of x_{N+1} (dashed), leading to the above decomposition. We interpret the gray circle as in figure 20.

per each of the four rightward-pointing branch cuts respectively anchored to x_1, x_2, x_3, and x_4, and the product of all four factors is one. Thus, the left and right halves of the simple loop separate into a left loop Γ_l tightly wrapped around $[x_1, x_4]$ and a right loop Γ_r surrounding Γ_1 (figure 22 with $N = 3$). Because integration around the original loop gives zero by the Cauchy integral theorem, the integration around Γ_l gives the opposite of the integration around Γ_r.

Interestingly, the integration along $\Gamma_r \times \Gamma_1$ gives zero too. To see why, we note that (6) with $N = 3$ gives an element of $\mathcal{S}_3$ whenever Γ_1 and Γ_2 are two nonintersecting closed contours, as is the case here with $\Gamma_2 = \Gamma_r$. (Indeed, Γ_r closes because the integrand of (7) does not acquire a phase factor as this contour crosses the interval $[x_4, x_5]$.) Then according to item a in section II, (x_1, x_2), (x_2, x_3), and (x_3, x_4) are two-leg intervals of this element of $\mathcal{S}_3$. However, every equivalence class in $\mathscr{B}_3^*$ has a limit that brings together the endpoints of one of these intervals, annihilating this element. As such, this element is in the kernel of the map $v : \mathcal{S}_N \to \mathbb{R}^{C_N}$ with $v(F)_\varsigma := [\mathscr{L}_\varsigma]F$. According to lemma 15 of [6], it must therefore be zero.

It immediately follows from the previous paragraph and the last sentence of the paragraph preceding it that the integration along $\Gamma_l \times \Gamma_1$ gives zero too (figure 22 with $N = 3$). After decomposing the integration around Γ_l into integrations along the three intervals $[x_1, x_2]$, $[x_2, x_3]$, and $[x_3, x_4]$ that Γ_l surrounds, we find that

$$0 = \mathcal{J}(\kappa \,|\, \Gamma_1, \Gamma_l) \propto [I_{15} - nI_{25} + (n^2 - 1)I_{35}](\kappa), \quad n(\kappa)^2 = 2, \tag{A8}$$

with I_{ij} and $n(\kappa)$ defined in (26) and (21) respectively. This result follows from factoring out phase factors in such a way that each I_{ij} is real and combining terms as in the previous sections. (If $\kappa \leq 4$, then these improper integrals diverge. We regularize them via the replacement (16).) Because (A8) is identical to (A6), we conclude that κ is a removable singularity of (A4).

Interestingly, (A8) implies the linear dependence of the Temperley-Lieb set $\mathcal{B}_3$ for $\varkappa = \kappa = \kappa_{4,q'}$ (definitions 4 and 5 of [8]), previously determined by other means in the proof of lemma 6 in [8]. Indeed, by integrating u_1 in (A8) around a loop surrounding $[x_1, x_6]$ and repeating the above steps, we may express I_{15}, I_{25}, and I_{35} in (A8) as linear combinations of I_{ij} with $i, j \neq 5$. After inserting these expressions into (A8) and multiplying the result by the algebraic factors preceding $\mathcal{J}(\Gamma_1, \Gamma_2)$ in (6) with $N = 3$ and $c = 5$, we find a linear combination of elements in $\mathcal{B}_3$ vanishing for $\varkappa = \kappa = \kappa_{4,q'}$. (See also corollary 9 of [8].)

Thus, the first hexagon connectivity weight (28) is an analytic function of $\varkappa \in (0, 8) \times i\mathbb{R}$.

Equation (32) gives a formula for the second hexagon connectivity weight. After using (16) to extend the integration in this formula to all speeds $\varkappa \in (0, 8) \times i\mathbb{R}$, we write it as

$$\frac{n(\varkappa)^2 \Gamma(2 - 8/\varkappa)^2}{4^2 \sin^2(-4\pi/\varkappa) \sin^2(12\pi/\varkappa) \Gamma(1 - 4/\varkappa)^4} \cdots \oint_{\mathscr{P}(x_4, x_5)} (x_5 - u_2)^{12/\varkappa - 2}$$

$$\times (u_2 - x_4)^{-4/\varkappa} \cdots \oint_{\mathscr{P}(x_5, x_6)} (x_6 - u_1)^{-4/\varkappa} (u_1 - x_5)^{12/\varkappa - 2} \cdots \mathrm{d}u_1 \, \mathrm{d}u_2, \tag{A9}$$

where the ellipses stand for omitted factors analytic over $\varkappa \in (0, 8) \times i\mathbb{R}$, over $u_1 \in A$, and over $u_2 \in B$, where A and B are open regions containing $\mathscr{P}(x_5, x_6)$ and $\mathscr{P}(x_4, x_5)$ respectively. Among speeds $\varkappa \in (0, 8) \times i\mathbb{R}$, the prefactor in (A9) is singular at all κ such that $8/\kappa \in \mathbb{Z}^+ + 1$ or $12/\kappa \in \mathbb{Z}^+ + 1$. We divide these singularities into three cases.

5. $8/\kappa \in \mathbb{Z}^+ + 1$ and $4/\kappa \notin \mathbb{Z}^+$: The treatment of this case is identical to that of item 1 in section A 1.

6. $12/\kappa \in \mathbb{Z}^+ + 1$ and $4/\kappa \notin \mathbb{Z}^+$: The treatment of this case is identical to that of item 2 in section A 1.

7. $4/\kappa \in \mathbb{Z}^+$: In this case, almost every factor in (A9) vanishes or has a pole at $\varkappa = \kappa$. Upon writing (A9) as

$$\frac{n(\varkappa)^2}{4^2} \underbrace{\frac{\Gamma(2 - 8/\varkappa)^2}{\sin^2(-4\pi/\varkappa) \Gamma(1 - 4/\varkappa)^4}}_{1.} \cdots \underbrace{\frac{1}{\sin^2(12\pi/\varkappa)} \oint_{\mathscr{P}(x_4, x_5)} \cdots \oint_{\mathscr{P}(x_5, x_6)} \cdots}_{2.} \tag{A10}$$

and using (14), we see that κ is a removable singularity of the first and second factors in (A10) and hence of (A9).

From these facts, we conclude that the second hexagon connectivity weight (32) is an analytic function of $\varkappa \in (0, 8) \times i\mathbb{R}$.

3. Singularities of the octagon connectivity weights

The content of this section is almost identical to that of sections A 1 and A 2, except that the analysis of singularities of the first octagon connectivity weight Π_1 (46) at all κ such that $n(\kappa)^2 = 2$ is considerably more involved. There are also differences between the treatment of the other octagon weights Π_2, Π_3 and their analogues in sections A 1 and A 2. Because these differences are at times significant, we include a complete analysis of singularities of octagon connectivity weights here.

There are three distinct octagon connectivity weights. We begin with the formula (35) for the second connectivity weight Π_2. After using (16) to extend it to all speeds $\varkappa \in (0, 8) \times i\mathbb{R}$, we find four terms, all with the form

$$
\frac{n(\varkappa)^3 \Gamma(2 - 8/\varkappa)^3}{4^3 \sin^4(-4\pi/\varkappa) \sin^2(12\pi/\varkappa) \Gamma(1 - 4/\varkappa)^6 [n(\varkappa)^4 - 3n(\varkappa)^2 + 1]} \cdots \oint_{\mathscr{P}(x_i, x_{i+1})} (x_{i+1} - u_3)^{-4/\varkappa} (u_3 - x_i)^{-4/\varkappa} \cdots
$$

$$
\oint_{\mathscr{P}(x_6, x_7)} (x_7 - u_2)^{12/\varkappa - 2} (u_2 - x_6)^{-4/\varkappa} \cdots \oint_{\mathscr{P}(x_7, x_8)} (x_8 - u_1)^{-4/\varkappa} (u_1 - x_7)^{12/\varkappa - 2} \cdots \mathrm{d}u_1 \, \mathrm{d}u_2 \, \mathrm{d}u_3, \quad i \in \{1, 2, 3, 4\},
$$
(A11)

where the ellipses stand for omitted factors analytic over $\varkappa \in (0, 8) \times i\mathbb{R}$, over $u_1 \in A$, over $u_2 \in B$, and over $u_3 \in C$, where A, B, and C are open regions containing $\mathscr{P}(x_7, x_8)$, $\mathscr{P}(x_6, x_7)$, and $\mathscr{P}(x_i, x_{i+1})$ respectively. Among speeds $\varkappa \in (0, 8) \times i\mathbb{R}$, the prefactor in (A11) is singular at all κ such that $8/\kappa \in \mathbb{Z}^+ + 1$, $12/\kappa \in \mathbb{Z}^+ + 1$, or $n(\varkappa)^4 - 3n(\varkappa)^2 + 1 = 0$. We divide these singularities into four cases.

1. $8/\kappa \in \mathbb{Z}^+ + 1$ and $4/\kappa \notin \mathbb{Z}^+$: The treatment of this case is identical to that of item 1 in section A 1.

2. $12/\kappa \in \mathbb{Z}^+ + 1$ and $4/\kappa \notin \mathbb{Z}^+$: The treatment of this case is identical to that of item 2 in section A 1.

3. $4/\kappa \in \mathbb{Z}^+$: In this case, almost every factor in (A11) vanishes or has a pole at $\varkappa = \kappa$. Upon writing (A11) as

$$
\frac{n(\varkappa)^3}{4^3 [n(\varkappa)^4 - 3n(\varkappa)^2 + 1]} \overbrace{\frac{\Gamma(2 - 8/\varkappa)^3}{\sin^3(-4\pi/\varkappa) \Gamma(1 - 4/\varkappa)^6}}^{1.} \cdots
$$

$$
\cdots \underbrace{\frac{1}{\sin(-4\pi/\varkappa)} \oint_{\mathscr{P}(x_i, x_{i+1})}}_{2.} \cdots \underbrace{\frac{1}{\sin(12\pi/\varkappa)} \oint_{\mathscr{P}(x_6, x_7)}}_{3.} \cdots \underbrace{\frac{1}{\sin(12\pi/\varkappa)} \oint_{\mathscr{P}(x_7, x_8)}}_{4.} \cdots
$$
(A12)

and using (14), we see that κ is a removable singularity of the first, second, third, and fourth factors in (A12) and hence of (A11).

4. $n(\kappa)^4 - 3n(\kappa)^2 + 1 = 0$: In this case, we have $n(\kappa) \in \{(1 \pm \sqrt{5})/2, -(1 \pm \sqrt{5})/2\}$. That is, $\kappa \in (0, 8) \times i\mathbb{R}$ is any of the exceptional speeds $\kappa_{5,q'} = 20/q'$ [8], where $q' > 1$ is an integer coprime with five. Here, $n(\varkappa)^4 - 3n(\varkappa) + 1 = O(\varkappa - \kappa)$ as $\varkappa \to \kappa$ (21). Also, (35, A11) with the factor $[n(\varkappa)^4 - 3n(\varkappa) + 1]^{-1}$ dropped is an analytic function of $\varkappa \in (0, 8) \times i\mathbb{R}$. Thus, if it vanishes at $\varkappa = \kappa$, then it is $O((\varkappa - \kappa)^m)$ as $\varkappa \to \kappa$ for some $m \in \mathbb{Z}^+$, and κ is a removable singularity of (35, A11). Indeed, this function does vanish at $\varkappa = \kappa$, as

$$
[n(I_{167} - nI_{267}) + (n^2 - 1)(nI_{367} - I_{467})](\kappa) = 0, \quad n(\kappa)^4 - 3n(\kappa)^2 + 1 = 0. \tag{A13}
$$

To derive (A13), we repeat the steps of item 4 in section A 2, with appropriate adjustments. We integrate u_3 of (A11) around a simple loop that surrounds $[x_1, x_8]$, $\Gamma_1 = [x_7, x_8]$, and $\Gamma_2 = [x_6, x_7]$, pinch the upper and lower halves of the loop together between x_5 and x_6, and divide the loop into a left half that tightly surrounds $[x_1, x_5]$ and a right half that surrounds Γ_1 and Γ_2. Now, as we cross the interval (x_5, x_6), the integrand of (7) with $N = 4$ and $c = 7$ does not acquire a phase factor. Indeed, the integrand accumulates one phase factor of

$$
e^{2\pi i(-4/\kappa)} = e^{2\pi i(-4q'/20)} = e^{2\pi i(-q'/5)} \tag{A14}
$$

per each of the five rightward-pointing branch cuts respectively anchored to $x_1, x_2, \ldots, x_5$, and the product of all five factors is one. Thus, the left and right halves separate into a left loop Γ_l tightly wrapped around $[x_1, x_5]$ and a right loop Γ_r surrounding Γ_1 and Γ_2 (figure 22 with $N = 4$ as shown). Because integration around the original loop gives zero by the Cauchy integral theorem, the integration around Γ_l gives the opposite of the integration around Γ_r.

Interestingly, the integration along $\Gamma_r \times \Gamma_2 \times \Gamma_1$ gives zero as well, and the argument for why this is true is identical to the argument made for the vanishing integration along $\Gamma_r \times \Gamma_1$ in item 4 of section A 2, with obvious adjustments (figure 22 with $N = 4$ as shown). Thus, we conclude that the integration along $\Gamma_l \times \Gamma_2 \times \Gamma_1$ gives zero too. After decomposing the integration around Γ_l into integrations along the four intervals $[x_1, x_2]$, $[x_2, x_3]$, $[x_3, x_4]$, and $[x_4, x_5]$ that Γ_r surrounds, we find that

$$0 = \mathcal{J}(\kappa \,|\, \Gamma_1, \Gamma_2, \Gamma_l)$$
$$\propto [I_{167} - nI_{267} + (n^2 - 1)I_{367} - n(n^2 - 2)I_{467}](\kappa) = 0, \quad n(\kappa)^4 - 3n(\kappa)^2 + 1 = 0, \quad \text{(A15)}$$

with I_{ijk} and $n(\kappa)$ defined in (33) and (21) respectively. (If $\kappa \leq 4$, then these improper integrals diverge. We regularize them via the replacement (16).) Because (A15) is identical to (A13), we conclude that κ is a removable singularity of (A11).

Interestingly, (A15) implies the linear dependence of the Temperley-Lieb set $\mathcal{B}_4$ for $\varkappa = \kappa = \kappa_{5,q'}$, previously determined by other means in the proof of lemma 6 in [8]. The argument for this claim is identical to the argument in the paragraph beneath (A8), up to obvious adjustments.

From these facts, we conclude that the second octagon connectivity weight Π_2 (35) is an analytic function of $\varkappa \in (0, 8) \times i\mathbb{R}$.

Equation (39) gives a formula for the third octagon connectivity weight Π_3. Here, there are two terms for us to consider. After using (16) to extend the formula to all speeds $\varkappa \in (0, 8) \times i\mathbb{R}$, we write the term of (39) including I_{567} as (figure 14)

$$\frac{n(\varkappa)^3 \Gamma(2 - 8/\varkappa)^3}{4^3 \sin^4(-4\pi/\varkappa) \sin^2(12\pi/\varkappa) \Gamma(1 - 4/\varkappa)^6} \cdots \oint_{\mathscr{P}(x_5, x_6)} (x_6 - u_3)^{-4/\varkappa} (u_3 - x_5)^{-4/\varkappa} \cdots$$
$$\cdots \oint_{\mathscr{P}(x_6, x_7)} (x_7 - u_2)^{12/\varkappa - 2} (u_2 - x_6)^{-4/\varkappa} \cdots \oint_{\mathscr{P}(x_7, x_8)} (x_8 - u_1)^{-4/\varkappa} (u_1 - x_7)^{12/\varkappa - 2} \cdots \mathrm{d}u_1 \, \mathrm{d}u_2 \, \mathrm{d}u_3, \quad \text{(A16)}$$

and we write the term of (39) including I_{667} as (figure 14)

$$\frac{n(\varkappa)^4 \Gamma(2 - 8/\varkappa)^3}{4^3 e^{-12\pi i/\varkappa} \sin^3(-4\pi/\varkappa) \sin(8\pi/\varkappa) \sin^2(12\pi/\varkappa) \Gamma(1 - 4/\varkappa)^6} \cdots \oint_{\mathscr{P}(x_6, x_7)} (x_7 - u_2)^{12/\varkappa - 2} (u_2 - x_6)^{-4/\varkappa} \cdots$$
$$\cdots \oint_{\mathscr{P}(x_6, u_2)} (u_2 - u_3)^{8/\varkappa} (u_3 - x_6)^{-4/\varkappa} \cdots \oint_{\mathscr{P}(x_7, x_8)} (x_8 - u_1)^{-4/\varkappa} (u_1 - x_7)^{12/\varkappa - 2} \cdots \mathrm{d}u_1 \, \mathrm{d}u_3 \, \mathrm{d}u_2, \quad \text{(A17)}$$

where the ellipses in (A16, A17) stand for omitted factors analytic over $\varkappa \in (0, 8) \times i\mathbb{R}$, over $u_1 \in A$, over $u_2 \in B$, and over $u_3 \in C$, where A, B, and C are open regions containing $\mathscr{P}(x_7, x_8)$, $\mathscr{P}(x_6, x_7)$, and $\mathscr{P}(x_5, x_6) \cup \mathscr{P}(x_6, x_7)$ respectively. Using the double-angle identity and (21) to write $\sin(8\pi/\varkappa) = -n(\varkappa) \sin(4\pi/\varkappa)$, we see that the prefactors of (A16) and (A17) are equal to within a phase factor. Among speeds $\varkappa \in (0, 8) \times i\mathbb{R}$, this common prefactor is singular at all κ such that $8/\kappa \in \mathbb{Z}^+ + 1$ or $12/\kappa \in \mathbb{Z}^+ + 1$. We divide these singularities into three cases.

5. $8/\kappa \in \mathbb{Z}^+ + 1$ and $4/\kappa \notin \mathbb{Z}^+$: The treatment of this case is identical to that of item 1 in section A 1.

6. $12/\kappa \in \mathbb{Z}^+ + 1$ and $4/\kappa \notin \mathbb{Z}^+$: The treatment of this case is identical to that of item 2 in section A 1.

7. $4/\kappa \in \mathbb{Z}^+$: In this case, almost every factor in (A16) vanishes or has a pole at $\varkappa = \kappa$. Upon writing (A16) as

$$\frac{n(\varkappa)^3}{4^3} \overbrace{\frac{\Gamma(2 - 8/\varkappa)^3}{\sin^3(-4\pi/\varkappa) \Gamma(1 - 4/\varkappa)^6}}^{1.} \cdots$$
$$\cdots \underbrace{\frac{1}{\sin(-4\pi/\varkappa)} \oint_{\mathscr{P}(x_5, x_6)}}_{2.} \cdots \underbrace{\frac{1}{\sin^2(12\pi/\varkappa)} \oint_{\mathscr{P}(x_6, x_7)} \cdots \oint_{\mathscr{P}(x_7, x_8)}}_{3.} \cdots \quad \text{(A18)}$$

and using (14), we see that κ is a removable singularity of the first, second, and third factors in (A18) and hence of (A16). Next, almost every factor in (A17) vanishes or has a pole at $\varkappa = \kappa$. Upon writing (A17) as

$$\frac{n(\varkappa)^4}{4^3 e^{-12\pi i/\varkappa}} \overbrace{\frac{\Gamma(2-8/\varkappa)^3}{\sin^3(-4\pi/\varkappa)\Gamma(1-4/\varkappa)^6}}^{1.} \cdots$$

$$\cdots \underbrace{\frac{1}{\sin^2(12\pi/\varkappa)} \oint_{\mathscr{P}(x_6,x_7)} \cdots \oint_{\mathscr{P}(x_7,x_8)}}_{2.} \cdots \underbrace{\frac{1}{\sin(8\pi/\varkappa)} \oint_{\mathscr{P}(x_6,u_2)}}_{3.} \cdots \quad \text{(A19)}$$

and using (14), we see that κ is a removable singularity of the first, second, and third factors in (A19) and hence of (A17).

From these facts, we conclude that the third octagon connectivity weight Π_3 (39) is an analytic function of $\varkappa \in (0,8) \times i\mathbb{R}$.

Finally, (46) gives a formula for the first octagon connectivity weight Π_1, and as (45) shows, this formula comprises two terms. One term is $-n(\varkappa)[n(\varkappa)^2 - 2]^{-1}$ multiplied by the third octagon connectivity weight Π_3 (39), and having found that the third weight is analytic over $\varkappa \in (0,8) \times i\mathbb{R}$, we conclude that this entire term has a pole only at the κ values in this region with $n(\kappa)^2 = 2$. Equation (42) gives the other term, denoted as Π_0. After replacing all simple integration contours in (42) with elementary Pochhammer contours via (16), we see that among the speeds $\varkappa \in (0,8) \times i\mathbb{R}$, the prefactor of each term in (42) is singular at all κ such that $8/\kappa \in \mathbb{Z}^+ + 1$, $12/\kappa \in \mathbb{Z}^+ + 1$, or $n(\kappa)^2 = 2$. By decomposing every term in (42) as we did in items 5–7 above, we show that (42), and therefore all of (46) is analytic at any κ such that $8/\kappa \in \mathbb{Z}^+ + 1$ or $12/\kappa \in \mathbb{Z}^+ + 1$. Thus, we are left with determining that (46) is analytic at all $\kappa \in (0,8) \times i\mathbb{R}$ such that

$$n(\kappa)^2 = 2 \quad \iff \quad \kappa = 16/q', \text{ where } q' \in \mathbb{Z}^+ + 1 \text{ is coprime with four.} \quad \text{(A20)}$$

To prove that the first octagon connectivity weight Π_1 (46) is analytic at $\varkappa = \kappa$, where κ satisfies (A20), is somewhat involved because showing that the bracketed linear combination of definite integrals in (46) vanishes there is no longer sufficient. Indeed, because any $\varkappa = \kappa$ satisfying (A20) is an order-two pole of the prefactor in (46), we must show

$$\overbrace{\begin{bmatrix} I_{357} - nI_{347} + n^2 I_{337} - 2nI_{237} + 2I_{137} \\ -nI_{257} + n^2 I_{247} + n^2 I_{227} - nI_{127} + I_{157} \\ -nI_{147} - (n^2 - 2)(nI_{567} - n^2 I_{667}) \end{bmatrix}}^{\text{bracketed linear combination in (46)}} (\varkappa \,|\, x_1, x_2, \ldots, x_8) = O((\varkappa - \kappa)^2) \quad \text{as } \varkappa \to \kappa \text{ (A20)}, \quad \text{(A21)}$$

in order to conclude that $\varkappa = \kappa$ is a removable singularity of the first octagon connectivity weight Π_1 (46).

To begin our proof of (A21), we first show that every κ satisfying (A20) is a zero of the left side of (A21). Obviously, the last two terms on the left side of (A21) vanish at $\varkappa = \kappa$ thanks to their vanishing common coefficient of $n(\kappa)^2 - 2$. Moreover, the sum of the remaining terms on the left side of (A21), which is the same as the sum of bracketed terms in (42) or boxed terms in figure 17, vanish at $\varkappa = \kappa$ too. To see why, we produce all of these terms by inserting an elementary Pochhammer contour $\mathscr{P}(y, z)$ into the following quantity (which vanishes thanks to (A6)),

$$\left(\prod_{\substack{i<j \\ i,j \neq 5}}^{6} (x_j - x_i)^{2/\kappa} \right) \left(\prod_{i \neq 5}^{6} |x_5 - x_i|^{1-6/\kappa} \right) [nI_{25} - I_{15} - I_{35}](\kappa \,|\, x_1, x_2, \ldots, x_6) = 0, \quad n(\kappa)^2 = 2. \quad \text{(A22)}$$

This new contour $\mathscr{P}(y, z)$ has two new endpoints $y < z$ and is in one of three locations. (If $\kappa > 4$, then this contour is simple thanks to (15).) This insertion promotes the left side of (A22) from an element of $\mathcal{S}_3$ to an element of $\mathcal{S}_4$.

The first location has $y < z < x_1$, and this insertion sends the left side of (A22) to

$$\left(\prod_{\substack{i<j \\ i,j \neq 5}}^{6} (x_j - x_i)^{2/\kappa} \right) \left((z - y)^{2/\kappa} \prod_{k \neq 5}^{6} (x_k - y)^{2/\kappa} (x_k - z)^{2/\kappa} \right)$$

$$\left((x_5 - y)^{1-6/\kappa} (x_5 - z)^{1-6/\kappa} \prod_{k \neq 5}^{6} |x_5 - x_k|^{1-6/\kappa} \right) [nI_{147} - I_{137} - I_{157}](\kappa \,|\, y, z, x_1, x_2, \ldots, x_6), \quad \text{(A23)}$$

where (26, 33) respectively define the contour integrals I_{ij} and I_{ijk}. The three terms in (A23) correspond one-to-one with the three terms to the right of the first brace, counting from the left, in the boxed part of figure 17. According to the discussion beneath (44) in [8], the inserted interval (y, z) is an identity interval of each of these terms.

The second (resp. third) location of the inserted contour has $x_1 < y < z < x_2$ (resp. $x_2 < y < z < x_3$), and similar to the first, this insertion produces the three terms to the right of the second (resp. third) brace, counting from the left, in the boxed part of figure 17. In each of these three locations, (y, z) is an identity interval of all generated terms. In total, these three insertions generate nine terms (the entire boxed collection in figure 17), and they combine to give the left side of (A21), excluding the last two terms multiplied by $n(\varkappa)^2 - 2$.

To finish our proof that the left side of (A21) vanishes at $\varkappa = \kappa$ satisfying (A20), we must show that the combination of nine terms described at the end of the previous paragraph vanishes at $\varkappa = \kappa$. To prove this claim for the sum of the three terms with $y < z < x_1$, we assume the contrary. Recalling that (y, z) is an identity interval of each of these terms, it follows from this assumption and theorem 2 and corollary 9 of [9] that (y, z) is an identity interval of their sum. In particular, (y, z) is not a two-leg interval of this sum, so its limit (8), with $x_{i+1} \mapsto z$ and $x_i \mapsto y$, may not be zero. But according to item 2 in the proof of lemma 6 of [8], this limit sends the sum to a multiple of (A22), which vanishes. From this contradiction, we conclude that the sum of three terms with $y < z < x_1$ vanishes at $\varkappa = \kappa$. The same argument shows that the sum of three terms with either $x_1 < y < z < x_2$ or $x_2 < y < z < x_3$ vanishes at $\varkappa = \kappa$ too. Because these nine terms combine to give the left side of (A21), excluding the last two terms multiplied

FIG. 23: With $\Gamma_1 = \mathscr{P}(x_7, x_8)$, $\Gamma_2 = \mathscr{P}(x_6, \Gamma_1)$, and $\Gamma_3 = \mathscr{P}(x_5, \Gamma_2)$ (figure 14) (we explain the notation $\mathscr{P}(x, \Gamma)$ above (47)), $\mathcal{J}(\varkappa | \Gamma_1, \Gamma_2, \Gamma_3)$ (7) is proportional to the boxed part of figure 17 plus terms that are $O((\varkappa - \kappa)^2)$ as $\varkappa \to \kappa$ (A20).

by $n(\varkappa)^2 - 2$, we conclude that the entire left side of (A21) vanishes at $\varkappa = \kappa$, as desired.

Having proven that $\varkappa = \kappa$ satisfying (A20) is a zero of the left side of (A21), we now show that its order is no less than two. For this purpose (and, for the sake of brevity, omitting any motivation), we reconsider the collection of Pochhammer contours $\Gamma_1 = \mathscr{P}(x_7, x_8)$, $\Gamma_2 = \mathscr{P}(x_6, \Gamma_1)$, and $\Gamma_3 = \mathscr{P}(x_5, \Gamma_2)$, illustrated in the left part of figure 14. (We explain the notation $\mathscr{P}(x, \Gamma)$ above (47).) Using the analysis surrounding items 1 and 2 of section II E (figures 20, 21), we deform Γ_2 and Γ_3 into a collection of simple contours (replaced by elementary Pochhammer contours via (16) if $\kappa \leq 4$) with endpoints among $x_1, x_2, \ldots, x_6$. We find

$$\mathcal{J}(\varkappa \,|\, \Gamma_1, \Gamma_2, \Gamma_3) = -64 e^{28\pi i/\varkappa} \sin^5\left(\frac{4\pi}{\varkappa}\right) \sin\left(\frac{12\pi}{\varkappa}\right) \Big\{ \text{boxed terms in figure 23} \Big\}(\varkappa). \qquad \text{(A24)}$$

Next, as indicated in figure 23, we rewrite the boxed terms of that figure as a sum of the boxed terms in figure 17 with seven other terms. These latter terms, appearing beneath "$O((n \pm \sqrt{2})^2)$" in figure 23, sort into three groups:

1. *sum of first three terms (top row):* We may generate this sum by inserting into every term of (A22) an elementary Pochhammer contour with two new endpoints between x_4 and x_5, as in the discussion surrounding (A22, A23). Because (A22) vanishes at $\varkappa = \kappa$ satisfying (A20), it follows from the second paragraph beneath (A23) that this sum vanishes too. Multiplied by $n(\varkappa)^2 - 2$, this sum thus has a zero at $\varkappa = \kappa$ with order at least two.

2. *sum of second three terms (middle row):* By the argument just given in the previous item 1, but with $(x_4, x_5) \mapsto (x_2, x_3)$, this sum also has a zero at $\varkappa = \kappa$ satisfying (A20) with order at least two.

3. *last term (bottom row):* With its factor of $[n(\varkappa)^2 - 2]^2$, this term manifestly has a zero at $\varkappa = \kappa$ with order at least two.

In light of items 1–3 immediately above, we may write (A24) as (figure 23)

$$\left[-64 e^{28\pi i/\varkappa} \sin^5\left(\frac{4\pi}{\varkappa}\right) \sin\left(\frac{12\pi}{\varkappa}\right) \right]^{-1} \mathcal{J}(\varkappa \,|\, \Gamma_1, \Gamma_2, \Gamma_3) = \Big\{ \text{boxed terms in figure 17} \Big\}(\varkappa) + O((\varkappa - \kappa)^2). \quad \text{(A25)}$$

Moreover, we may use (47, 55) (with the $m = 1$ phase factor of (55) adjusted to account for the fact that $c = 2N - 1 = 7 \neq 2N$ here, see the discussion beneath (55)) followed by (39) to write the left side of (A25) as

$$\left[-64 e^{28\pi i/\varkappa} \sin^5\left(\frac{4\pi}{\varkappa}\right) \sin\left(\frac{12\pi}{\varkappa}\right) \right]^{-1} \mathcal{J}\left(\varkappa \,\Big|\, \Gamma_1, \Gamma_2, \Gamma_3 \,\Big|\, x_1, x_2, \ldots, x_8\right)$$

$$= \left[\frac{n(\varkappa)^3 e^{-12\pi i/\varkappa} e^{-4\pi i(4-3)/\varkappa} e^{-4\pi i(6-3)/\varkappa} \Gamma(2 - 8/\varkappa)^3}{4^3 \sin^3(-4\pi/\varkappa) \sin(12\pi/\varkappa) \sin(16\pi/\varkappa) \sin(20\pi/\varkappa) \Gamma(1 - 4/\varkappa)^6} \right]^{-1} \Pi_3(\varkappa \,|\, x_1, x_2, \ldots, x_8)$$

$$\times \left[-64 e^{28\pi i/\varkappa} \sin^5\left(\frac{4\pi}{\varkappa}\right) \sin\left(\frac{12\pi}{\varkappa}\right) \right]^{-1} \left(\prod_{\substack{i<j \\ i,j \neq 7}}^{8} (x_j - x_i)^{-2/\varkappa} \right) \left(\prod_{k \neq 7}^{8} |x_7 - x_k|^{6/\varkappa - 1} \right) \qquad \text{(A26)}$$

$$= -n(\varkappa)[n(\varkappa)^4 - 3n(\varkappa)^2 + 1][n(\varkappa)^2 - 2][I_{567} - n I_{667}](\varkappa \,|\, x_1, x_2, \ldots, x_8)$$

$$= -n(\varkappa)[-1 + O(\varkappa - \kappa)][n(\varkappa)^2 - 2][I_{567} - n I_{667}](\varkappa \,|\, x_1, x_2, \ldots, x_8)$$

$$= \ n(\varkappa)[n(\varkappa)^2 - 2][I_{567} - n I_{667}](\varkappa \,|\, x_1, x_2, \ldots, x_8) + O((\varkappa - \kappa)^2).$$

After replacing the left side of (A25) with the bottom-right side of (A26) and rearranging, we ultimately find

$$\overbrace{\Big\{ \text{boxed terms in figure 17} \Big\}(\varkappa) - n(\varkappa)[n(\varkappa)^2 - 2][I_{567} - n I_{667}](\varkappa)}^{\text{left side of (A21)}} = O((\varkappa - \kappa)^2) \quad \text{as } \varkappa \to \kappa. \qquad \text{(A27)}$$

As indicated, the left side of (A27) matches the left side of (A21). Indeed, the boxed terms in figure 17 correspond one-to-one with all of the terms on the left side of (A21), except the last two terms, which are multiplied by $n(\varkappa)^2 - 2$. Also, these last two terms match the last two terms on the left side of (A27). Thus, the left sides of (A21) and (A27) match, so this proves the claim (A21). We conclude that all singularities $\varkappa = \kappa$ such that $n(\kappa)^2 = 2$ (A20) of the first octagon connectivity weight formula Π_1 (46) are removable. As such, Π_1 is an analytic function of $\varkappa \in (0, 8) \times i\mathbb{R}$.

Appendix B: Connectivity weights and logarithmic CFT

In this appendix, we investigate the appearance of logarithmic terms in Frobenius series expansions of the connectivity weights in powers of the differences of neighboring coordinates from the point $\boldsymbol{x} = (x_1, x_2, \ldots, x_{2N}) \in \Omega_0$. We anticipate that for sufficiently large $N \in \mathbb{Z}^+$, such logarithmic terms may appear if and only if κ equals an exceptional speed $\kappa_{q,q'} := 4q/q'$, where by definition, q and q' are coprime positive integers with $q > 1$ [8, 9]. (In the following discussion, we justify this expectation with CFT considerations. If the reader is not familiar with CFT, then he/she may skip our references to it, since they are only used to motivate the results.)

The prediction that logarithmic terms appear in Frobenius series expansions of some connectivity weights if $\kappa \in (0, 8)$ is an exceptional speed follows from CFT. Indeed, such speeds correspond with CFT minimal models [9], whose operator content is restricted to the Kac table [25–27]. Now, some connectivity weights do not respect this truncation in the sense that they (by hypothesis) satisfy the usual system of PDEs (2, 3) but not the larger "extended system" of CFT null-state PDEs that includes the former system. As discussed in section V of [9], the extra PDEs of the extended system arise from the presence of extra null-state conditions imposed on the affiliated CFT correlation functions, in addition to those associated with the CFT Kac operators $\psi_1 = \phi_{1,2}$ or $\phi_{2,1}$ that appear in the correlation functions. By conjecture 17 of that section, if the extended PDEs are not satisfied, then the corresponding connectivity weights, used to calculate observables, such as crossing probabilities [19, 31, 45], in the corresponding statistical mechanics models, must arise from operator content beyond the Kac table, extending the minimal model. Including these operators typically introduces logarithmic operators into the theory too [45–50]. Thus, logarithmic terms should appear in the Frobenius series expansions of some connectivity weights.

Many observables in statistical mechanics models with CFT descriptions, such as crossing probabilities, are closely related to the connectivity weights determined in this article. From the CFT perspective, it is customary to (loosely) "interpret" the latter functions, solving (2, 3) (and subject to the duality condition (10)), as CFT correlation functions of $2N$ one-leg boundary operators ψ_1 (or more generally as linear combinations of such functions) [6]:

$$F(x_1, x_2, \ldots, x_{2N}) = \langle \psi_1(x_1)\psi_1(x_2) \cdots \psi_1(x_{2N}) \rangle. \tag{B1}$$

In section IV of [9], we observe that the exceptional speed $\kappa_{q,q'}$ with $q' > 1$ corresponds to an $\mathcal{M}(p, p')$ CFT minimal model with $p = \max\{q, q'\} > 1$ and $p' = \min\{q, q'\} > 1$. In the logarithmic extension of this model, we find a pre-logarithmic operator at the $(1, q)$ (resp. $(q, 1)$) position of the Kac grid if $\kappa > 4$ (resp. $\kappa \le 4$). This operator is beyond the edge of the Kac table, whose first column (resp. row) terminates at $(1, q-1)$ (resp. $(q-1, 1)$). Loosely speaking, because we may advance by at most one position up (resp. left) along the leftmost column (resp. bottommost row) of the Kac grid through fusion with a one-leg boundary operator, we must fuse together at least $q - 1$ adjacent one-leg boundary operators in order to observe the pre-logarithmic operator. However, we may advance from the $(1, 2)$ (resp. $(2, 1)$) position in the Kac grid to at most the $(1, N+1)$ (resp. $(N+1, 1)$) position (i.e., we may generate at most an N-leg boundary operator) by consecutive fusions of adjacent one-leg boundary operators within the $2N$-point function (B1). Hence, pre-logarithmic operators play significant roles in connectivity weights only if $q - 1 \le N$. These cases correspond exactly with all of those for which the Temperley-Lieb set $\mathcal{B}_N \subset \mathcal{S}_N$ (defined in [8]) of solutions for the system (2, 3) is not a basis of $\mathcal{S}_N$. (See Lemma 6 of [8].)

Next, we find a logarithmic operator at the $(1, q+1)$ (resp. $(q+1, 1)$) position of the Kac grid. To arrive at this position, we must fuse together at least q adjacent one-leg boundary operators, or equivalently, we must fuse a pre-logarithmic operator with an adjacent one-leg boundary operator. By the arguments of the previous paragraph, it follows that logarithmic operators play significant roles in connectivity weights only if $q \le N$. In particular, logarithmic terms may appear in Frobenius series expansions of $2N$-point connectivity weights only if $q \le N$.

In summary, pre-logarithmic fusions occur in all cases with $q \le N + 1$, and both pre-logarithmic and logarithmic fusions occur in all cases with $q \le N$. However, we should note that this last point does not imply that Frobenius series expansions of any $2N$-point connectivity weight must have logarithmic terms if $q \le N$. Indeed, in some cases, correlation functions (B1) with such pre-logarithmic and logarithmic operators may lack logarithmic terms.

Rather than considering all cases, for brevity we give examples of elements of $\mathcal{S}_N$ with Frobenius series expansions as described above for $\kappa = \kappa_{q,q'}$ with $q = 2$ and for $q = 3 = N$ only. (The corresponding results for Frobenius series expansions for the case $\kappa = \kappa_{2,q'} = 8/r$ with $r > 1$ odd are already given in theorem 2 of [9]. See also appendix A of [9].) The work that we present below generalizes to the remaining cases of $q = 3 < N$ and $3 < q \le N$ in an evident way. For convenience, we adopt the notation of [6–9]

$$\psi_s(x) = \begin{cases} \phi_{1,s+1}(x), & \kappa > 4 \\ \phi_{s+1,1}(x), & \kappa \le 4 \end{cases}, \quad \theta_s := \left\{ \begin{array}{ll} h_{1,s+1}, & \kappa > 4 \\ h_{s+1,1}, & \kappa \le 4 \end{array} \right\} = \frac{s(2s + 4 - \kappa)}{2\kappa}, \tag{B2}$$

where $\phi_{1,s}$ (resp. $\phi_{s,1}$) is a CFT $(1, s)$ (resp. $(s, 1)$) Kac operator (and we call ψ_s an *s-leg boundary operator*), and we

adopt the following notation of [45]:

$$\mathbf{1} := \psi_0 \text{ (the identity operator)}, \quad \phi := \psi_1, \quad \upsilon := \psi_2, \quad \psi := \psi_3. \tag{B3}$$

We reference articles in logarithmic CFT below that use the CFT central charge instead of the SLE_κ parameter κ. For $\kappa \neq 4$ (resp. $\kappa = 4$), these quantities are related two-to-one (resp. one-to-one) via

$$c(\kappa) = \frac{(6-\kappa)(3\kappa - 8)}{2\kappa}, \quad \kappa > 0. \tag{B4}$$

Furthermore, if $c(\kappa) = c(\hat{\kappa})$, then $\hat{\kappa} = 16/\kappa$, with one speed in the dense phase ($\kappa > 4$) of SLE_κ and the other in the dilute phase ($0 < \kappa \leq 4$). The relation between κ and $\hat{\kappa}$ is known as *duality* in SLE_κ [42, 43].

To begin, we consider the exceptional speeds $\kappa = \kappa_{2,q'}$ (i.e., $8/\kappa = r \in 2\mathbb{Z}^+ + 1$). One speed belonging to this case is $\kappa = 8/3$, and this example is unusual because the one-leg boundary operator $\phi = \phi_{2,1}$ is pre-logarithmic, sitting just outside the Kac table of the $\mathcal{M}(3,2)$ minimal model [25–27]. Thus, the first logarithmic operators for this speed appear in the operator product expansion (OPE) of $\phi(x)$ with $\phi(x+\varepsilon)$. Using CFT arguments, V. Gurarie determined this OPE, finding

$$\phi(x)\phi(x+\varepsilon) \underset{\varepsilon \to 0}{\sim} a_0 \varepsilon^{-2\theta_1} \mathbf{1} + b_0 \varepsilon^{-2\theta_1 + \theta_2} \hat{\upsilon}(x) + \cdots + (b_0 \log \varepsilon + c_0)\varepsilon^{-2\theta_1 + \theta_2} L_{-2}\mathbf{1}(x) + \cdots, \quad \kappa = 8/3. \tag{B5}$$

(see (45) of [46], but note that our $L_{-2}\mathbf{1}(x)$ is the stress-energy tensor $T(x)$ in [46]) Here, $\hat{\upsilon}$ is the logarithmic partner that couples with $L_{-2}\mathbf{1}$ [46], and (B2, B3) give the other powers and operators of (B5). Moreover, the ellipses following the second and third term of (B5) stand for descendent terms of the corresponding conformal family [26], with factors respectively of the form $b_m \varepsilon^m$ and $(b_m \log \varepsilon + c_m)\varepsilon^m$ for all $m \in \mathbb{Z}^+$. The regular and logarithmic operators of (B5) belong to the same staggered logarithmic module [47, 48]. As such, if we fix the value of a_0, then the b_m are fixed for all $m \in \mathbb{Z}^+ \cup \{0\}$. In particular if $a_0 = 0$ then $b_m = 0$.

The terms of (B5) with the coefficients c_m are algebraically independent of those with coefficients a_0 and b_m. Indeed, the invariance of the logarithmic CFT operator algebra under the shift $\hat{\upsilon} \mapsto \hat{\upsilon} + kL_{-2}\mathbf{1}$ induces this feature. This symmetry of the operator algebra implies that the descendants of $L_{-2}\mathbf{1}$ effectively form a second, independent fusion channel, even though they are produced from within the logarithmic fusion channel. Here, we have glossed over a logarithmic CFT subtlety, namely that if the staggered module appears in this fusion, then $a_0 \neq 0$. However, connectivity weights, which are the subject of this article, often correspond to a difference of two staggered module blocks with different values for c_0, which effectively allows $a_0 = b_m = 0$ while $c_0 \neq 0$.

Another speed belonging to the case $\kappa = \kappa_{2,q'}$ is $\kappa = 8$. This example is also special because κ sits on the border of the range $(0,8)$ of SLE_κ speeds to which the results of our previous articles [6–9] apply. Assuming that theorems 1 and 2 of [9] are true if $\kappa = 8$, we again consider the operator product expansion (OPE) of $\phi(x)$ with $\phi(x + \varepsilon)$. V. Gurarie explicitly determines this OPE in [49]. Summing (11) and (12) of [49], his result amounts to

$$\phi(x)\phi(x+\varepsilon) \underset{\varepsilon \to 0}{\sim} (a_0 + b_0 \log \varepsilon)\varepsilon^{-2\theta_1 + \theta_0} \mathbf{1} + \cdots + b_0 \varepsilon^{-2\theta_1 + \theta_2} \hat{\upsilon}(x) + \cdots, \quad \kappa = 8, \tag{B6}$$

where the powers, operators, ellipses, and coefficients are as described beneath (B5), except that $\hat{\upsilon}$ is now a logarithmic partner to $\mathbf{1}$. (From (B2), we observe that $\theta_0 = 0$, and $\theta_2 = 0$ if $\kappa = 8$. In spite of this, we exhibit these quantities in (B6) to capture the structure of a two-point OPE [26].) Now, if we insert either of (B5, B6) with $x = x_i$ and $x+\varepsilon = x_{i+1}$ for some $i \in \{1, 2, \ldots, 2N-1\}$ into the correlation function (B1) and use the formula (B2) for the conformal weights θ_s, we find an expansion of the form (π_i projects the ith coordinate from $\boldsymbol{x} \in \Omega_0$, and $8/\kappa = r \in 2\mathbb{Z}^+ - 1$)

$$F(\boldsymbol{x}) = (x_{i+1} - x_i)^{1 - 6/\kappa} \sum_{m=0}^{r-2} [(A_m \circ \pi_i)(\boldsymbol{x})] (x_{i+1} - x_i)^m + (x_{i+1} - x_i)^{2/\kappa} \sum_{m=0}^{\infty} [(B_m \circ \pi_i)(\boldsymbol{x})] (x_{i+1} - x_i)^m$$
$$+ \log(x_{i+1} - x_i)(x_{i+1} - x_i)^{2/\kappa} \sum_{m=0}^{\infty} [(C_m \circ \pi_i)(\boldsymbol{x})] (x_{i+1} - x_i)^m. \tag{B7}$$

(We note that, with $8/\kappa = r \in \mathbb{Z}^+$, the powers of the second and third series begin where the powers of the first series end.) As expected, the form (B7) exactly matches the known form of the Frobenius series expansion for a generic solution $F \in \mathcal{S}_N$ with $8/\kappa = r \in 2\mathbb{Z}^+ + 1$. (See (18) and appendix A of [9].) As stated in theorem 2 of [9], if $A_0 = 0$ or $C_0 = 0$ in (B7), then we have $A_m = 0$ for all $m \in \{0, 1, \ldots, r-2\}$ and $C_m = 0$ for all $m \in \mathbb{Z}^+ \cup \{0\}$. (Furthermore, if $A_0 = B_0 = 0$, then F is zero.)

It is interesting to observe the appearance of logarithms in the Frobenius series expansions of some of the connectivity weights in the case $\kappa = \kappa_{2,q'}$. As the sentence ending the paragraph above (B1) implies, not every connectivity weight

contains a logarithmic term as $x_{i+1} \to x_i$ for some fixed $i \in \{1, 2, \ldots, 2N - 1\}$. As an example, we let $N = 2$ and consider the rectangle connectivity weight $\Pi_1(\kappa)$ (24, 25). As we send $x_2 \to x_1$, we observe only the second series (i.e., $A_m = C_m = 0$, $B_m \neq 0$) in (B7), generated solely by the regular operator in the logarithmic pair, that is, $L_{-2}\mathbf{1}$ in (B5) and $\mathbf{1}$ in (B6). But if we consider the rectangle connectivity weight $\Pi_2(\kappa)$, obtained by changing the integration contour in (24) to $\mathscr{P}(x_2, x_3)$ (or equivalently replacing $\lambda \mapsto 1 - \lambda$ in (25)), then we observe all of the three series (i.e., $A_m, B_m, C_m \neq 0$) in (B7), including the series multiplied by a logarithm. In particular, if $\kappa = 8$, then a logarithm appears in the leading term of (B7), and if $\kappa = 8/3$, then a logarithm appears in the second-to-leading term of (B7).

In appendix A of [9], we find that whether $A_m = C_m = 0$ or $A_m, C_m \neq 0$ in (B7) depends on how an integration contour interacts with the contracting interval (x_i, x_{i+1}). Assuming that neither x_i nor x_{i+1} bears the conjugate charge (see below (6)), we summarize those findings as follows: with $8/\kappa \in 2\mathbb{Z}^+ + 1$, if no integration contour of $F \in \mathcal{S}_N \setminus \{0\}$ touches or surrounds either of x_i and x_{i+1}, or if one contour of (6) surrounds both of x_i and x_{i+1}, then $A_m = C_m = 0$ in (B7), so no logarithm appears in the expansion (B7). Otherwise $A_m, C_m \neq 0$, so a logarithm multiplying a Frobenius series does appear in the expansion (B7). (We expect that this is true for $\kappa = 8$ too.)

Next, we consider the exceptional speeds $\kappa = \kappa_{3,q'}$ (i.e., $12/\kappa = r \in \mathbb{Z}^+ + 1$ is coprime with three). Just as with the previous case $\kappa = \kappa_{2,q'}$, we find logarithmic terms in Frobenius series expansions of connectivity weights. But now (as discussed beneath (B1)), we must bring together not just two but at least three adjacent points, $x_i < x_{i+1} < x_{i+2}$ with $i \in \{1, 2, \ldots, 2N - 2\}$, in order to observe such a term. To anticipate the result, we recall the OPE of three adjacent one-leg boundary operators for $\kappa = \kappa_{3,2} = 6$, from appendix A of [45]:

$$\{\phi(x)\phi(x + \lambda\varepsilon)\}_v \phi(x + \varepsilon) \underset{\varepsilon \to 0}{\sim} \Pi_1(\lambda)\varepsilon^{-3\theta_1 + \theta_1}\phi(x) + \varepsilon^{-3\theta_1 + \theta_3}\mathcal{F}_3(\lambda)\hat{\psi}(x)$$
$$+ \varepsilon^{-3\theta_1 + \theta_3}\Big[\mathcal{F}_2(\lambda) + \log(c\,\varepsilon)\mathcal{F}_3(\lambda)\Big]\partial\phi(x) + \cdots, \quad \lambda \in (0, 1), \quad \kappa = 6. \quad \text{(B8)}$$

Here, the powers and operators are given in (B2, B3), $\hat{\psi}$ is the logarithmic partner of the first descendant $L_{-1}\phi = \partial\phi$ of ϕ, c is an unspecified constant, the notation $\{\phi(x)\phi(y)\}_v$ indicates that we allow only the two-leg channel to propagate between the enclosed one-leg boundary operators $\phi(x)$ and $\phi(y)$ (i.e., we restrict the OPE of these two operators to contain the two-leg boundary operator only), $\Pi_1(\lambda)$ is given by (25) with $\kappa = 6$, now strictly a function of only λ (indeed, it is Cardy's formula [19] for critical percolation), and finally

$$\mathcal{F}_2(\lambda) := \frac{3\Gamma(5/3)}{4\Gamma(1/3)^2}\lambda^{4/3}(1 - \lambda)^{1/3}\,_3F_2(2/3, 1, 1; 2, 7/3 \,|\, \lambda), \quad \mathcal{F}_3(\lambda) := \frac{\sqrt{3}\Gamma(5/3)^2}{\pi\Gamma(7/3)}\lambda^{1/3}(1 - \lambda)^{1/3}. \quad \text{(B9)}$$

(Although the conformal weight θ_1 (B2) vanishes for $\kappa = 6$, we include it in (B8) to exhibit the formal structure of an OPE [26]. Moreover, as the powers of (B8) suggest, $\partial\phi$ is a primary operator with conformal weight $\theta_3 = 1$. Its consequent close relation with ψ_3 is exploited to compute new percolation crossing observables in [51].)

Inserting (B8) with $x = x_i$, $x + \lambda\varepsilon = x_{i+1}$, and $x_{i+2} = x + \varepsilon$ for some $i \in \{1, 2, \ldots, 2N - 2\}$, $\varepsilon > 0$, and $\lambda \in (0, 1)$ into (B1) then gives a candidate form for the expansion of an element of $\mathcal{S}_N$ if $12/\kappa = r \in \mathbb{Z}^+ + 1$ is coprime with three. The form is (here, $\pi_{i,i+1}$ projects the ith and $(i + 1)$th coordinate from $\boldsymbol{x} \in \Omega_0$)

$$F\Big(x_1, x_2, \ldots, x_i,\, x_{i+1} = (1 - \lambda)x_i + \lambda x_{i+2},\, x_{i+2}, \ldots, x_{2N}\Big) =$$
$$(x_{i+2} - x_i)^{1 - 6/\kappa}\sum_{m=0}^{r-2}\Big[A_m\big(\lambda, \pi_{i,i+1}(\boldsymbol{x})\big)\Big](x_{i+2} - x_i)^m + (x_{i+2} - x_i)^{6/\kappa}\sum_{m=0}^{\infty}\Big[B_m\big(\lambda, \pi_{i,i+1}(\boldsymbol{x})\big)\Big](x_{i+2} - x_i)^m$$
$$+ \log(x_{i+2} - x_i)(x_{i+2} - x_i)^{6/\kappa}\sum_{m=0}^{\infty}\Big[C_m\big(\lambda, \pi_{i,i+1}(\boldsymbol{x})\big)\Big](x_{i+2} - x_i)^m. \quad \text{(B10)}$$

Rather than prove that all elements of $\mathcal{S}_N$ admit a Frobenius expansion of the form (B10) if $12/\kappa = r \in \mathbb{Z}^+ + 1$ is coprime with three (and $N > 2$, see below), for brevity we limit ourselves to showing that the hexagon connectivity weight $\Pi_1(\kappa)$ (28) has this feature. The analysis closely follows the arguments of appendix A in [9].

To find a Frobenius series expansion for the hexagon connectivity weight $\Pi_1(\kappa)$ (28) in the form (B10), we consider the formula for $\Pi_1(\kappa)$ in two pieces. With $\varkappa \in (0, 8)$ denoting an arbitrary SLE$_\kappa$ speed and $\kappa \in (0, 8)$ denoting an exceptional speed with $12/\kappa = r \in \mathbb{Z}^+ + 1$ coprime with three (and recalling definitions (21, 26)), we have

$$\Pi_1(\varkappa) \propto [nI_{25} - I_{15} - I_{35}](\varkappa) \propto \underbrace{\sin(4\pi/\varkappa)I_{15}(\varkappa) + \sin(8\pi/\varkappa)I_{25}(\varkappa)}_{1.} + \underbrace{\sin(4\pi/\varkappa)I_{35}(\varkappa)}_{2.}. \quad \text{(B11)}$$

Next, we show that the first brace and the second brace in (B11) each equal a Frobenius series or a sum of Frobenius series of the form (B10) with $i = 1$.

To begin, we study the first brace in (B11). The analysis of this term is somewhat similar to what we find in case 2 of appendix A in [9]. Supposing that $\varkappa = \kappa > 4$ so the integration contours of I_{ij} are simple, the integrand of $I_{15}(\kappa)$ (resp. $I_{25}(\kappa)$) (26), as a function of u_2 (integrated along $[x_1, x_2]$ (resp. $[x_2, x_3]$)), has no branch cut along the segment $[x_3, x_4]$. (Indeed, this immediately follows from the property that $12/\kappa \in \mathbb{Z}^+$.) In light of this fact, it is easy to see that the two terms of the first brace in (B11) combine to give an integration around a simple loop surrounding $[x_1, x_3]$. (If $\kappa \leq 4$, then the integration contours of $I_{ij}(\kappa)$ are not simple but are replaced by Pochhammer contours, as in (16). By analytically continuing the first part of the right side of (B11) to the region $\varkappa \in (0, 8) \times i\mathbb{R}$, we find the same result.) Because this loop is not tangled with the points x_1, x_2, and x_3 inside it, the loop is not constrained to contract to a point as we send $x_3, x_2 = (1 - \lambda)x_1 + \lambda x_3 \to x_1$. Hence, the integration around this loop, contained in the first brace of (B11), is $O(1)$ in this limit. After multiplying this integration by the power-law factors in (28) (which are omitted from (B11)), and now with $x_2 = (1 - \lambda)x_1 + \lambda x_3$, we find that these terms contribute exclusively to the second series on the right side of (B10) with $i = 1$ if $\varkappa = \kappa$. This outcome is similar to what we find in case 2 of appendix A in [9].

Next, we study the second part of the right side of (B11). The analysis of this term is somewhat similar to what we find in case 3 of appendix A in [9]. Again supposing that $\varkappa > 4$ so the integration contours of I_{ij} are simple, we use (26) to write

$$I_{35}(\varkappa \,|\, x_1, x_2, \ldots, x_6) = \int_{x_5}^{x_6} \cdots I_3(\varkappa \,|\, x_1, x_2, \ldots, x_5, u_1, x_6) \, \mathrm{d}u_1, \tag{B12}$$

$$I_k(\varkappa \,|\, x_1, x_2, \ldots, x_7) := \int_{x_k}^{x_{k+1}} \mathcal{N}\left[\prod_{j=1}^{7}(u_2 - x_j)^{\beta_j}\right] \mathrm{d}u_2, \quad x_8 := x_1, \quad \int_{x_7}^{x_8} := \int_{x_7}^{\infty} + \int_{-\infty}^{x_8}, \tag{B13}$$

where the ellipses in (B12) stand for omitted factors from the integrand of (26), we have relabeled $u_1 \mapsto x_6$ and $x_6 \mapsto x_7$ in (B13) (but not in (B12)), $\mathcal{N}[\,\ldots\,]$ orders the differences of its enclosed factors so $I_k(\varkappa)$ is real-valued, and

$$\beta_j = -4/\varkappa, \quad j \in \{1, 2, 3, 4, 7\}, \quad \beta_5 = 12/\varkappa - 2, \quad \beta_6 = 8/\varkappa. \tag{B14}$$

The integrand of each $I_k(\varkappa)$, as a function of u_2, is manifestly analytic in the upper and lower half-planes. Furthermore, because $\beta_1 + \beta_2 + \cdots + \beta_7 = -2$, this integrand has no singularity at infinity either. As such, we find that

$$\sum_{k=1}^{7} e^{\pm \pi i \sum_{l=1}^{k} \beta_l} I_k = \sum_{k=1}^{6} e^{\pm \pi i \sum_{l=1}^{k} \beta_l} I_k + I_7 = 0 \tag{B15}$$

after integrating the integrand of I_k around a large semicircle in the upper half-plane ($-$ sign in the exponent) or lower half-plane ($+$ sign in the exponent) with its base flush against the real axis and sending the radius of that semicircle to infinity. Solving (B15) for I_3 in terms of I_1, I_2, I_4, I_5, and I_6 gives (compare with (A7) of [9])

$$I_3 = \frac{1}{\sin \pi(\beta_1 + \beta_2 + \beta_3)}\left[-\sin(\pi\beta_1)I_1 - \sin \pi(\beta_1 + \beta_2)I_2 - \sum_{k=4}^{6}\left(\sin \pi \sum_{l=1}^{k} \beta_l\right) I_k\right]. \tag{B16}$$

From (B14), we see that the factor multiplying the bracketed terms on the right side of (B16) is $-\sin(12\pi/\varkappa)^{-1}$ and thus has a simple pole at $\varkappa = \kappa = 12/r$. But because I_3 is an analytic function of $\varkappa \in (0, 8) \times i\mathbb{R}$ (after we extend it to this region via (16)), the bracketed factor on the right side of (B16) must vanish at $\varkappa = \kappa$. Hence, to find $I_3(\kappa)$, we expand the terms and denominator on the right side of (B16) to first order in $\varkappa - \kappa$ and send $\varkappa \to \kappa$. We find

$$I_3(\kappa) = (-1)^r \left(\frac{\kappa^2}{12\pi}\right) \sum_{k=4}^{6}\left[\left(\sin \pi \sum_{l=1}^{k} \beta_l(\kappa)\right) \partial_\varkappa I_k(\kappa) + \left(\cos \pi \sum_{l=1}^{k} \beta_l(\kappa)\right)\left(\pi \sum_{l=1}^{k} \partial_\varkappa \beta_l(\kappa)\right) I_k(\kappa)\right] \tag{B17}$$

$$+ (-1)^r \left(\frac{\kappa^2}{12\pi}\right)\left[\cos\left(\frac{4\pi}{\kappa}\right)\left(-\frac{4\pi}{\kappa^2}\right) I_1(\kappa) + \sin\left(\frac{4\pi}{\kappa}\right) \partial_\varkappa I_1(\kappa)\right] \tag{B18}$$

$$+ (-1)^r \left(\frac{\kappa^2}{12\pi}\right)\left[\cos\left(\frac{8\pi}{\kappa}\right)\left(-\frac{8\pi}{\kappa^2}\right) I_2(\kappa) + \sin\left(\frac{8\pi}{\kappa}\right) \partial_\varkappa I_2(\kappa)\right]. \tag{B19}$$

Because the terms in (B17) do not involve an integration contour with an endpoint at x_1, x_2 or x_3, they are analytic at $x_1 = x_2 = x_3$. Multiplied by the power-law factors in (28) (not included in (B11)), and now with $x_2 = (1 - \lambda)x_1 + \lambda x_3$, they contribute exclusively to the second sum in (B10) with $i = 1$.

Next, the term in (B18) (resp. (B19)) with $I_1(\kappa)$ (resp. $I_2(\kappa)$) not differentiated has an integration contour with an endpoint at x_1, x_2, or x_3. As a result, its asymptotic behavior is more complicated. Substituting $u_2(t) = x_i(1-t) + x_{i+1}t$ with $i = 1$ (resp. $i = 2$) and $x_2 = (1-\lambda)x_1 + \lambda x_3$ into (B13) with $k = 1$ (resp. $k = 2$), we find that this term is $O((x_3 - x_1)^{1-12/\kappa})$ as $x_3, x_2 \to x_1$ with $\lambda \in (0,1)$ fixed. Multiplied by the power-law factors in (28) (not included in (B11), and now with $x_2 = (1-\lambda)x_1 + \lambda x_3$), it contributes exclusively to the first sum in (B10) with $i = 1$.

The behavior as $x_3, x_2 = (1-\lambda)x_1 + \lambda x_3 \to x_1$ of the final terms in (B18) and (B19) with $I_1(\kappa)$ and $I_2(\kappa)$ respectively differentiated is more complicated and interesting. Using (B13), after inserting $u_2(t) = (1-t)x_i + tx_{i+1}$ with $i = 1$ (resp. $i = 2$) into the former (resp. latter) term and inserting $x_2 = (1-\lambda)x_1 + \lambda x_3$ with $\lambda \in (0,1)$ into both terms, we find

$$I_1\Big(x_1, x_2 = (1-\lambda)x_1 + \lambda x_3, \ldots, x_7\Big) = \lambda^{1-8/\varkappa}(x_3 - x_1)^{1-12/\varkappa}$$
$$\times \int_0^1 t^{-4/\varkappa}(1-t)^{-4/\varkappa}(1-\lambda t)^{-4/\varkappa}\mathcal{N}\left[\prod_{j=4}^7 \big[x_j - (1-\lambda t)x_1 - \lambda t x_3\big]^{\beta_j(\varkappa)}\right]\mathrm{d}t, \qquad \text{(B20)}$$

$$I_2\Big(x_1, x_2 = (1-\lambda)x_1 + \lambda x_3, \ldots, x_7\Big) = (1-\lambda)^{1-8/\varkappa}(x_3 - x_1)^{1-12/\varkappa}\int_0^1 \big[1 - (1-\lambda)(1-t)\big]^{-4/\varkappa}t^{-4/\varkappa}(1-t)^{-4/\varkappa}$$
$$\times \mathcal{N}\left[\prod_{j=4}^7 \big[x_j - (1-\lambda)(1-t)x_1 - (1-(1-\lambda)(1-t))x_3\big]^{\beta_j(\varkappa)}\right]\mathrm{d}t. \qquad \text{(B21)}$$

With (B20, B21), the asymptotic behaviors of $\partial_\varkappa I_1(\kappa)$ and $\partial_\varkappa I_2(\kappa)$ as $x_3, x_2 = (1-\lambda)x_1 + \lambda x_3 \to x_1$ become evident. Indeed, differentiating (B20, B21) with respect to $\varkappa$, and setting $\varkappa = \kappa$ in the result, we find

$$(-1)^r\left(\frac{\kappa^2}{12\pi}\right)\left[\sin\left(\frac{4\pi}{\kappa}\right)\partial_\varkappa I_1(\kappa\,|\,x_1, x_2, \ldots, x_7) + \sin\left(\frac{8\pi}{\kappa}\right)\partial_\varkappa I_2(\kappa\,|\,x_1, x_2, \ldots, x_7)\right] =$$

$$\frac{(-1)^r}{\pi}\log(x_3 - x_1)\overbrace{\left[\sin\left(\frac{4\pi}{\kappa}\right)I_1(\kappa\,|\,x_1, x_2, \ldots, x_7) + \sin\left(\frac{8\pi}{\kappa}\right)I_2(\kappa\,|\,x_1, x_2, \ldots, x_7)\right]}^{1.} + (-1)^r\left(\frac{\kappa^2}{12\pi}\right)$$

$$\times (x_3 - x_1)^{1-12/\kappa}\overbrace{\left[\sin\left(\frac{4\pi}{\kappa}\right)\partial_\varkappa\left\{\begin{matrix}\lambda^{1-8/\varkappa}\times \text{ integral on}\\ \text{right side of (B20)}\end{matrix}\right\} + \sin\left(\frac{8\pi}{\kappa}\right)\partial_\varkappa\left\{\begin{matrix}(1-\lambda)^{1-8/\varkappa}\times \text{ integral}\\ \text{on right side of (B21)}\end{matrix}\right\}\right]}^{2.}\Bigg|_{\varkappa=\kappa}. \qquad \text{(B22)}$$

The right side of (B22) gives the asymptotic behavior as $x_3, x_2 = (1-\lambda)x_1 + \lambda x_3 \to x_1$ of the sum of terms in (B18) and (B19) that have $I_1(\kappa)$ and $I_2(\kappa)$ respectively differentiated. As a part of $I_3(\kappa)$, these terms also form a part of $I_{35}(\kappa)$ via (B12). In particular, the first brace in (B22) gives rise to terms of $I_{35}(\kappa)$ whose sum is proportional to the first brace in (B11). In the paragraph beneath (B11), we determine that this brace contributes exclusively to the second series on the right side of (B10). However, $\log(x_3 - x_1)$ multiplies this quantity in our present situation (B22). Hence, the first brace in (B22) contributes to the third series on the right side of (B10) with $i = 1$. In fact, these latter terms are the only terms appearing on the right side of (B11) that contribute to the logarithmic series of the Frobenius series expansion (B10) for $\Pi_1(\kappa)$ (28).

Finally, the terms beneath the second brace in (B22) are analytic at $x_3 = x_2 = x_1$. Multiplied by the preceding factor of $(x_3 - x_1)^{1-12/\kappa}$ in (B22) and then by the power-law factors in (28) (not included in (B11), and now with $x_2 = (1-\lambda)x_1 + \lambda x_3$), these last terms evidently give a Frobenius series in powers of $x_3 - x_1$ and with indicial power $1 - 6/\kappa$. Because $12/\kappa = r \in \mathbb{Z}^+$, the difference $r - 1$ between this power and $6/\kappa$ is a positive integer. Hence, the terms beneath the second brace in (B22) contribute exclusively to both the first and second sum in (B10) with $i = 1$. Putting everything together, we conclude that $\Pi_1(\kappa)$ (28) equals a sum of Frobenius series of the form (B10) with $i = 1$. (So far for the case where $12/\kappa = r \in \mathbb{Z}^+ + 1$ is coprime with three, we have assumed that $\kappa > 4$. As usual, we easily extend these results to other such $\kappa \in (0,4]$ via analytic continuation (16) to $\varkappa \in (0,8) \times i\mathbb{R}$.)

To finish, we note some interesting facts. First, the first and third series of (B10) (and in particular, the third series, which has a logarithm) do not arise from terms that sum to give an integration contour surrounding the interval to be collapsed, which is $[x_1, x_3]$ here. Indeed, the terms that sum to give such a contour are those of the first brace in (B11). Rather, the first and third series of (B10) arise from terms with an integration contour terminating at just one endpoint of the interval to be collapsed. All of these terms arise from the second brace in (B11). (This is exactly the same circumstance that we observed in appendix A of [9], where we investigated the case with $8/\kappa \in 2\mathbb{Z}^+ + 1$. There, we referred to these two scenarios as case 2 and case 3 respectively.)

A second observation follows from the above analysis. Either both the first sum and the third sum (containing the logarithm) are present together on the right side of (B10) ($A_m, C_m \neq 0$), or neither is present ($A_m = C_m = 0$), at least

if $N > 2$. (See the following paragraph for $N = 2$.) Previously, we observed that the series expansion (B7) in the case with $8/\kappa = r \in 2\mathbb{Z}^+ - 1$ has the same property. (See the discussion beneath (B7).) This is natural from the following CFT point-of-view: the expansion of (B8) either contains contributions for all elements of the staggered logarithmic module (i.e., ϕ, $\hat{\psi}$, and $\partial\phi$), or only contributions from the regular partner $\partial\phi$. We may isolate the $\partial\phi$ contributions in the OPE (B8) by altering the value of c in this OPE and subtracting the result from (B8). This subtraction leaves only terms proportional to $\varepsilon^{-3\theta_1 + \theta_3}\mathcal{F}_3(\lambda)\partial\phi(x)$ and its descendants, and these in turn produce only the terms of the second series in (B10). Thus, reasoning using logarithmic CFT explains this second observation.

For a final observation, we consider the exceptional case $N = 2$ mentioned in the previous paragraph. Indeed, if $12/\kappa = r \in \mathbb{Z}^+ + 1$ is coprime with three, then any element of $\mathcal{S}_2$ admits the expansion (B10) with $C_m = 0$ for all $m \in \mathbb{Z}^+$, although we may have $A_m \neq 0$. This fact demonstrates the at times wraithlike behavior of logarithmic terms in logarithmic CFT, or more precisely, the fact that N must be sufficiently large in order for such terms to appear in Frobenius series expansions of correlation functions. We can justify this claim for $\kappa = 6$ and $i = 1$ by considering the rectangle crossing weight $\Pi_1(\kappa = 6)$ (24) and the constant solution 1. Taken together, these two functions span $\mathcal{S}_2$ (but only if $\kappa = 6$). Obviously, the claim is true for the latter solution, so we turn our attention to the former. Inserting the OPE (B8) into the correlation function (B1) with $N = 2$, $x_1 = x$, $x_2 = x + \lambda\varepsilon$, $x_3 = x + \varepsilon$, $\varepsilon > 0$, and $\lambda \in (0,1)$ gives (with $\kappa = 6$, we have $\theta_1 = 0$ and $\theta_3 = 1$)

$$\langle \{\phi(x)\phi(x + \lambda\varepsilon)\}_\upsilon \phi(x + \varepsilon)\phi(x_4) \rangle \underset{\varepsilon \to 0}{\sim} \Pi_1(\lambda)\langle \phi(x)\phi(x_4) \rangle + \varepsilon\mathcal{F}_3(\lambda)\langle \hat{\psi}(x)\phi(x_4) \rangle$$
$$+ \varepsilon\left[\mathcal{F}_2(\lambda) + \log(c\,\varepsilon)\mathcal{F}_3(\lambda)\right]\partial_x\langle \phi(x)\phi(x_4) \rangle + \cdots . \quad \text{(B23)}$$

From within the correlation function on the left side of (B23), the two-leg channel exclusively propagating between $\phi(x)$ and $\phi(x + \lambda\varepsilon)$ exclusively projects out the two-leg channel between $\phi(x + \varepsilon)$ and $\phi(x_4)$. That is,

$$\langle \{\phi(x)\phi(x + \lambda\varepsilon)\}_\upsilon \phi(x + \varepsilon)\phi(x_4) \rangle = \langle \{\phi(x)\phi(x + \lambda\varepsilon)\}_\upsilon \{\phi(x + \varepsilon)\phi(x_4)\}_\upsilon \rangle. \quad \text{(B24)}$$

With only the two-leg channel propagating between the two leftmost one-leg boundary operators of (B24) and between the two rightmost, the correlation functions of (B24), and that of the left side of (B23), equal Cardy's formula: $\Pi_1(\kappa = 6 \,|\, x, x + \lambda\varepsilon, x + \varepsilon, x_4)$ (24, 25) [19]. Furthermore, with $\theta_1 = 0$ for $\kappa = 6$, the two-point function $\langle \phi(x)\phi(y) \rangle = (y - x)^{-2\theta_1}$ is a constant. As a result, the logarithmic term in (B23) vanishes (and so too do all of its descendants). Although perhaps counterintuitive, it then follows that logarithms do not appear in the Frobenius series expansion (B10) with $i = 1$ of Cardy's formula, in spite of the presence of logarithmic operators in (B8) [50]. (Of course, we may also verify this claim from the explicit formula (24) for $\Pi_1(\kappa = 6)$.) This is an example of the $q - 1 = N$ case (here, with $q = 3$ and $N = 2$) attributable to pre-logarithmic operators, as discussed in the paragraphs following (B1). In conclusion, because the collection $\{1, \Pi_1(\kappa = 6)\}$ spans $\mathcal{S}_2$, the above arguments imply that the third series in (B10) with $i = 1$ vanishes (while the first series may or may not) for all elements of $\mathcal{S}_2$. Invoking symmetry arguments and/or the alternative basis $\{1, \Pi_2(\kappa = 6)\}$ (where Π_2 is the second rectangle connectivity weight, generated from Π_1 by replacing $\mathscr{P}(x_3, x_4) \mapsto \mathscr{P}(x_2, x_3)$ in (24)), we easily extend this fact to $i = 2$.

Returning to other values of κ and $N = 2$ we note that logarithmic terms do not appear in the Frobenius series expansions of solutions in $\mathcal{S}_2$ if $12/\kappa \in \mathbb{Z}^+ + 1$ is coprime with three (which as mentioned occurs for $\kappa = \kappa_{3,q'}$), but such terms may appear for $\kappa = \kappa_{2,q'}$ if $8/\kappa \in 2\mathbb{Z}^+ - 1$, which includes the case $\kappa = 8/3$ mentioned above. Interestingly, $\kappa = 8/3$ is the SLE_κ dual [42, 43] of $\kappa = 6$, where logarithmic terms do not appear.

Finally, for the case $\kappa = 6$, we mention that the two-point function $\langle \phi(x)\phi(y) \rangle$ is normalized to equal one in the OPE (B8). To see this, we note that the correlation function on the left side of (B24), being Cardy's formula $\Pi_1(\kappa = 6 \,|\, x, x + \lambda\varepsilon, x + \varepsilon, x_4)$ (24, 25), depends exclusively on the cross-ratio

$$\eta = \frac{(x + \lambda\varepsilon - x)(x_4 - x + \varepsilon)}{(x + \varepsilon - x)(x_4 - x - \lambda\varepsilon)} \underset{\varepsilon \to 0}{\sim} \lambda + O(\varepsilon). \quad \text{(B25)}$$

The asymptotic behavior given in (B25) implies that the left side of (B23, B24), equaling $\Pi_1(\kappa = 6 \,|\, \eta)$, approaches $\Pi_1(\kappa = 6 \,|\, \lambda)$ as $\varepsilon \to 0$. Meanwhile, the right side of (B23) approaches $\Pi_1(\kappa = 6 \,|\, \lambda)\langle \phi(x)\phi(x_4) \rangle$ in this limit. Matching these two quantities gives $\langle \phi(x)\phi(x_4) \rangle = 1$, as claimed.

---

[1] M. Bauer, D. Bernard, and K. Kytölä, *Multiple Schramm-Löwner evolutions and statistical mechanics martingales*, J. Stat. Phys. **120** (2005), 1125.

[2] J. Dubédat, *Commutation relations for SLE*, Comm. Pure Applied Mathematics **60** (2007), 1792–1847.

[3] K. Graham, *On multiple Schramm-Loewner evolutions*, J. Stat. Mech. (2007), P03008.

[4] M. J. Kozdron and G. Lawler, *The configurational measure on mutually avoiding SLE paths*, Fields Institute Communications **50** (2007), 199–224.

[5] K. Sakai, *Multiple Schramm-Loewner evolutions for conformal field theories with Lie algebra symmetries*, Nucl. Phys. B **867** (2013), 429–447.

[6] S. M. Flores and P. Kleban, *A solution space for a system of null-state partial differential equations I*, Commun. Math. Phys. **333** (2015), 389–434.

[7] S. M. Flores and P. Kleban, *A solution space for a system of null-state partial differential equations II*, Commun. Math. Phys. **333** (2015), 435–481.

[8] S. M. Flores and P. Kleban, *A solution space for a system of null-state partial differential equations III*, Commun. Math. Phys. **333** (2015), 597–667.

[9] S. M. Flores and P. Kleban, *A solution space for a system of null-state partial differential equations IV*, Commun. Math. Phys. **333** (2015), 669–715.

[10] M. Bauer and D. Bernard, *2D growth processes: SLE and Loewner chains*, Phys. Rept. **432** (2006), 115–221.

[11] G. Lawler, O. Schramm, and W. Werner, *Conformal invariance of planar loop-erased random walks and uniform spanning trees*, Annals Probab. **32** (2004), 939–995.

[12] G. Lawler, O. Schramm, and W. Werner, *On the scaling limit of planar self-avoiding walk*, in Fractal geometry and applications: a jubilee of Benoit Mandelbrot, Part 2, eds. M. L. Lapidus and M. V. Frankenhuysen (2002).

[13] G. Lawler, O. Schramm, and W. Werner, *Values of Brownian intersection exponents I: Half-plane exponents*, Acta Math. **187** (2001), 237–273.

[14] S. Smirnov, *Critical percolation in the plane*, C. R. Acad. Sci. Paris Sr. I Math. **333** (2001), 239–244.

[15] G. Lawler, *Scaling limits and the Schramm-Loewner evolution*, Probab. Surveys **8** (2011), 442–495.

[16] J. Cardy, *SLE for theoretical physicists*, Annals Phys. **318** (2005), 81–118.

[17] P. M. Morse and H. Feshbach, *Methods of Theoretical Physics*, McGraw-Hill (1953).

[18] M. Abramowitz and I. Stegun, *Handbook of Mathematical Functions with Formulas, Graphs, and Mathematical Tables*, Dover Publications, New York (1972).

[19] J. Cardy, *Critical percolation in finite geometries*, J. Phys. A: Math. Gen. **25** (1992), L201–L206.

[20] S. Smirnov, *Towards conformal invariance of 2D lattice models*, Proc. Int. Congr. Math. **2** (2006), 1421–1451.

[21] H. Duminil-Copin and S. Smirnov, *Conformal invariance of lattice models*, preprint: arXiv:1109.1549v1 (2011).

[22] A. Gamsa and J. Cardy, *Schramm–Loewner evolution in the three-state Potts model – a numerical study*, J. Stat. Mech. (2007), P08020.

[23] O. Schramm and S. Sheffield, *The harmonic explorer and its convergence to SLE4*, Ann. Prob. **33** (2005), 2127–2148.

[24] S. M. Flores, P. Kleban, J. J. H. Simmons, and R. M. Ziff, *Partition functions and crossing probabilities for critical systems inside polygons*, in preparation.

[25] A. A. Belavin, A. M. Polyakov, and A. B. Zamolodchikov, *Infinite conformal symmetry in two-dimensional quantum field theory*, Nucl. Phys. B **241** (1984), 333–380.

[26] P. Di Francesco, R. Mathieu, and D Sénéchal, *Conformal Field Theory*, Springer-Verlag, New York (1997).

[27] M. Henkel, *Conformal Invariance and Critical Phenomena*, Springer-Verlag, Berlin Heidelberg (1999).

[28] M. Bauer and D. Bernard, *Conformal field theories of stochastic Loewner evolutions*, Commun. Math. Phys. **239** (2003), 493–521.

[29] V.S. Dotsenko and V.A. Fateev, *Conformal algebra and multipoint correlation functions in 2D statistical models*, Nucl. Phys. B **240** (1984), 312–348.

[30] V.S. Dotsenko and V.A. Fateev, *Four-point correlation functions and the operator algebra in 2D conformal invariant theories with central charge $c \leq 1$*, Nucl. Phys. B **251** (1985), 691–673.

[31] J. Dubédat, *Euler integrals for commuting SLEs*, J. Stat. Phys. **123** (2006), 1183–1218.

[32] S. Smirnov, *Conformal invariance in random cluster models. I. Holomorphic fermions in the Ising model*, Ann. Math. **172** (2010), 1435–1467.

[33] K. Kytölä and E. Peltola, *Pure partition functions of multiple SLEs*, in preparation.

[34] K. Kytölä and E. Peltola, *Conformally covariant boundary correlation functions with a quantum group*, preprint: arXiv:1408.1384.

[35] S. M. Flores, R. M. Ziff, and J. J. H. Simmons, *Percolation crossing probabilities in hexagons: a numerical study*, J. Phys. A Math. Theor. **48** (2015), 025001.

[36] S. Sheffield, *Exploration trees and conformal loop ensembles*, Duke Math. J. 147 (2009), 79–129.

[37] S. Sheffield and W. Werner, *Conformal loop ensembles: the Markovian characterization and the loop-soup construction*, Annals of Math. **176** (2012), 1827–1917.

[38] B. Doyon, *Conformal loop ensembles and the stress-energy tensor*, Lett. Math. Phys. **103** (2013), 233–284.

[39] I. A. Gruzberg, *Stochastic geometry of critical curves, Schramm-Loewner evolutions, and conformal field theory*, J. Phys. A **39** (2006), 12601–12656.

[40] I. Rushkin, E. Bettelheim, I. A. Gruzberg, and P. Wiegmann, *Critical curves in conformally invariant statistical systems*, J. Phys. A **40** (2007), 2165–2195.

[41] P. Di Francesco, O. Golinelli, and E. Guitter, *Meanders and the Temperley-Lieb algebra*, Commun. Math. Phys. **186** (1997), 1–59.

[42] S. Rohde and O. Schramm, *Basic properties of SLE*, Ann. Math. **161** (2005), 879920.

[43] W. Kager, B. Nienhuis, and L. P. Kadanoff, *A guide to stochastic Loewner evolution and its applications*, J. Stat. Phys. **115** (2004), 1149–1229.

[44] B. Duplantier, *Conformal fractal geometry and boundary quantum gravity*, Fractal geometry and applications: a jubilee of Benoît Mandelbrot, Part 2: Multifractals, probability and statistical mechanics, applications (Providence), Proc. Sympos. Pure Math. **72**, Amer. Math. Soc., (2004), 365–482.

[45] J. J. H. Simmons, *Logarithmic operator intervals in the boundary theory of critical percolation*, J. Phys. A: Math. Theor. **46** (2013), 494015.

[46] V. Gurarie, *Logarithmic operators and logarithmic conformal field theories*, J. Phys. A: Math. Theor. **46** (2013), 494003.

[47] K. Kytölä and D. Ridout, *On staggered indecomposable Virasoro modules*, J. Math. Phys. **50** (2009), 123503.

[48] T. Creutzig and D. Ridout, *Logarithmic conformal field theory: beyond an introduction*, J. Phys. A: Math. Theor. **46** (2013), 494006.

[49] V. Gurarie, *Logarithmic operators in conformal field theory*, Nucl. Phys. B **410** (1993), 535–549.

[50] P. Mathieu and D. Ridout, *From percolation to logarithmic conformal field theory*, Phys. Lett. B **657** (2007), 120–129.

[51] J. J. H. Simmons and P. Kleban, *Percolation crossing formulas and conformal field theory*, J. Phys. A **40** (2007), F771.